Project No. 13-4783

Development of Fuel Cycle Data Packages for Two-Stage Fast Reactor Fuel Cycle Options for Optimum Resource Utilization and Waste Management

Fuel Cycle Research and Development

W. S. Yang
Purdue University

Kenneth Kellar, Federal POC
Gilles Youinou, Technical POC

NEUP Nuclear Energy University Programs
U.S. Department of Energy

PURDUE UNIVERSITY

Argonne NATIONAL LABORATORY

PU/NE-16/01

Final Report on Two-Stage Fast Spectrum Fuel Cycle Options

W. S. Yang, C. S. Lin, J. S. Hader, T. K. Park, P. Deng, G. Yang, Y. S. Jung
School of Nuclear Engineering
Purdue University

T. K. Kim, N. E. Stauff
Nuclear Engineering Division
Argonne National Laboratory

January 30, 2016

Executive Summary

This report presents the performance characteristics of two "two-stage" fast spectrum fuel cycle options proposed to enhance uranium resource utilization and to reduce nuclear waste generation. One is a two-stage fast spectrum fuel cycle option of continuous recycle of plutonium (Pu) in a fast reactor (FR) and subsequent burning of minor actinides (MAs) in an accelerator driven system (ADS). The first stage is a sodium-cooled FR fuel cycle starting with low-enriched uranium (LEU) fuel; at the equilibrium cycle, the FR is operated using the recovered Pu and natural uranium without supporting LEU. Pu and uranium (U) are co-extracted from the discharged fuel and recycled in the first stage, and the recovered MAs are sent to the second stage. The second stage is a sodium-cooled ADS in which MAs are burned in an inert matrix fuel form. The discharged fuel of ADS is reprocessed, and all the recovered heavy metals (HMs) are recycled into the ADS. The other is a two-stage FR/ADS fuel cycle option with MA targets loaded in the FR. The recovered MAs are not directly sent to ADS, but partially incinerated in the FR in order to reduce the amount of MAs to be sent to the ADS. This is a heterogeneous recycling option of transuranic (TRU) elements.

To evaluate the proposed two-stage fuel cycle options, design studies were performed to develop reference designs for a 1000 MWt sodium-cooled fast reactor core, named LEUFBR (LEU-fueled fissile break-even reactor), an 840 MWt sodium-cooled ADS blanket, and a moderated MA target assembly. It was assumed that after an assumed plant lifetime of 60 years, the recovered U and Pu from LEUFBR spent fuel including the core inventory at the end-of-life (EOL) is used to start a new Pu-fueled FR. The electricity sharing in a nuclear fleet between Pu-fueled FR and MA-fueled ADS was evaluated at the equilibrium state such that the TRU consumption in the second-stage ADS is balanced with the recovered MA and surplus Pu from the first-stage Pu-fueled fast reactors. Using the fuel cycle performance and electricity sharing data, the mass flow data at the equilibrium state in a nuclear fleet of 100 GWe-yr electricity production were evaluated for the two proposed two-stage fuel cycle options. For comparison, a single-stage fast reactor fuel cycle with homogeneous recycling of TRU was evaluated as well.

The reference core designs for FR and ADS and the reference assembly design for MA target were developed through a detailed neutronics and thermal-hydraulic analyses. Fuel cycle analyses were performed with the DIF3D/REBUS-3 code system. Using 3-dimensional hexagonal-z geometry models, equilibrium and non-equilibrium cycle analyses were performed. Region-dependent, 33-group neutron cross section sets and 21-group gamma cross sections were generated using the MC^2-3 code and the ENDF/B-VII.0 data. The cross sections of moderated MA target assemblies were generated by combining MCNP6 and MC^2-3 calculations. Reactivity coefficients and kinetics parameters were calculated using the VARI3D perturbation theory, DIF3D diffusion, and VARIANT transport codes. Coupled neutron and gamma heating calculations were performed using the DIF3D and GAMSOR codes. Thermal-hydraulic analyses were carried out using the SE2-ANL sub-channel analysis code. The radioactivity of the nuclear waste was calculated with the ORIGEN2 code. In addition, to facilitate the cycle-by-cycle transition analyses of LEUFBR, a search capability to determine the feed enrichment of fresh assemblies for non-equilibrium cycle problems with partial reloading was implemented into the REBUS-3 code.

Starting from a metal fuel core design of the 1000 MWt Advanced Burner Reactor (ABR), a compact core configuration of LEUFBR was developed by increasing the active core height and replacing six primary control assemblies with fuel assemblies. Figure 0.1 shows the radial core layout of the 1000 MWt LEUFBR core concept. The core is composed of 186 drivers, 114 reflectors, 66 radial shields, and 9 primary and 4 secondary control assemblies. The core is divided into three enrichment zones (i.e., inner, middle and outer cores) in order to flatten the power distribution. The primary control system consists of three assemblies in the fourth hexagonal row and six assemblies in the seventh row, and the secondary control system consists of one central assembly and three assemblies in the fourth row. The core is surrounded by two rows of steel reflectors and one row of B_4C shield assemblies. The ABR design parameters were adopted for the primary and secondary control assemblies, steel reflectors and B_4C shields.

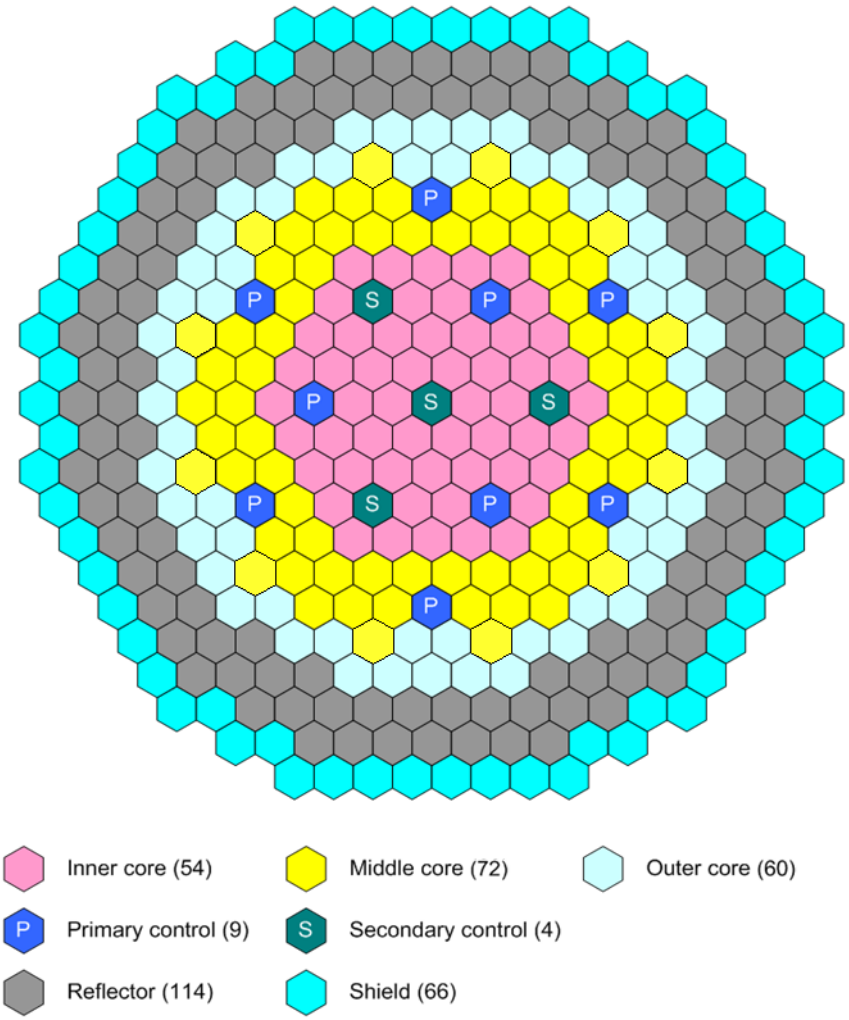

Figure 0.1. Radial Core Layout of LEU-Fueled Fissile Break-Even Reactor (LEUFBR)

Using this core configuration, scoping studies based on equilibrium cycle calculations were performed to determine the fuel volume fraction to achieve a fissile break-even core and the fuel management scheme to maximize the discharge burnup within the fast fluence limit of cladding material. A fixed cycle length of 18 months with a capacity factor of 90% was selected

with a three-batch fuel management scheme for the inner and middle core zones and a four-batch scheme for the outer core zone. The results showed that the minimum fuel volume fraction to achieve a fissile break-even core with external feed of depleted uranium is 35.3%. It was also found that the maximum fuel volume fraction achievable within the imposed thermal design limits was 39.4%. The assembly design parameters corresponding to these fuel volume fractions are compared in Table 0.1 along with selected performance parameters.

Table 0.1. Key Assembly Design Parameters for Minimum and Maximum Fuel Volume Fractions of LEUFBR

Fuel volume fraction, %	35.3	39.4
Core height, cm	100	100
Pin outer diameter, mm	8.9	10.5
Number of fuel pins per assembly	217	169
Assembly lattice pitch, cm	16.14	16.14
Inter-assembly gap, mm	4.0	4.0
Duct thickness, mm	3.0	3.0
Pin pitch-to-diameter ratio	1.14	1.10
Cladding thickness, mm	0.5	0.5
Equilibrium cycle fissile conversion ratio	1.01	1.07
Average linear power, kW/m	22.7	29.2
Peak linear power (PLP), kW/m	36.2	45.4
PLP limit (fuel/cladding eutectic), kW/m	37.7	46.5
PLP limit (fuel centerline), kW/m	56.1	62.6

At the equilibrium cycle, the LEUFBR core concept reached a fissile break-even core with recovered plutonium and natural uranium only without any supporting LEU fuel. Since the core starts with LEU fuel, it would take some time to reach an equilibrium cycle by building sufficient plutonium. For this reason, the overall fuel cycle characteristics of LEUFBR were evaluated through transitional cycle-by-cycle analyses over an assumed plant lifetime of 60 years. The same fuel management scheme as used in equilibrium cycle was employed in the transitional cycle analyses. It was assumed that the recovered Pu from the discharged fuel at the end of n-th cycle can be loaded into the core at the beginning of (n+2)-th cycle.

A cycle-by-cycle analysis of the LEUFBR was performed by searching the required U-235 enrichment of charged fuel to achieve the targeted cycle length (18 months). In the initial uranium cores, the fuel assembly design with a fuel volume fraction of 39.4% was used in order to maximize the natural resource utilization by maximizing Pu production. When the core becomes close to the equilibrium-cycle Pu core, the fuel assembly design with a fuel volume fraction of 35.3% was used to reduce the surplus Pu buildup. At the equilibrium state, the fuel volume fraction of Pu-fueled FR was further reduced to 35.1% to minimize the TRU generation while maintaining a fissile break-even core with external feed of natural uranium.

Table 0.2 summarizes the performance parameters of the LEUFBR core. At the beginning of life (BOL), the core is loaded with LEU fuel of 13.6% enrichment. The fissile conversion ratio is initially 0.67 and gradually increases with operating cycles. It reaches a fissile break-

even point at the 14-th cycle. For the succeeding cycles, the required fresh fuel is fabricated from the recycled U and Pu and the continued external feed of depleted uranium. For a 60-year operation time, the total natural uranium requirement (with an enrichment tail of 0.2%) is 814.3 metric ton (MT), which is about one-fifth of that for a typical pressurized water reactor (PWR) with same amount of electricity generation. The total amount of accumulated Pu and MAs including the unprocessed inventories at EOL are 3.7 MT and 533 kg, respectively. The remaining Pu and MA inventory at EOL can be used to start a new FR or in an ADS.

Table 0.2. Fuel Cycle Performance Parameters of the LEUFBR Core

U-235 mass fraction at BOL HM inventory, %	13.6
Core inventory of LEU at BOL, MT	15.5
Core inventory of depleted U at BOL, MT	7.2
Fissile conversion ratio at BOL	0.67
Natural U resource required for 60 years, MT	814.3
Surplus Pu over cycle 1-38, kg	92.5
Discharged Pu at cycle 39, kg	827.8
Remaining Pu inventory at cycle 40, kg	2745.0
Accumulated Pu for 60 years, MT	3.7
Accumulated MAs over 60 years, kg	533

To examine the safety characteristics of the reference LEUFBR design, kinetics parameters and reactivity coefficients were calculated for the uranium and Pu cores. The control requirements for both cores were also evaluated by accounting for the temperature and power defects (including 15% overpower), the burnup reactivity swing, and the associated uncertainties. The estimated total control requirement for primary control system is about 3.4$ in uranium core and 4.2$ in Pu core. The total control requirement for the secondary control systems is about 0.9$ in uranium core and 1.7$ in Pu core. The shutdown margins of primary and secondary control systems were determined with the assumption that the most reactive assembly is stuck. The minimum shutdown margins of the primary system for the uranium and Pu cores are ~10.7$ and ~13.2$, respectively. The minimum shutdown margins of the secondary system for the uranium and Pu cores are ~3.0$ and ~6.1$, respectively. The evaluated reactivity coefficients provided sufficient negative feedback. In addition, the integral reactivity parameters for the quasi-static reactivity balance model indicate that both the uranium and Pu cores have passive safety features.

A reference blanket design was developed for an 840 MWt sodium-cooled ADS by utilizing non-uranium metallic dispersion fuel in which MA-10Zr fuel particles are dispersed in a zirconium metal matrix. In this study, similar design goals and analysis techniques were adopted from the previous analyses for 840 MWt accelerator transmutation of waste (ATW) blanket designs with lead-bismuth eutectic and sodium coolants. The design objectives were maximizing discharge burnup and minimizing burnup reactivity loss over an operating cycle. The core was divided into three zones with different fuel particle fractions (i.e., inner, middle and outer cores) in order to flatten the power distribution.

Table 0.3 shows the equilibrium-cycle performance characteristics of the sodium-cooled ADS blanket design. The MA-10Zr particle fraction in fuel was determined to attain a

multiplication factor of 0.97 at the beginning of equilibrium cycle (BOEC). The heavy metal inventory at BOEC required to achieve the desired multiplication factor is 4.2 MT. A high fuel inventory was obtained by increasing the fuel volume fraction of dispersion fuel. The volume fractions of fuel particles in the charged fuel are 25.4%, 34.4%, and 38.2% in the inner, middle and outer zones, respectively. Because of the large fuel inventory, the burnup reactivity loss is relatively small, but the average discharge burnup is also relatively low. The average discharged burnup was determined to be 19.6% and the burnup reactivity loss was 1.3% with a six-month short cycle design.

Table 0.3. Equilibrium Cycle Performance of Sodium-Cooled ADS Blanket Design

Parameter		ADS
Thermal power, MW		840
Cycle length, EFPD		135
Capacity factor, %		75
BOEC heavy metal inventory, kg		4208
Fuel particle fraction, volume % in matrix	Inner zone Middle zone Outer zone	25.4 34.4 38.2
Multiplication factor	BOEC EOEC*	0.97007 0.95726
Burnup reactivity loss, %Δk		1.3
Core-average power density, kw/l		247.6
Power peaking factor at BOEC/EOEC		1.55/1.58
Peak linear power, kW/m	Inner zone Middle zone Outer zone	37.8 37.2 37.1
Average discharge burnup, atom %		19.6
Peak fast fluence, 10^{23} n/cm^2		3.52
Net TRU consumption rate (kg/year)		233
Equilibrium loading, kg/year	FR TRU Recycled HM Total HM	233 974 1206

* EOEC: End of Equilibrium Cycle

A reference MA target assembly design was developed to transmute the recovered MA isotopes from the discharged fuels of LEUFBR. The major isotopes in the MAs of the used fuels are Np-237 and Am-241, so they can be effectively converted into fissile nuclides in a moderated target by utilizing their large capture cross sections in the thermal energy region. Using $ZrH_{1.6}$ moderator, the moderator volume fraction was maximized within the peak linear power limit on MA-40Zr target during one cycle irradiation time. In order to reduce the local power peaking in the adjacent fuel assemblies due to the thermal neutron leakage from the moderated target assembly, the long-lived fission product (LLFP) pins were used as thermal neutron filters. The target assembly contains 169 pins of 9.5 mm diameter and has the same assembly dimensions as the driver fuel assembly. Twenty-four MA target pins, one hundred and twenty-seven moderator pins, nine technetium pins and nine calcium iodide pins are almost evenly distributed in the target assembly.

Using the MA target assembly design, the transmutation performance of LEUFBR was investigated by non-equilibrium cycle-by-cycle analyses for the assumed lifetime of 60 years. It was assumed that a target assembly would be fabricated only when the recovered amount of MAs is sufficient to fabricate at least one assembly. Based on the available amount of recovered MA, six target assemblies were loaded in the core from the 9-th cycle. Total one hundred and ninety-two target assemblies were loaded in the core over an assumed plant lifetime of 60 years. With the use of 192 target assemblies, overall transmutation fractions of 88.6% and 36.1% were obtained for MAs and LLFPs, respectively. At the equilibrium state, the use of MA target assemblies in LEUFBR reduces the amount of MA to be sent to ADS by a factor of six compared to that of the fuel cycle with no recycling of MA in FR. Through whole-core sub-channel thermal-hydraulic analyses, it was also confirmed that the peak cladding inner wall and fuel centerline temperatures including 2-sigma uncertainties satisfy the imposed thermal design limits for all the fuel and target assemblies.

The two proposed two-stage fuel cycle options are illustrated schematically in Figures 0.2 and 0.3. In both options, the first-stage fast reactors are divided into uranium-fueled cores (i.e., LEUFBR) and Pu-fueled cores based on the external fuel feed at BOL. The LEUFBR is operated for an assumed plant lifetime of 60 years starting from an initial uranium core, and the accumulated U and Pu fuel including the core inventory at EOL is used to start the Pu-fueled FR. For both FR cores, Pu and U are co-extracted from the discharged fuel and recycled back into the reactor. The recovered MAs from the discharged fuel are sent to the second-stage ADS directly in the first option, but in the second option, MAs are partially transmuted in the FR using moderated MA targets. The initial HM inventory of ADS is extracted from the discharged fuel of LEUFBR. The discharged fuel of ADS is reprocessed, and all the recovered HMs are recycled into the ADS along with the MAs from the first-stage FRs.

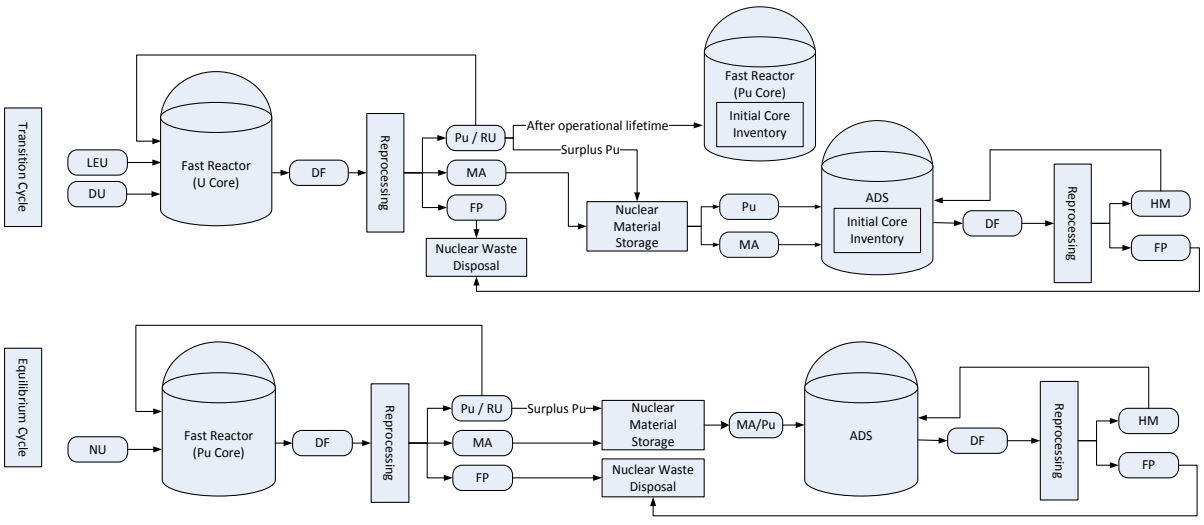

Legend:

LEU = Low-Enriched Uranium	DF = Discharged Fuel	MA = Minor Actinides
ADS = Accelerator Driven System	DU = Depleted Uranium	RU = Recovered Uranium
FP = Fission Products	HM = Heavy Metals	NU = Natural Uranium

Figure 0.2. Schematic Illustration of First Two-stage Fuel Cycle Option

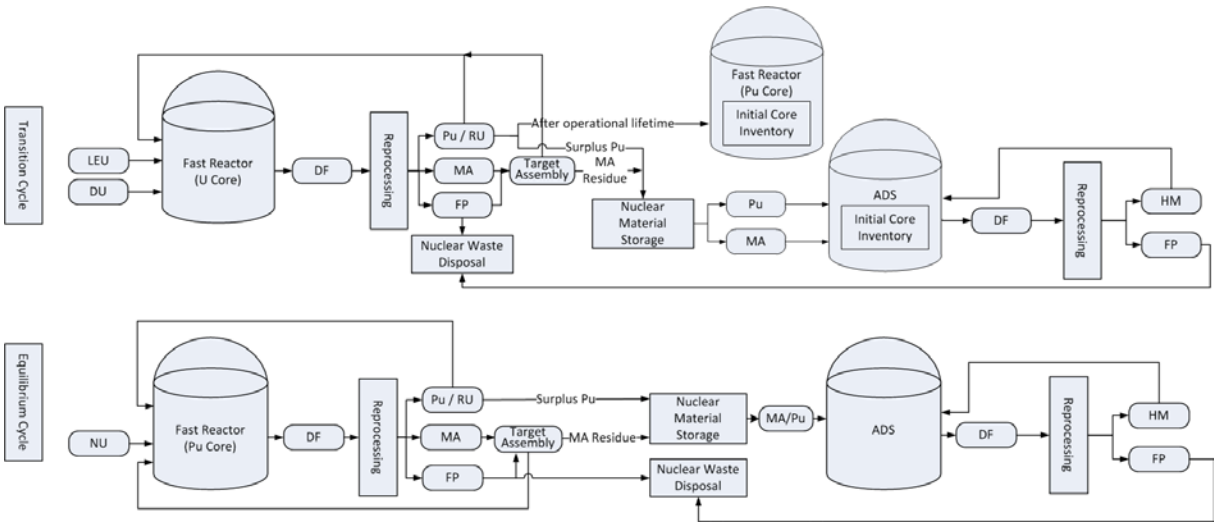

Figure 0.3. Schematics of Second Two-Stage Fuel Cycle Option with MA Targets in FR

The fuel cycle performance characteristics of the first two-stage fuel cycle option are summarized in Table 0.4. The MAs generation rate in the Pu-fueled FRs is 6.5 kg/year, while the TRU consumption rate of the ADS is 232.6 kg/year. The number of Pu-fueled FRs to be supported by one ADS was estimated to be 37 based on the mass balance of MAs at the equilibrium state. With an assumed separation loss of 1% and a fabrication loss of 0.2%, the Pu-fueled FR produces only negligible amount of surplus Pu (0.2 kg/year) for an equilibrium

Table 0.4. Comparison of the First Two-stage Fuel Cycle Performance Parameters

Parameter		U-fueled FR	Pu-fueled FR	ADS
Reactor power, MWt		1000	1000	840
Fuel form		U-10Zr/ U-Pu-10Zr	U-Pu-10Zr	MA-10Zr dispersion
Cycle length, months		18	18	6
Capacity factor, %		90	90	75
Specific power, MW/MT		42.5	47.6	203.7
Number of batches		3/3/4	3/3/4	7/8/8
Average fuel residence time, year		4.98	4.98	3.79
Fuel inventory in core, MT		22.8	20.4	4.2
Charge fuel mass per batch, MT		7.2	6.4	0.6
Charge fuel mass fraction, %	U Pu MAs	100/87.2* 0/12.8 0	86.7 13.3 0	3.4 35.8 60.8
Surplus Pu plus EOL Pu inventory, MT		3.7	---	---
Pu inventory at BOEC+2nd cycle feed, MT		---	3.5	---
Discharged MAs from FR, kg/year		---	6.5	---
TRU consumption in ADS, kg/year		---	---	232.6
Number of systems		35	37	1

* BOL/EOL

cycle. This surplus Pu would be burned with MA in the ADS. The amount of Pu required to start a Pu-fueled FR is 3.5 MT, while each reference LEUFBR (with a fuel volume fraction of 39.4% and 35.3%) produces 3.7 MT of Pu over its assumed lifetime of 60 years. As a result, 35 LEUFBRs are required to support 37 Pu-fueled FRs from the plutonium mass balance. For the second two-stage fuel cycle option, the amount of MAs to be sent to ADS is reduced to 1.1 kg/year, and hence the demand for ADS is reduced by a factor of about six relative to the first option.

Using the performance parameters of LEUFBR and ADS, the mass flow data at the equilibrium state were assessed for a nuclear fleet of 100 GWe-yr electricity production. The production rates of MA and surplus Pu in the first-stage FRs and the TRU consumption rates in the second-stage ADS are 18 kg/GWe-yr and 958 kg/GWe-yr, respectively, for the first two-stage fuel cycle option, and 3 kg/GWe-yr and 1045 kg/GWe-yr for the second two-stage fuel cycle option. Based on the TRU production and consumption rates, the electricity sharing between FRs and ADSs in the nuclear fleet were estimated to be 98.1% to 1.9%, respectively, for the first fuel cycle option and 99.7% to 0.3% for the second two-stage fuel cycle option.

Table 0.5 summarizes the performance characteristics of the two two-stage fuel cycle options (Options 1 and 2) and the single-stage fuel cycle option (Option 3). The electricity sharing of ADS in FR/ADS nuclear for the second two-stage fuel cycle option was reduced due to the reduced amount of MAs produced in the first-stage FRs. The total amount of natural uranium (with an enrichment tail of 0.2%) required for a 100 GWe-yr electricity production in the whole nuclear fleet is 102.8 MT for Option 1, 103.2 MT for Option 2, and 102.6 for Option 3. Since the Pu and MA are continuously recycled, these fuel cycle options do not release Pu or MA except for the loss from the fuel fabrication and separation. For the overall fuel cycle, the fission products and reprocessing loss of HM sent to the repository are 90.5 MT and 13.1 MT for Option 1, 88.9 MT and 13.6 MT for Option 2, and 90.4 MT and 13.1 MT for Option 3.

Table 0.5. Comparison on Equilibrium Cycle Performance

			Option 1	Option 2	Option 3
TRU recycle option			Pu in FR/ MA in ADS	With MA targets in FR	Homo. recycle of TRU in FR
Electricity sharing of ADS in FR/ADS nuclear fleet, %			1.9	0.3	0
Mass flow (MT) per 100 GWe-yr	Natural U resource required		102.8	103.2	102.6
	Separation/fabrication loss of U		11.1	11.6	11.1
	Separation/fabrication loss of TRU		2.0	2.0	2.0
	Fission product sent to the repository		90.5	88.9	90.4
Core performance parameters	Average discharge burnup, GWd/t	Fuel/Target in FR	72.7	70.5/278.1	73.7
		Fuel in ADS	177.5	231.0	- -
	TRU fraction of HM inventory, %	Fuel/Target in FR	14.2	14.2/100	14.8
		Fuel in ADS	96.4	98.2	- -

For the driver fuel assemblies, the average discharge burnup was determined to be approximately 70 GWd/t and the TRU fraction of HM inventory in the two two-stage fuel cycle options was 14.2% while that increased to 14.8% for Option 3. Since LLFP pins were used as the thermal neutron filters in the target assemblies, a transmutation fraction of 14.5% in LLFPs is attained at the equilibrium cycle. The accumulated LLFPs to be send to repository could be further reduced by loading multiple targets with a larger amount of LLFPs. Calculation result showed that the reduced amount of Tc-99 to be sent to repository would result in a significant reduction in activity value at 100,000 year after fuel discharge.

All the three fuel cycle options employ the same fast spectrum reactor concept and continuously recycle U and TRU. Thus, they show similar fuel cycle performances in term of mass flow data. In Options 1 and 2, U/Pu and U/TRU were recycled in FR, respectively, and MAs were recycled in ADS. In Option 3, U/TRU was recycled in FR. The FR in the Options 1 and 2 may have potential benefit from the fuel fabrication and reprocessing points of view. In these options where TRU elements are partitioned into Pu and MA streams, the normal fuel fabrication methods can be applied to the most of the fuel assemblies since all the MA are concentrated in a few ADSs or in a few target assemblies. On the other hand, Option 3 with homogeneous recycle of TRU in FR may have economic advantage over Options 1 and 2. Moreover, co-extraction of Pu and MA would reduce the proliferation risk.

In summary, the two proposed two-stage fuel cycle options (consisting of first-stage FR with and without MA target assemblies and second-stage ADS) and the single-stage fast reactor option with homogeneous recycling of TRU showed similar performances in terms of natural uranium utilization and waste generation. All the three fuel cycles considered can be operated with natural or depleted uranium only at the equilibrium state, since all the uranium, plutonium and MAs are continuously recycled. The results from the equilibrium cycle analysis showed that the three fuel cycle options could achieve high reductions in waste generation because of the continuous recycle of the Pu and MA. In addition, the mass flow data showed that the proposed two-stage fast spectrum fuel cycle options increase the efficiency of natural uranium utilization and reduce the nuclear waste generation compared to the conventional two-stage fuel cycle options based on thermal and fast spectrum systems.

Table of Contents

List of Figures

List of Tables

1. Introduction

The Department of Energy, Office of Nuclear Energy (DOE-NE) has recently developed a roadmap for its research, development and demonstration activities to ensure that nuclear energy remains a compelling and viable energy option for the United States, based on its ability to provide abundant and stable electricity supply while helping to meet clean air and carbon reduction goals. One of the key objectives stated in the Nuclear Energy Research and Development (R&D) Roadmap [1] is to develop sustainable nuclear fuel cycles, where the nuclear fuel cycle is the progression of nuclear fuel from mining and enrichment to power generation to ultimate disposal of the used nuclear fuel or derived waste products. In order to provide information about potential benefits and challenges of nuclear fuel cycles and to identify promising fuel cycles with potential to provide substantial improvements relative to the current U.S. fuel cycle, the Office of Fuel Cycle Technologies (FCT) of DOE-NE conducted an Evaluation and Screening (E&S) study [2] for a wide range of nuclear fuel cycle options. The study showed that the most promising advanced fuel cycles have one or more of the following characteristics: continuous recycle of actinides (U/Pu or U/transuranics (TRU)), fast spectrum critical reactors, high internal conversion, and no uranium enrichment required once steady-state conditions are established.

The purpose of this study is to provide supporting data for the E&S study by evaluating the two proposed "two-stage" fast spectrum fuel cycle options, which offer efficient use of uranium resources and the ability to burn minor actinides (MAs) and long-lived fission products (LLFPs). One is a two-stage fuel cycle option of continuous recycle of plutonium (Pu) in a fast reactor (FR) and subsequent burning of MAs in an accelerator driven system (ADS), hereafter called the first two-stage fuel cycle option. The other is a two-stage FR/ADS fuel cycle option with MA targets, hereafter called the second two-stage fuel cycle option. This study was performed in two phases in two years. The first phase of the research during the first year involved the development of a point reference FR core design and a point reference ADS blanket design. The second phase of the research during the second year focused on the development of MA target design and the evaluation of the fuel cycle metrics and preparation of fuel-cycle data package.

This report documents the outcome of this two-year research on the two "two-stage" fast spectrum fuel cycle options for optimum resource utilization and waste management. The performance characteristics of the proposed two-stage fast spectrum fuel cycle options were evaluated by developing optimum core designs for a 1000 MWt sodium-cooled fast reactor starting with low-enriched uranium (LEU) fuel, which was named the LEU-fueled fissile break-even reactor (LEUFBR), and an 840 MWt MA-fueled ADS. For the second fuel cycle option with MA targets, moderated target assembly designs were developed.

A point reference design of the 1000 MWt LEUFBR was developed starting from the metal fuel core design of the 1000 MWt Advanced Burner Reactor (ABR) [3,4]. Using the core configuration design, equilibrium cycle calculations were performed to determine the minimum fuel volume fraction to achieve a fissile break-even core without supporting LEU fuel. Parametric studies were carried out to optimize the cycle length and the fuel management scheme so that the discharge burnup is maximized within the fast fluence limit of cladding material.

Using a zirconium matrix MA dispersion fuel, a point reference design of the 840 MWt sodium-cooled ADS blanket was developed based on the 840 MWt sodium-cooled accelerator transmutation of waste (ATW) blanket design [5] with zirconium-matrix TRU dispersion fuel. Using the core configuration of the ATW blanket design, parametric studies were carried out to determine the optimum design parameters. The burnup reactivity loss was reduced with short irradiation cycle approach, and the optimum fuel volume fraction was determined to maximize the discharge burnup while satisfying the imposed thermal design constraints.

In the second two-stage fuel cycle option, MAs are partially transmuted in FR through MA target assemblies in order to reduce the amount of MA to be sent to the second-stage ADS. A reference MA target design was developed for partially transmuting the MA in the FR. The major isotopes among the MAs in the used LEUFBR fuel are NP-237 and Am-241. These nuclides have relatively small fission-to-absorption cross section ratios in the fast energy range, but they have large thermal capture cross sections. Therefore, it would be a promising option to convert them first into fissile nuclides in moderated target assemblies and to fission the product fissile nuclides. The optimum moderator fraction in the target assembly was determined to maximize the MA transmutation performance while satisfying the imposed thermal design constraints.

In order to evaluate the relative performances of the proposed two-stage fuel cycle options, a single-stage fast rector fuel cycle option where all the TRU elements are homogeneously (i.e., without partitioning into Pu and MA elements) recycled into FR was also evaluated. Using the performance parameters of the LEUFBR and ADS, the mass flow data at equilibrium state in a nuclear fleet of 100 GWe-yr electricity production were assesses for the three fuel cycle options. In addition, the activity, toxicity and decay heat of spent nuclear fuel were also compared for the three fuel cycle options.

This report is organized as follows. In Section 2, the reference LEUFBR core design and performance characteristics are discussed along with the design objectives, design constraints, and computational methods and models. The results of scoping equilibrium cycle analyses and transition cycle analyses are also discussed along with the reactivity coefficients, control requirement, and shutdown margins. Section 3 discusses the scoping design studies of the sodium-cooled ADS system. In Section 4, the design and performance characteristics of moderated MA target assembly are described, including moderator and fuel materials, design constraints, transmutation characteristics of MAs, and sub-channel thermal-hydraulics analysis results. Section 5 compares the performance characteristics of the three fuel cycle options. Conclusions are summarized in Section 6.

2. Development of Reference LEUFBR Core Design

2.1. LEUFBR Core Concept

A sodium-cooled fast reactor core design for the first-stage of the proposed two-stage fuel cycle options was developed through detailed neutronics and thermal-hydraulics design studies. This sodium-cooled FR starts with low-enriched (less than 20%) uranium (LEU) fuel. Pu and uranium are co-extracted from the discharged fuel and recycled in the reactor. The recovered MAs from the discharged fuel are sent to the second-stage ADS directly in the first two-stage fuel cycle option, while they are first transmuted in the FR using MA target assemblies and only remaining MAs are sent to the second-stage ADS in the second two-stage fuel cycle option. At the equilibrium cycle, the FR of the first-stage operates with the recovered plutonium and depleted or natural uranium only without supporting LEU.

The main design goal for the sodium-cooled FR was to develop a compact, fissile break-even core without the use of a fertile blanket while maximizing the uranium resource utilization and minimizing the nuclear waste or plutonium buildup. In order to achieve these goals, several design decisions were made. High discharge burnup was pursued to enhance the uranium resource utilization and to minimize the loss of TRU elements to the waste stream. A blanket-free core concept was selected to reduce the risk of proliferation, and a long fuel cycle length was selected by trade-off between the plant capacity factor and burnup reactivity swing. Finally, to reduce construction and material costs, the core size was minimized within the imposed thermal design limits.

In order to enhance the neutron economy required for a high fissile conversion ratio, the well-known U-10Zr and U-Pu-10Zr metal alloy fuels [6,7] were selected for startup and recycled fuels, respectively. These two metal alloy fuels are favorable because of their inherent passive safety characteristics [8,9]. A low-swelling stainless steel cladding (HT-9) was selected for cladding and assembly duct. The thermal-hydraulic and material-related design constraints were adopted from the ABR studies conducted by Argonne National Laboratory (ANL) [3,4].

Starting from a metal fuel core design of 1000 MWt ABR, a compact core configuration was developed for a 1000 MWt sodium-cooled fast reactor, named the LEU-fueled fissile break-even reactor (LEUFBR). Using this core configuration, scoping studies based on equilibrium cycle analyses were performed to determine the minimum fuel volume fraction to achieve a fissile break-even core without supporting LEU fuel. The fuel management scheme was optimized to maximize the discharge burnup within the fast fluence limit of HT-9 cladding. Candidate assembly designs were developed to yield an equilibrium-cycle fissile conversion ratio slightly greater than 1.0 while satisfying the imposed thermal-hydraulic and material-related design constraints.

Using these fuel assembly designs, cycle-by-cycle transition analyses were performed for an assumed plant lifetime of 60 years starting from an initial uranium core. A reference core design was developed to maximize the uranium resource utilization while minimizing TRU generation during the 60-year plant lifetime. The performance characteristics of fuel cycle, including the mass flow rates of the reference design, were evaluated using the transition cycle analysis for the 60-year plant lifetime.

2.2. Design Constraints

For the binary (U-10Zr) and ternary (U-Pu-10Zr) metal fuels, an as-built smeared density of 75% was assumed to allow free fuel swelling of approximately 33%, at which point porosity becomes largely interconnected and open to the outside of the fuel, releasing a large fraction of fission gas to the fission gas plenum at the top of the fuel pin [6]. A fast fluence limit for HT-9 cladding was assumed approximately 4×10^{23} n/cm^2, based on the irradiation data obtained in Fast Flux Test Facility (FFTF) that showed no duct elongation or cladding breach after a fast fluence of 3.9×10^{23} n/cm^2 [7] with HT-9 structural material.

The power in the hottest fuel pin was required to be less than the minimum value for incipient bulk fuel melting. Although bulk fuel melting is less likely to cause cladding damage in metallic fuel pins because the melting temperature of the fuel (~1100°C) is lower than the melting temperature of the cladding, the criterion of not allowing bulk fuel melting during normal operation was imposed in this study. The relatively benign effect of bulk melting in metallic fuels was shown by the results from experimental irradiations of EBR-II Mark-IA fuel fabricated with bond sodium only in the lower half of the pins. Even though the absence of the bond sodium caused extensive fuel melting, the molten fuel simply relocated to close the fuel-cladding gap and froze in place without failure of the cladding. Only a small area of eutectic interaction with the cladding was noted with a maximum wall penetration of 10% of the thickness.

An additional constraint was imposed such that the power-to-flow ratio and power in the hottest fuel pin are less than the minimum value for macroscopic eutectic liquefaction at the fuel-cladding interface. The source of the eutectic liquefaction at the interface is the metallurgical interaction of metallic U-Pu-Zr fuel and fission products with the iron-based cladding to form a low melting point phase. Based on a series of out-of-pile experiments, the threshold temperature for high burnup U-20Pu-10Zr fuel with HT-9 cladding was determined to be between 650°C and 660°C [10]. It was also shown that the threshold temperature is much higher at lower burnups. Although the eutectic melting temperature of the initial U-10Zr fuel is significantly higher than that of U-Pu-10Zr fuel, the minimum value of 650°C was used in this study to accommodate the recycled U-Pu-10Zr fuel.

2.3. Computational Methods and Models

The ANL suite of fast reactor analysis codes was used in this study. Fuel cycle analyses were performed with the DIF3D/REBUS-3 code system [11-13]. Using 3-dimensional hexagonal-z geometry models, equilibrium and non-equilibrium cycle analyses were performed. Region-dependent, 33-group neutron cross section sets were generated using the MC^2-3 code [14] and the ENDF/B-VII.0 cross section library. The initial scoping study to determine the region-wise fuel compositions required for cross section generation was performed using the 21-group cross section set used in the ABR design studies [3,4], which was generated with the ETOE-2/MC^2-2/SDX code system [15,16] based on ENDF/B-V.2. The details of cross section generation method are discussed in the Section 2.4.2.

Material thermal expansion at operating condition was modeled by adjusting the hexagonal pitch, axial meshes, and the fuel and structure volume fractions appropriately. Irradiation

swelling of metal fuel was considered, and the bond sodium was displaced into the lower part of fission gas plenum. Uniform axial swellings of 5% and 8% were assumed for U-Pu-10Zr and U-10Zr fuel forms, respectively. An enrichment zoning strategy was employed to flatten the power distribution, and the fuel discharge burnup was maximized by adjusting the fuel residence time such that the peak fast fluence is within the fast fluence limit of HT-9 cladding.

Equilibrium and non-equilibrium cycle calculations were performed with REBUS-3. Block nuclide depletion was performed by dividing each fuel assembly into five axial depletion zones. The fuel enrichment was defined as the fraction of U-235 and Pu in heavy metal in this study, and the required enrichment to maintain the criticality throughout a burn cycle was determined using the enrichment search option of REBUS-3. In order to accommodate the computational modeling and fabrication uncertainties, the criticality was estimated with a multiplication factor (k-effective) of 1.003. For a fissile burning cycle where the k-effective decreases with time, the critical enrichment at the end of cycle (EOC) was searched. On the other hand, for a fissile breeding cycle where the k-effective increases with burnup, the critical enrichment at the beginning of cycle (BOC) was searched.

Flux calculations were mainly performed using the hexagonal-z nodal diffusion theory option of DIF3D [12]. However, the DIF3D nodal option often yields unreliable peak flux values for the fuel assemblies adjacent to control or reflector assemblies because they are determined under the assumption that the neutron flux within each node is separable in axial and radial directions [17]. Therefore, the peak values of flux, power density and fluence were calculated for the finalized designs using the finite-difference option of DIF3D [11]. The kinetics parameters, reactivity coefficients, and shutdown margins were estimated using the VARI3D [18] perturbation theory, DIF3D diffusion, and VARIANT [19] transport codes.

For the parametric studies to determine the assembly design parameters, the thermal margins were evaluated simply by comparing the peak linear power density to the linear power limit. The linear power limits were estimated using a single channel thermal-hydraulics model. The average flow rate was determined such that the coolant temperature rise across the core is 155 °C with assumed coolant inlet temperature of 355 °C. A chopped cosine shape was assumed for the axial power distribution. Hot channel factors for the film, cladding, gap and coolant regions were obtained from the Clinch River Breeder Reactor Plant (CRBRP) homogeneous core design with 3σ confidence level [20]. The linear power limit was determined such that the peak fuel centerline and peak cladding temperatures were lower than the fuel melting and fuel-cladding eutectic temperatures, respectively.

For finalized core designs, reactor orifice zoning and flow allocation were determined through detailed steady-state thermal-hydraulic analyses. Heating rates for thermal-hydraulic calculations were determined by coupled neutron and gamma heating calculations. The SE2-ANL code [21] was employed for whole core temperature calculations. SE2-ANL is a modified version of the SUPERENERGY-2 thermal-hydraulic code [22] interfaced with Argonne heating calculations. Reactor hot spot analysis methods as well as fuel and cladding temperature calculation models were also added to the original version of SUPERENERGY-2. Both nominal and 2-sigma temperatures were calculated for the fuel and cladding.

Orifice zoning of assemblies and flow allocation to the assemblies in each orifice zone were iteratively determined with the overall goal of equalizing the accrual of fuel pin damage and thus pin reliability. The coolant inlet and bulk outlet temperatures were assumed 355°C and 510°C, respectively. The average flow rate was determined such that the coolant temperature rise across the core is 155°C. The fuel assemblies were grouped into several orifice zones, and the assembly flow rates were determined such that the peak 2σ cladding inner-wall temperatures of individual orifice zones over the 18-month cycle are approximately equal to each other. The non-fueled assemblies were grouped into separate orifice zones, and the flow rates were determined in proportion to the heating rates in order to obtain uniform coolant outlet temperatures. Hot channel factors were included in temperature predictions to account for core design, analysis, fabrication and operational uncertainties and variations.

2.4. Reference LEUFBR Core Design

2.4.1. LEUFBR Core Configuration

Scoping studies were performed to develop a LEUFBR core design of 1000 MWt power rating. Starting from a metal fuel core design of 1000 MWt ABR [3,4], a compact core configuration was developed for a 1000 MWt fissile break-even core. Using this core configuration, equilibrium cycle calculations were performed to determine the minimum fuel volume fraction for a fissile break-even core without supporting LEU fuel. Parametric studies were also performed to optimize the cycle length and the number of batches such that the discharge burnup is maximized within the fast fluence limit of HT-9 cladding.

The reference ABR core concepts were developed for effective consumption of TRU elements recovered from light water reactor (LWR) spent fuel [3,4]. Using U-TRU-10Zr ternary metal alloy and mixed oxide fuels, compact core designs of a medium TRU conversion ratio of ~0.7 were developed by trade-off between burnup reactivity loss and TRU conversion ratio. The burnup reactivity loss over a one-year cycle length was constrained to ~ 3.5% Δk in order to achieve a sufficient shutdown margin with a reasonable number of primary control assemblies that could be accommodated in a compact core and to limit a single assembly reactivity fault less than ~0.7$. It was also shown that break-even fissile and TRU conversion ratios could be achieved in metal fuel cores without blanket only by employing different assembly designs [4].

Figure 2.1 shows the radial core layout of the reference 1000 MWt ABR metal core concept. The core is composed of 180 drivers, 114 reflectors, 66 radial shields, and 15 primary and 4 secondary control assemblies. The core was divided into two enrichment zones to flatten the power distribution. The fuel assembly consisted of 271 fuel pins, and the duct outside flat-to-flat distance was 15.71 cm. The fuel volume fraction was 29.2 %, and the active core height was 81.3 cm. The heavy metal inventory at the beginning of equilibrium cycle (BOEC) was ~13.2 metric ton (MT) and the core average TRU fraction in heavy metal (HM) was 22.1 %. The resulting TRU conversion ratio was 0.73 and the TRU consumption rate was ~10 kg/ TWh. The average discharge burnup was determined to be 93 MWd/kg with a peak discharge fast fluence of 4.09×10^{23} /cm^2.

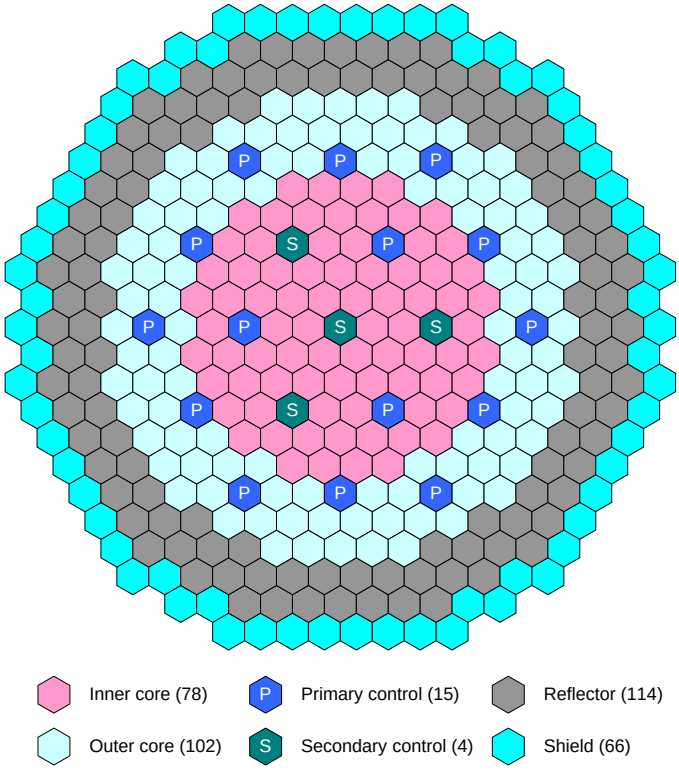

Figure 2.1. Radial Core Layout of Metal Core of Advanced Burner Reactor

As mentioned in Section 2.1, the LEUFBR is designed as a blanket-free core concept. As shown in Reference 4, break-even fissile and TRU conversion ratios can be achieved in metal fuel cores without blanket. A high conversion ratio metal core design of ABR was developed without a blanket by retaining the configuration shown in Figure 2.1 with an increased fuel volume fraction from 29.2% to 34.3% and an increased active core height from 81.3 cm to 96.5 cm. The resulting TRU and fissile conversion ratios were determined to be 1.0 and 0.99, respectively. Compared to the reference ABR metal core design of TRU conversion ratio of 0.73, the TRU fraction in HM was decreased to 14.4% from 22.1%, but the HM loading was increased to 18.5 MT from 13.2 MT. The increase in HM loading reduced the average discharge burnup from 93 MWd/kg to 67 MWd/kg. Additionally, the burnup reactivity swing for a one-year cycle length (with 90% capacity factor) was reduced to 0.14% Δk from 2.2% Δk.

Although the LEUFBR core design starts with LEU fuel and thus the fuel composition is different from that of ABR, these results suggest that a fissile break-even core (at least at the equilibrium cycle with Pu recycling) can be obtained by relatively minor modifications of the high TRU conversion ratio metal core design of ABR. To increase the fissile conversion ratio, it is necessary to lower the core average fissile enrichment. In order to maintain the criticality with low fissile enrichment fuel, it is necessary to increase the fuel loading, which in turn requires increasing the active core volume and/or the fuel volume fraction in each fuel assembly. To increase the fuel loading, it was decided to increase the active core volume by increasing the active core height while maintaining the compact core configuration and the radial dimensions of fuel assemblies in the ABR. A significant decrease in the burnup reactivity swing of LEUFBR relative to ABR results in a reduction in the core control requirement.

Therefore, it was also decided to replace some of the control assemblies with fuel assemblies. Finally, the fuel volume fraction in fuel assemblies was increased by increasing the fuel pin size within the imposed thermal design limits.

The increased active core height reduces the total flux level (for the same power rating) and thus allows a longer fuel residence time within the fast fluence limit of HT-9. On the other hand, the sodium void worth becomes more positive and the pressure drop across the core increases. In order to increase the fuel loading without affecting the sodium void worth noticeably, the active core height of the fissile break-even core was only slightly increased to 100 cm (from 96.5 cm of the high TRU conversion ABR core design) for the U-Pu-10Zr ternary fuel with recycled Pu. The active core was only increased to 97.2 cm for the initial U-10Zr loading to accommodate the higher axial irradiation swelling.

The ABR was designed to be operated for a wide range of TRU conversion ratios, so the number of control assemblies was determined to provide a sufficient shutdown margin for a low TRU conversion ratio core design with a burnup reactivity loss of 3.5% Δk. The worth of 14 primary control assemblies excluding the most reactive assembly was 17.5% Δk [23]. The estimated reactivity control requirement for the low TRU conversion ratio core design was determined to be ~5.1% Δk including the burnup reactivity loss. It was expected that the burnup reactivity swing of the LEUFBR would be similar to that of the high conversion ratio ABR, so the reactivity control requirement was estimated to be ~1.8% Δk. Therefore, the number of primary control assemblies was reduced from 15 to 9 by replacing the six control assemblies in the seventh row of hexagon with fuel assemblies, as shown in Figure 2.2.

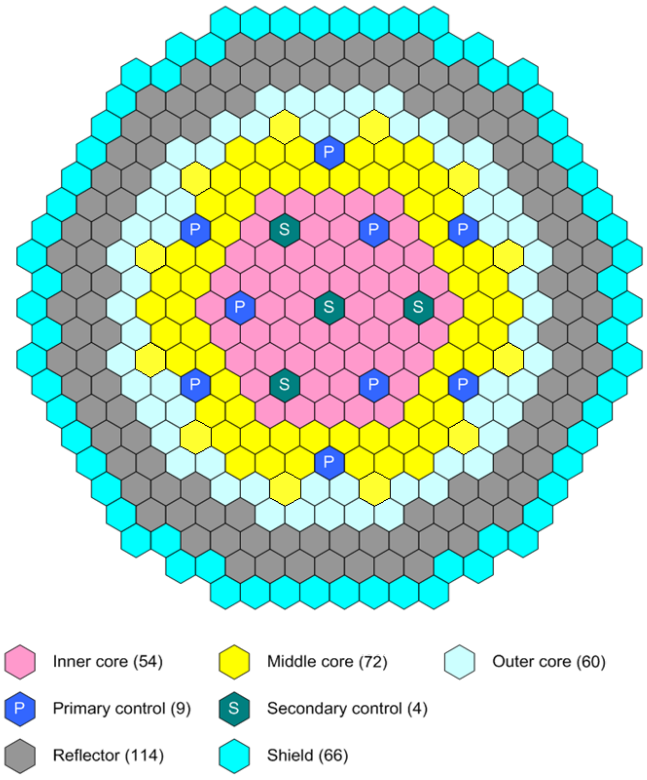

Figure 2.2. Radial Core Layout of LEU-Fueled Fissile Break-Even Reactor (LEUFBR)

Figure 2.2 shows the radial core layout of the 1000 MWt LEUFBR core concept. The core is composed of 186 drivers, 114 reflectors, 66 radial shields, and 9 primary and 4 secondary control assemblies. The core is divided into three enrichment zones (i.e., inner, middle and outer cores) to flatten the power distribution. The primary control system consists of three assemblies in the fourth row of hexagon and six assemblies in the seventh row, and the secondary control system consists of one central assembly and three assemblies in the fourth row. The core is surrounded by two rows of steel reflectors and one row of B_4C shield assemblies.

2.4.2. Region-Dependent Multi-group Cross Section Generation

Using the core configuration shown in Figure 2.2, region-dependent 33-group cross sections were generated based on the ENDF/B-VII.0 cross section library with the MC^2-3 code [14]. The material compositions required for multi-group cross section generation were not initially known at the beginning of analysis, and thus the multi-group cross sections were generated in two steps. In the first step, preliminary design studies were performed using the 21-group cross section set (based on the ENDF/B-V.2 library) used in ABR design studies. A parametric study based on equilibrium cycle analyses suggested that a fuel volume fraction of 35.3% would be a feasible fuel volume fractions that yield a fissile conversion ratio larger than 1.0 while satisfying the imposed thermal design constraints. Using this fuel volume fraction, REBUS-3 equilibrium cycle calculations were performed for a hexagonal-z model of the LEUFBR core configuration discussed in Section 2.4.1. The fraction of Pu in the HM was searched with recycling of Pu to yield an 18-month cycle length with 90% capacity factor.

Using the resulting nuclide densities, a cylindrical-z core model was developed as shown in Figure 2.3. The core was divided into three regions, and the homogenized nuclide densities of each region were determined by the average values of the corresponding densities at the beginning of equilibrium cycle (BOEC) and at the end of equilibrium cycle (EOEC). The nuclide densities of fission products were determined by multiplying the lumped fission product densities by the corresponding fission yield data of each fissionable isotope in the ENDF/B-VII data. For the reflector and shield regions, the ABR designs were adopted and the ABR nuclide densities were used.

In the second step, region-dependent 33-group cross sections were generated using the MC^2-3 code [14]. In this MC^2-3 calculation, self-shielded 2082-group isotopic cross sections were first prepared for each region by numerical integration of the pointwise cross sections based upon the narrow resonance approximation. Then, a 2082-group transport calculation was conducted for the whole-core model shown in Figure 2.3 using the discrete ordinate transport code TWODANT [24]. Finally, region-dependent 33-group cross sections were determined by condensing the 2082-group cross sections of each region using the 2082-group TWODANT flux solution. The fission products were modeled using fissionable-isotope-dependent lumped fission products. Lumped fission product cross sections were generated for U-235, U-238, Np-237, Pu-238, Pu-239, Pu-240, Pu-241, Pu-242, Am-241, Am-243, and Cm-244 using the fission product yield data of ENDF/B-VII.0. In order to account the fraction of rare-earth fission products carried over by the recycled fuel in the assumed pyroprocessing, region-dependent multi-group cross sections were separately generated for rare-earth fission products.

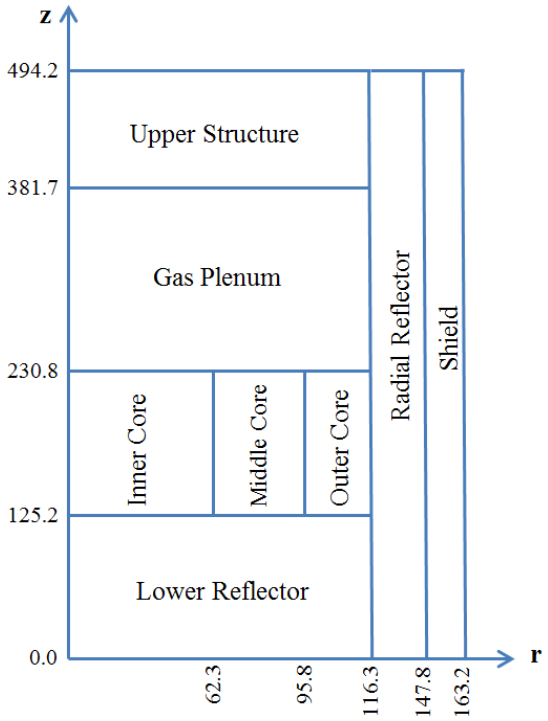

Figure 2.3. Cylindrical-z Model of 1000 MWt LEUFBR Core Design

2.4.3. Scoping Equilibrium Cycle Analyses and Fuel Assembly Designs

Using the LEUFBR core configuration depicted in Figure 2.2 and the cross section set discussed in Section 2.4.2, scoping studies based on equilibrium cycle analyses were performed to determine the minimum fuel volume fraction to achieve a fissile break-even core without supporting LEU fuel. In order to facilitate the design optimization to achieve a high discharge burnup as well as a high fissile conversion ratio, an optimum fuel management scheme was also investigated to maximize the discharge burnup within the fast fluence limit of HT-9 cladding.

Parametric studies were performed by varying the cycle length and the number of batches. To minimize fluctuations of system performance characteristics, cycle-to-cycle variations in the number of replaced assemblies in each core zone should be minimized. Accordingly, the number of batches was determined such that the number of assemblies in each core zone equal to an integer multiple of the corresponding number of fuel batches. In order to maximize the average discharge burnup, one additional batch was used in the outer core zone where the flux level is significantly lower than in the inner and middle core zones. A three-batch fuel management scheme was used for the inner and middle core zones, and a four-batch scheme was used in the outer core zone. A fuel cycle length of eighteen months with a 90% capacity factor was determined such that the peak fast fluence is maximized within the HT-9 irradiation limit.

Using these cycle length and fuel management schemes, parametric studies were carried out to determine the minimum fuel volume fraction to achieve a fissile conversion ratio slightly greater than 1.0. By performing the REBUS-3 equilibrium cycle analyses with different fuel volume fractions, the U-235 and Pu fraction in HM (i.e., Pu fraction in the equilibrium cycle)

to maintain the criticality throughout the cycle duration and the fissile conversion ratio were calculated as a function of fuel volume fraction. In this core of a conversion ratio greater than 1.0, the reactivity increases with time, so the Pu enrichment of fresh fuel was determined such that the multiplication factor at BOEC is 1.003.

Figure 2.4 shows the Pu fraction in HM required to achieve the criticality at BOEC and the resulting fissile conversion ratio as a function of the fuel volume fraction. As expected, the required Pu fraction at BOEC decreases as the fuel volume fraction increases, and thus the fissile conversion ratio increases. It can be seen that to achieve a fissile conversion ratio greater than 1.0 for the specified fuel management scheme, the fuel volume fraction should be greater than 35.3%.

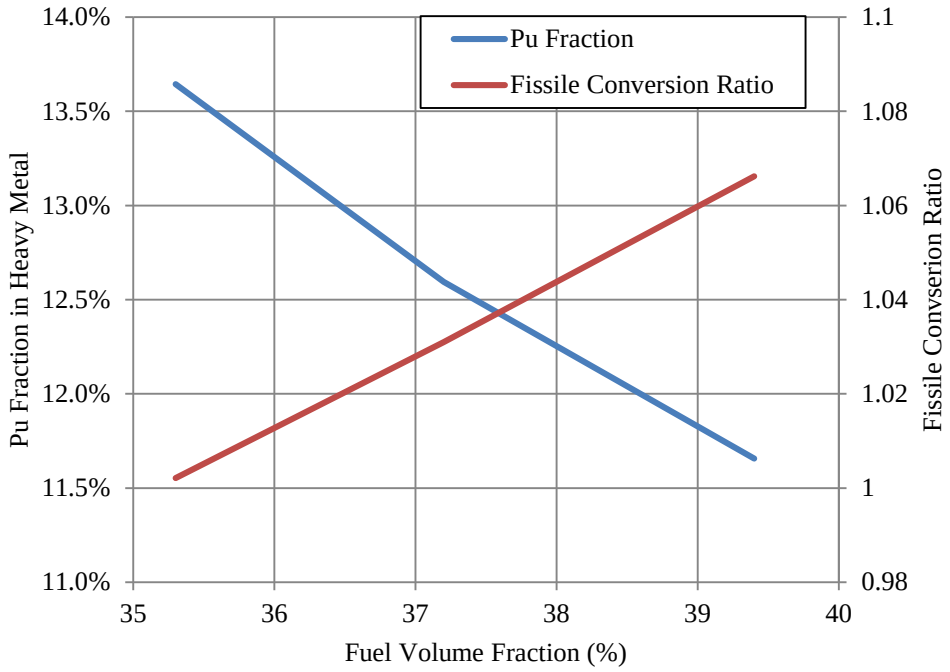

Figure 2.4. Pu Fraction in Heavy Metal and Conversion Ratio vs. Fuel Volume Fraction

Assembly design studies were conducted using the REBUS-3 equilibrium cycle option to determine the maximum fuel volume fraction achievable with fixed assembly dimensions based on the ABR design. In this study, various fuel volume fractions were obtained by varying the number of fuel pins and the fuel pin diameter. In order to increase the fuel volume fraction for fixed assembly dimension and cladding thickness, the pin diameter should be increased, which in turn reduces the number of fuel pins. As a result, the average and peak linear powers increase with increasing fuel volume fraction. Therefore, the fuel volume fraction should be limited to satisfy the thermal design criteria imposed on the fuel centerline and cladding inner wall temperatures.

In order to estimate the upper limit for fuel volume fraction, a single channel thermal-hydraulics analysis was conducted. The single channel thermal-hydraulics model used an assembly pitch of 16.14 cm, a duct outside flat-to-flat distance of 15.74 cm, and a cladding

thickness of 0.05 cm. A smeared fuel density of 75% was used, and the initial thermal bond between the fuel column and the cladding was sodium. The coolant inlet and bulk outlet temperatures were assumed 355 °C and 510 °C, respectively. The average flow rate was determined such that the coolant temperature rise across the core is 155 °C. A chopped cosine shape was assumed for the axial power distribution and hot channel factors of 2.67, 1.10 and 1.24 were used for the film, cladding and coolant temperature rises, respectively [25].

Table 2.1 shows the selected core performance parameters of LEUFBR along with the assembly design parameters for two candidates for fuel assembly design. The volume faction was increased from Case 1 to Case 2 by increasing the fuel pin diameter and reducing the number of pins, while retaining the assembly duct dimensions and cladding thickness of ABR. The fuel pin diameter was increased from 8.9 mm to 10.5 mm and the number of fuel pins was reduced from 217 to 169. Consequently, the fuel volume fraction was increased from 35.3% to 39.4%.

Table 2.1. Core Performance Characteristics of LEUFBR for Two Fuel Assembly Designs

	Case 1	Case 2
Core height, cm	100	100
Assembly lattice pitch, cm	16.14	16.14
Inter-assembly gap, mm	4.0	4.0
Duct thickness, mm	3.0	3.0
Number of fuel pins per assembly	217	169
Pin outer diameter, mm	8.9	10.5
Cladding thickness, mm	0.5	0.5
Wire-wrap diameter, mm	1.00	1.00
Pin pitch-to-diameter ratio	1.14	1.10
Material volume fraction, % - Fuel - Bond sodium - Structure - Coolant	 35.3 11.8 20.5 32.4	 39.4 13.1 19.4 28.1
Pressure drop, MPa	0.31	0.46
Equilibrium cycle fissile conversion ratio	1.01	1.07
Average linear power, kW/m	22.7	29.2
Peak linear power (PLP), kW/m	36.2	45.4
PLP limit (cladding inner-wall temp.), kW/m	37.7	46.5
PLP limit (fuel centerline temp.), kW/m	56.1	62.6

In Table 2.1, the peak linear power deduced from the peak power density of REBUS-3 calculation is compared with the two limiting values of the peak linear power estimated based on the limit on the cladding inner-wall temperature (i.e., 650 °C limit determined from fuel-

cladding eutectic melting) and the limit on the fuel centerline temperature (i.e., fuel solidus temperature). It can be seen that the peak linear power limit estimated based on the cladding inner-wall temperature is significantly lower than that based on the limit on the fuel centerline temperature. As the fuel volume fraction increases, the Pu fraction required to achieve the criticality decreases, and thus the thermal conductivity and solidus temperature of the U-Pu-10Zr ternary fuel increase. As a result, the peak linear power limit increases with the fuel volume fraction. The peak linear power limit based on the fuel cladding eutectic temperature also increases with increasing fuel volume fraction since for a fixed thickness the thermal resistance of cladding decreases with increasing pin diameter. Table 2.1 shows that the minimum fuel volume fraction to achieve a fissile break-even core with external feed of depleted uranium would be 35.3% (Case 1). By increasing the fuel pin diameter and reducing the number of fuel pins per assembly, a maximum fuel volume fraction of 39.4% (Case 2) could be attained while staying the imposed thermal design constraints.

2.4.4. Transition Cycle Performance of Reference LEUFBR Design

The results of equilibrium cycle analyses discussed in Section 2.4.3 showed that in an equilibrium cycle, a LEUFBR with a fuel volume fraction in the range from 35.3% to 39.4% could be operated with recovered plutonium only without supporting LEU fuel while satisfying the imposed thermal design constraints. However, the LEUFBR starts with LEU fuel and thus it would take a long time to reach an equilibrium cycle by building sufficient plutonium. This necessitates the cycle-by-cycle evaluation of transitional cores starting from the initial LEU core. Using the assembly designs discussed in Section 2.4.3, cycle-by-cycle calculations were performed for an assumed plant lifetime of 60 years using the non-equilibrium cycle option of the REBUS-3 code. The cycle-by-cycle calculations were carried out with two sets of cross section data: the cross section set of uranium core was used for cycles 1 through 8 and that of Pu core was used for cycles 9 through 40. Based on the results of these analyses, a reference core design of LEUFBR was developed by the trade-off of external LEU fuel requirement and surplus plutonium buildup.

The initial core of LEUFBR is loaded with LEU fuel. Pu and uranium are co-extracted from the discharged fuel and recycled in the core. It was assumed that 0.1% of fuel is lost in reprocessing/re-fabrication and 5% of rare-earth fission products are carried over by the recycled fuel. Minor actinides are accumulated for the future use in ADS. Since a long cooling time is not required, the turnaround time of the assumed pyroprocessing of metal fuel is relatively short (e.g., the average turnaround time in EBR-II was about two months from discharge to reload into the reactor). So it was assumed that the recovered uranium and Pu from the discharged fuel at the end of n-th cycle can be reloaded into the reactor at the beginning of (n+2)-th cycle. In the fresh fuel fabrication model of REBUS-3, the recovered uranium and Pu were used as the primary feed and the external LEU fuel was used as the makeup feed. That is, if the recovered fuel was not sufficient, the external LEU fuel was added to fabricate the required amount of fresh fuel. On the other hand, if the recovered fuel was more than necessary, the surplus was accumulated for the use in the later cycles. Even in this case, however, depleted uranium is required to compensate for the consumed HM. For the first two-cycles, the fresh fuel was fabricated using the external LEU fuel.

The function of feed enrichment search for partial reloading in REBUS-3 has been improved in this work to implement a wide range of fuel management strategies. Details of the modified search algorithm are discussed in Appendix A, and the associated modifications in the TYPE 03, 35 and 46 cards of the input dataset A.BURN are presented in Appendix B. For each cycle, the fraction of LEU (with enrichment of 20 wt. %) and Pu in heavy metal (defined as the enrichment in REBUS-3) required to maintain the criticality was searched for a fixed fuel management scheme. A fixed cycle length of 18 months with 90% capacity factor was used with a three-batch fuel management scheme for the inner and middle core zones and a four-batch scheme for the outer core zone. The numbers of assemblies in the inner, middle and outer core zones were selected to be 54, 72, and 60, respectively, so that the number of assemblies in each zone becomes an integer multiple of the number of fuel batches in that region. The enrichment zoning strategy was employed to flatten the power distribution. The enrichment splits among zones varied slightly over cycles, but no attempt was made to optimize the splits.

For initial fissile-burning cycles where the k-effective value decreases with time, the critical enrichment was searched at EOC. On the other hand, for later fissile-breeding cycles where the k-effective value increases with burnup, the critical enrichment was searched at BOC. In order to accommodate the computational modeling and fabrication uncertainties, the criticality was estimated with a k-effective value of 1.003. In the initial uranium cores, the fuel assembly design of Case 2 in Table 2.1 with a fuel volume fraction of 39.4% was employed in order to maximize the natural resource utilization by maximizing Pu production within the imposed thermal design limits. When the core becomes close to the equilibrium-cycle Pu core, the fuel assembly design of Case 2 was replaced by the fuel assembly design of Case 1 in Table 2.1 to reduce the surplus Pu buildup. Specifically, from the cycle 21 that is a middle of life (MOL) core, the fresh fuels were made of the fuel assembly design of Case 1.

Figure 2.5 presents the external uranium feeds (depleted and low enriched) and the fissile conversion ratio as a function of burnup cycle. The fissile conversion ratio was initially 0.67 for the uranium-fueled core and increases monotonically with burn cycles. From the cycle 3, the external LEU feed had a decreasing trend and at the cycle 14, the core reached a fissile break-even point. At this point, the British breeding gain [20], which accounts for the difference in the reactivity value of different nuclides, becomes slightly greater than zero and thus the core becomes fissile-self-sustaining although the conventional fissile conversion ratio is slightly less than one. This is because of the higher reactivity worth of produced Pu-239 than that of destroyed U-235. For the succeeding cycles, the required fresh fuel was fabricated from the recycled U and Pu and the external feed of depleted uranium. As can be seen in Figure 2.5, in the MOL, it took some time for the core to reach the equilibrium state with the new fuel assembly design. The fissile conversion ratio decreased due to the use of the fuel assembly design with a smaller fuel volume fraction. In this transition period, the surplus Pu over the cycles 14 through 20 was used as the external feed to maintain the criticality in the subsequent burn cycles. In addition to the Pu fuel, the external feed of depleted uranium was required to compensate for the consumed HM and it remained almost constant from the cycle 27 to the end of life (EOL) with an average of 520 kg per cycle.

Figure 2.6 shows the U and Pu fissile mass flows during the 60 years of operation. The core inventory of U-235 at the first cycle was at a maximum of 3088 kg and decreased with burn cycles. On the other hand, the Pu generation during the first cycle was at a maximum of 333 kg

and the core inventory of Pu increased with burnup cycles. From the cycle 24 until EOL, the core inventory of Pu fissile materials (Pu-239 and Pu-241) is near the equilibrium state with an average of 2002 kg. After a 60-year transition period, a plutonium core was achieved from the initial LEU core.

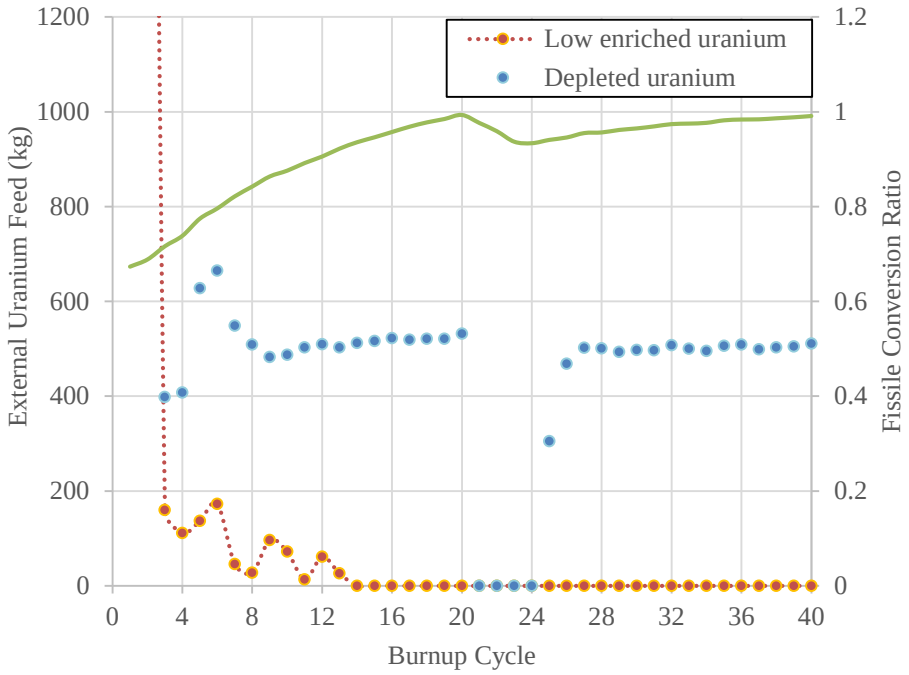

Figure 2.5. External Uranium Feed vs. Burn Cycle of Reference LEUFBR Core

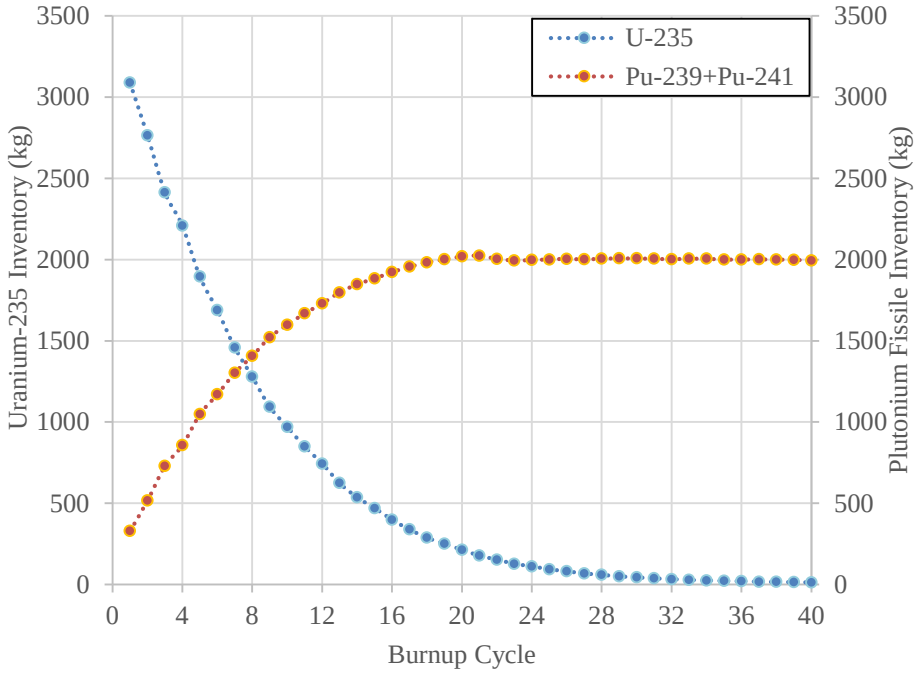

Figure 2.6. U-235 and Pu Fissile Mass Flow vs. Burn Cycle of Reference LEUFBR Core

Table 2.2 summarizes the performance parameters of the LEUFBR core. At the beginning of life (BOL), the core is loaded with LEU fuel of 13.6% enrichment. The fissile conversion ratio is initially 0.67 and gradually increases with operating cycles. It reaches a fissile break-even point at the 14-th cycle. For a 60-year operation time, the total natural uranium requirement (with an enrichment tail of 0.2%) is 814.3 MT, which is about one-fifth of that for a typical pressurized water reactor (PWR) with same amount of electricity generation. The total Pu inventory at EOL 3665 kg, including the surplus Pu of 92.5 kg accumulated over the cycles 1 through 38, the unprocessed Pu of 828 kg in the discharged fuel at the end of the cycle 39, and the core inventory of 2745 kg at the end of the plant lifetime. The total amount of accumulated MAs is 533 kg. These Pu and MAs inventories at EOL can be used to start a new FR or in an ADS.

Table 2.2. Fuel Cycle Performance Parameters of the LEUFBR Core

U-235 mass fraction at BOL HM inventory, %	13.6
Core inventory of LEU at BOL, MT	15.5
Core inventory of depleted U at BOL, MT	7.2
Fissile conversion ratio at BOL	0.67
Natural U resource required for 60 years, MT	814.3
Surplus Pu over cycle 1-38, kg	92.5
Discharged Pu at cycle 39, kg	827.8
Remaining Pu inventory at cycle 40, kg	2745.0
Accumulated Pu for 60 years, MT	3.7
Accumulated MAs over 60 years, kg	533

2.4.5. Kinetics Parameters and Reactivity Coefficients

Kinetics Parameters and reactivity coefficients were estimated using the VARI3D [18] perturbation theory code, the DIF3D [11,12] diffusion theory code, and the VARIANT [19] transport theory code. The kinetics parameters and reactivity coefficients were calculated for the uranium and Pu core configurations. Reactivity coefficients of uranium and Pu cores were evaluated at the third cycle and the equilibrium cycle, respectively. The primary control assemblies were located at the critical positions, while the secondary control assemblies were positioned at the top of the active core. The critical position of control rod tip from the bottom of the active core was estimated to be 87.0 cm for the uranium core and 82.0 cm for the Pu core.

Table 2.3 summarizes the calculated reactivity coefficients and kinetic parameters. The effective delayed neutron fraction (β_{eff}) and the prompt neutron lifetime were evaluated using the VARI3D perturbation theory code. The delayed neutron fraction is 0.00630 for the uranium core and 0.00357 for the Pu core. The prompt neutron lifetime is ~0.36 μs for the uranium core and ~0.34 μs for the Pu core. The axial and radial expansion coefficients were calculated using the DIF3D code by direct eigenvalue differencing between the base and perturbed cases. The uniform radial expansion coefficient increases to -0.22 ¢/°C from -0.11 ¢/°C and the axial expansion coefficient goes from -0.04 ¢/°C to -0.08 ¢/°C from the uranium core to the Pu core.

Compared to the ABR reference design, the radial expansion coefficient becomes less negative in the Pu core (-0.22 ¢/°C vs. -0.38 ¢/°C) due to reduced axial leakage because of an increased core height. The axial expansion coefficient is comparable to ABR core because a similar radial core layout was used. From these results, it is seen that the negative reactivity effect from the core expansion is more significant in the radial direction than in the axial direction.

Table 2.3. Kinetic Parameters and Reactivity Coefficients

Parameter		Uranium Core	Pu Core	ABR Startup
Delayed neutron fraction, β_{eff}		0.00630	0.00357	0.00334
Prompt neutron lifetime	μs	0.36	0.34	0.38
Axial expansion coefficient	¢/°C	-0.04	-0.08	-0.05
Radial expansion coefficient	¢/°C	-0.11	-0.22	-0.38
Fuel density coefficient	¢/°C	-0.32	-0.54	-0.67
Structure density coefficient	¢/°C	0.02	0.05	0.06
Sodium void worth	$	0.47	5.79	4.93
Sodium density coefficient	¢/°C	0.0017	0.029	0.13
Doppler coefficient	¢/°C	-0.08	-0.15	-0.12
Sodium-voided Doppler coefficient	¢/°C	-0.06	-0.09	-0.09

The Doppler coefficient along with the fuel, structure, and sodium density coefficients were estimated using the VARI3D perturbation theory code. The Doppler coefficient was evaluated by increasing the temperature of the fuel, structure, and coolant isotopes in the active core region. The fuel, structure, and sodium density coefficients were evaluated by perturbing the material densities by factors of 1.10, 1.25, and 0.85, respectively. The Doppler and fuel density coefficients are significantly more negative in the Pu core. The small positive sodium and structure density coefficients are also larger in the Pu core than in the U core.

The sodium void worth and sodium-voided Doppler coefficients were calculated using the VARIANT transport code through direct eigenvalue differencing. When estimating these coefficients, the flowing sodium coolant in the active core, upper gas plenum, and upper internal structure was completely voided. It is noteworthy that the exact perturbation theory option of VARI3D based on the diffusion theory was initially used, but upon further analysis, it was discovered that the diffusion theory overestimates the neutron leakage from the sodium-voided cores, and in turn, underestimates the sodium void worths. In the case of the uranium core, the VARI3D result showed a small negative value for the sodium void worth. The sodium void worth for uranium and Pu cores were determined to be 0.47 $ and 5.79$, respectively. It is noted that the sodium void worth in uranium core is significantly smaller than that in the Pu and ABR cores. This can be attributed to the fact that the spectrum hardening due to sodium voiding increases the reproduction factor η of Pu-239 significantly more than that of U-235. A neutron balance comparison also shows that the leakage effect during sodium voiding is similar between the uranium and Pu cores. A comparison of the Doppler coefficient shows that negative feedback is enhanced at further stages in the reactor lifetime with an initial coefficient of -0.08 ¢/°C and a final coefficient of -0.15 ¢/°C. If the flowing sodium within the active core is voided,

the negative Doppler feedback becomes less effective due to spectral hardening and reduced resonance absorption. This change between the Doppler coefficient and the sodium-voided Doppler coefficient is larger in Pu core than in uranium core mainly because of plutonium's larger reproduction factor η.

Using the reactivity coefficients in Table 2.3, the integral reactivity parameters [8,9] for a quasi-static reactivity balance were evaluated for the uranium and Pu cores and given in Table 2.4. For these calculations, the temperature was estimated with the assumed coolant inlet temperature of 355 °C, core-averaged coolant temperature of 433 °C, and core-averaged fuel temperature of 558 °C as well as the assumed refueling temperature of 205 °C. The asymptotic state of the core after the external perturbation is estimated by solving the quasi-static reactivity balance equation. The quasi-static reactivity for the new asymptotic stage can be denoted as the sum of the reactivity changes due to the variations in power, flow rate, coolant inlet temperature and the external reactivity insertion. The sufficient conditions for a stable reactor to reach a new asymptotic state for possible accident scenarios (unprotected transient overpower (TOP), unprotected loss of heat sink, unprotected loss of flow, chilled inlet and pump over-speed) are:

$$A/B \le 1, \quad 1 \le C\Delta T_c \le 2, \quad \Delta\rho_{TOP}/|B| \le 1$$

The integral parameters A, B, and C are different combinations of the reactivity feedback coefficients. The parameter A represents the reactivity decrement due to the average fuel temperature increase from the coolant average temperature, and it contains the Doppler and axial expansion effects. The parameter B accounts the reactivity decrement due to the coolant and fuel temperature rise from the zero-power isothermal condition at the coolant inlet temperature to the coolant average temperature. It contains the reactivity changes due to the Doppler effects, axial and radial expansion, sodium density change, and control rod driveline expansion. The inlet temperature parameter, C, is the sum of the Doppler coefficient, axial and radial expansion coefficients and sodium density coefficient.

For both the uranium and Pu core, the calculated values of A/B, $C\Delta T_c/B$ and $\Delta\rho_{TOP}/|B|$ satisfy the sufficient conditions for passive shutdown. After an external perturbation, both cores can reach a new asymptotic state after natural adjustment of the core power and temperature due to thermal feedbacks.

Table 2.4. Integral Reactivity Parameters for Quasi-Static Reactivity Balance

Parameter		Uranium Core	Pu Core
A, net reactivity decrement	¢	-10.5	-18.6
B, power/flow coefficient	¢	-12.9	-25.0
C, inlet temperature coefficient	¢/°C	-0.23	-0.42
Transient overpower initiator, $\Delta\rho_{TOP}$	¢/°C	0.12	0.20
A/B		0.81	0.74
$C\Delta T_c/B$		1.35	1.31
$\Delta\rho_{TOP}/\|B\|$		0.009	0.008

2.4.6. Reactivity Control Requirements and Shutdown Margins

The control requirements and shutdown margins were also estimated for the primary and secondary control systems. By definition, the primary system is required to shut down the reactor from any operating condition to the refueling temperature, with the assumption that the most reactive control assembly is stuck. Any operating condition includes an overpower condition combined with a reactivity fault. The primary system also serves to compensate for the reactivity effects of the fuel burnup and axial growth of metal fuel, and in addition, must accommodate any uncertainties in criticality and/or fissile loading during refueling. The secondary system is also required to have sufficient negative reactivity to shut down the reactor from any operating condition to the cold shutdown with the most reactive assembly inoperative.

Reactivity control requirements of uranium and Pu cores were evaluated at the third and equilibrium cycles. The third cycle of uranium core was selected because it has the maximum burnup reactivity swing among the transition cycles. To estimate the control requirements and shutdown margins, the reactivity worth was calculated for various combinations of control assemblies inserted, and the stuck-assembly worth was estimated for each control assembly. Table 2.5 presents the calculated control assembly worth for various combinations of control assemblies.

Table 2.5. Control Assembly Worth ($)

	Inserted assemblies	Uranium Core	Pu Core
Primary system			
- All assemblies	9	17.8	20.5
- All assemblies except one in 4th row	8	14.4	17.0
- All assemblies except one in 7th row	8	14.1	17.4
- All assemblies except one in 4th and one in 7th row	7	12.4	14.9
Secondary system			
- All assemblies	4	5.4	9.8
- All assemblies except central one	3	4.3	7.8
- All assemblies except one in 4th row	3	3.9	7.0
One stuck assembly worth			
- Most reactive primary assembly		3.7	3.1
- Most reactive secondary assembly		1.5	2.1

Figure 2.7 and Figure 2.8 show the primary system reactivity worth curves for the uranium and Pu cores, respectively. The dashed curve denotes the core reactivity as a function of the tip position of control rods from the bottom of active core for the case where all the primary control assemblies are moving together. The critical positions of primary control assemblies are indicated by the dashed vertical lines, and the solid curve represents the reactivity worth of the most reactive control assembly, which is one of the seventh row assemblies. The reactivity

insertion by the complete withdrawal of the most reactive control assembly from its critical position (maximum single rod fault) for uranium and Pu cores are ~0.12$ and ~0.20$, respectively.

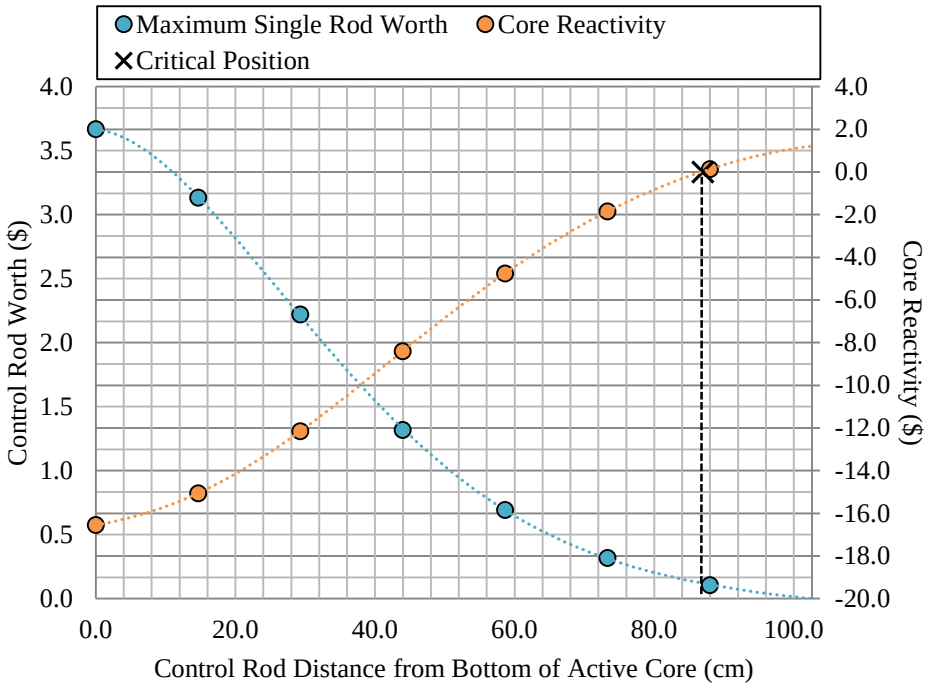

Figure 2.7. Reactivity Worth of Primary Control System of Uranium Core

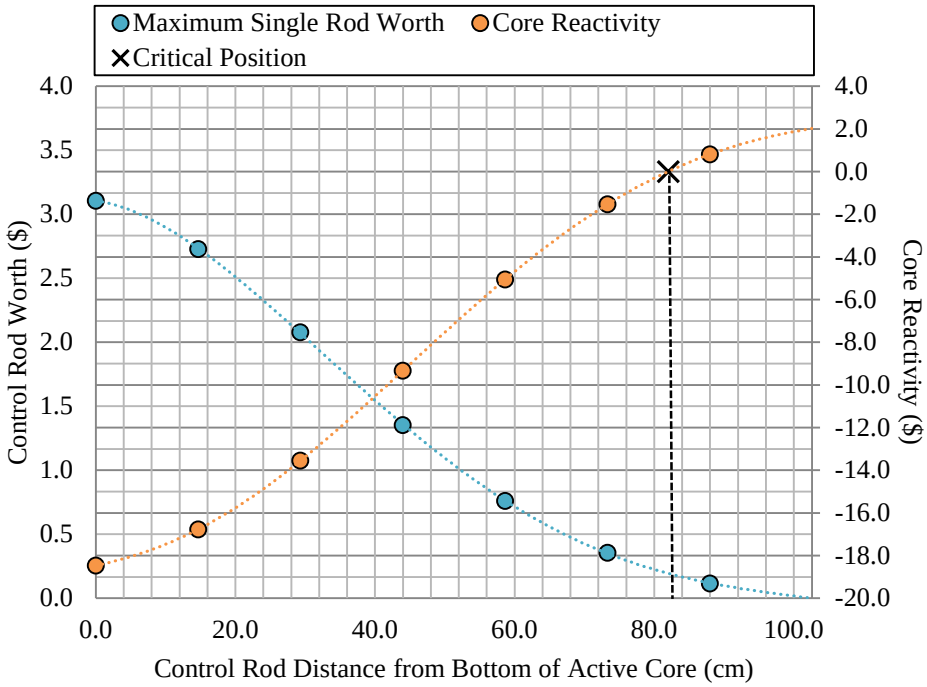

Figure 2.8. Reactivity Worth of Primary Control System of Pu Core

The control requirements for uranium and Pu cores were evaluated by accounting for the temperature and power defects, including overpower, the reactivity swing and the associated uncertainties. The temperature and power defects were estimated with the assumed coolant inlet temperature of 355 °C and assumed refueling temperature of 205 °C. Table 2.6 presents the temperature and power defects calculated with the reactivity coefficients in Table 2.3. Table 2.7 and 2.8 show the reactivity worth requirements and the available reactivity worths of the primary and secondary control systems of the uranium and Pu cores. Uncertainties include 15% overpower margin, 20% uncertainty for temperature defect, 20% uncertainty for burnup reactivity, and 1.0$ uncertainty for each of the critical prediction, fissile loading, and refueling.

The estimated total control requirement for primary control system is about 3.4$ in the uranium core and 4.2$ in the Pu core. The total control requirement for the secondary control systems is about 0.9$ in the uranium core and 1.7$ in the Pu core. The shutdown margins of the primary and secondary control systems were determined with the assumption that the most reactive assembly is stuck. The minimum shutdown margins of the primary system for the uranium and Pu cores are ~10.7$ and ~13.2$, respectively. The minimum shutdown margins of the secondary system for the uranium and Pu cores are ~3.0$ and ~6.1$, respectively.

Table 2.6. Temperature and Power Defects ($)

	Uranium Core	Pu Core
Hot full power to hot standby		
Doppler	0.17	0.30
Axial expansion	0.07	0.17
Radial expansion	0.22	0.45
Sodium density	0.00	-0.02
Total	**0.46**	**0.90**
Hot standby to refueling		
Doppler	0.13	0.22
Axial expansion	0.05	0.12
Radial expansion	0.16	0.33
Sodium density	0.00	-0.04
Total	**0.34**	**0.63**

Table 2.7. Shutdown Margin of Primary Control System ($)

	Uranium Core	Pu Core
Number of control assemblies	9	9
Total worth	17.8	20.5
Worth with one stuck assembly	**14.1**	**17.4**
Reactivity control requirement	**3.43**	**4.19**
- Temperature defect	0.80	1.53
HFP to hot standby	0.46	0.60
Hot standby to refueling	0.34	0.63
- Burnup reactivity loss	0.70	0.57
- Overpower (15%)	0.07	0.13
- Reactivity fault	0.12	0.20
- Uncertainties (RMS)	1.74	1.76
Temperature defect (20%)	0.16	0.31
Burnup reactivity (20%)	0.14	0.11
Criticality prediction	1.00	1.00
Fissile loading	1.00	1.00
Refueling	1.00	1.00
Shutdown margin	**10.7**	**13.2**

Table 2.8. Shutdown Margin of Secondary Control System ($)

	Uranium Core	Pu Core
Number of control assemblies	4	4
Total worth	5.4	9.8
Worth with one stuck assembly	**3.9**	**7.8**
Control requirement	**0.9**	**1.7**
- Power defect	0.46	0.90
- Temperature defect	0.34	0.63
- Overpower (15%)	0.07	0.13
Shutdown margin	**3.0**	**6.1**

3. Scoping Design Study of Sodium-Cooled Accelerator Driven System

In order to investigate the proposed two-stage fuel cycle options, a scoping design study was performed to develop an accelerator driven system (ADS). The main purpose of the proposed ADS system is to facilitate waste management by separating out MA elements from the spent FR fuels of the first-stage and transmuting these constituents in the ADS blanket. The design goal is to maximize the MA destruction per unit energy production (kg/GWe-yr) within the reasonable design constraints based on the current (or expected in near future) irradiation experience of the fuel and structural materials. A design study was built based on previous analyses for the sodium-cooled accelerator driven system with inert matrix minor actinides fuel [26] and the 840 MWt Accelerator Transmutation of Waste (ATW) blanket designs with lead-bismuth eutectic (LBE) and sodium coolants [5,27-30]. Similar design objectives and analysis techniques were utilized in this work.

The major assumptions made in developing the ADS system design are similar to those employed in the ATW roadmap [31]; they can be summarized as follows:

1. A high-power linear accelerator generates a beam of energetic (~1 GeV) protons. The spallation neutrons are produced by bombarding a target with intense proton beams that drive the subcritical blanket.
2. Beam delivery to the target is in the vertical direction; the target material is liquid LBE. A window cooled by the same LBE coolant is employed to separate the vacuum of the beam transport tube and the target.
3. The blanket is fueled with solid, uranium-free fuel and a low-swelling HT-9 stainless steel alloy cladding developed in the U.S. Advanced Liquid Metal Reactor (ALMR) Program [7,32].
4. Similar to the zirconium matrix TRU-dispersion fuel [33] used in the previous ATW studies, a metallic dispersion fuel form comprised of MA-10Zr alloy particles dispersed in Zr matrix is assumed. Extensive experience with U-10Zr and U-Pu-10Zr fuels in the EBR-II fuel development program demonstrated the comparability of similar fuel forms with sodium coolant.
5. The fission power level of each transmuter module is 840 MWt – consistent with the ALMR power level selected based on favorable economics (through modular fabrication and installation) and excellent safety (passive removal of decay heat using ambient air as an inexhaustible heat sink).

3.1. ADS Core Concept

The idea of combining an accelerator with a subcritical reactor for transmuting MAs has already been considered in several countries, such as Japan, France, and U.S. The accelerator produces large numbers of neutrons by impinging the proton beam onto the target in a process called spallation. The spallation neutrons then penetrate the target and the surrounding subcritical core. A self-sustaining system can be achieved with spallation neutrons by sustaining the desired fission power level and thus, the losses of neutron in the system can be compensated

for by the supplement of spallation neutrons from the target. The external neutron source and subcritical operation open new possibilities for the transmutation of MAs.

A sodium-cooled ADS blanket with a non-uranium metallic dispersion was selected as the reference design. A fast neutron spectrum system was chosen because of the higher fission-to-absorption ratio that leads to a higher fission fraction of the MA inventory. Uranium-free matrices are able to accommodate large amounts of MAs with maximized MAs consumption. The metallic fuels are favorable because of their relatively high thermal conductivity and because they are capable of reaching a harder neutron spectra than nitride/oxide fuels, which enhance the MAs consumption. Furthermore, the dispersion fuels have better swelling behavior since the fission products are contained in the fuel particles mixed in the matrix. The sodium liquid metal was selected since the low moderating power and its superior thermal hydraulic capabilities (i.e. liquid metals allow the system to be operated at atmospheric pressure, while the gas-cooled system requires high pressures to achieve similar heat transfer capability).

Maximized MA destruction per unit energy production could be achieved with minimizing the fraction of the initial TRU inventory that is not transmuted and lost to the waste stream. Since there is small amount (~1%) of inventory lost over reprocessing, development of highly efficient processing technology while minimizing the number of times the fuel is processed should be targeted. For the ADS blanket design, the studies have focused primarily on the high discharge burnup that suggests the smallest number of recycle/re-fabrication campaigns to destroy a given amount of material. As discussed in Section 3.2, the goal of minimizing the fractional loss of MA to the waste streams is accomplished by maximizing the discharge burnup of ADS fuel (to minimize the number of recycle passes) and minimizing the fractional TRU loss per pass in recycle and re-fabrication. On the other hand, the source multiplication in the subcritical blanket decreases significantly with burnup due to the reactivity loss. Therefore, maximizing discharge burnup and minimizing burnup reactivity loss over an operating cycle were chosen as the primary performance objectives in the design of the sodium-cooled ADS blanket.

Analyses of the sodium-cooled ADS point design have focused primarily on the equilibrium fuel cycle that is believed to be a good basis for design optimization. In the equilibrium cycle, the charged fuel contains the heavy metals recovered from previous ADS fuel cycles and the MAs recovered from the first-stage FRs. At present, the equilibrium composition of ADS has been determined without considering the small fractional losses of TRU during the recycling and re-fabrication stages.

3.2. Design Objectives and Constraints

The main purpose of the ADS system is to facilitate waste management by removing MA elements from the spent FR fuels and transmuting these constituents in the ADS blanket. Additionally, the overall performance objective for the ADS system is to minimize the fraction of the initial TRU inventory that is not transmuted and lost to the waste stream. Because there is a small fraction of the inventory lost every time the material is processed, developing high efficiency processing technology and minimizing the number of processing operations required are design targets. From the viewpoint of the ADS blanket design, high discharge burnup was pursued which gives the smallest number of recycle/re-fabrication campaigns needed to destroy

a given amount of material. On the other hand, the source multiplication in the subcritical blanket that determines the transmutation performance decreases with burnup due to the reactivity loss. Therefore, maximizing discharge burnup and minimizing burnup reactivity loss over an operating cycle were chosen as the primary performance objectives in the physics design of the sodium-cooled ADS blanket.

The fuel discharge burnup is proportional to the total fuel residence time in the reactor and rated power divided by the mass of TRU inventory of transmutation blanket. For maximizing discharge burnup, the system should be designed with a high power density and a long fuel residence time, while limiting the actinide inventory of the transmutation blanket. However, limiting inventory of TRU increases the burnup reactivity loss. For uranium-free fuel, one major problem is the complete loss of internal conversion of the uranium matrix, which creates fissile material (Pu-239) with fuel burnup. This leads to magnified reactivity losses with fuel burnup compared to conventional uranium fuel systems. The fission power produced by a subcritical blanket is inversely proportional to the sub-criticality level (i.e., absolute value of static reactivity). Absence of compensating measure for the reactivity loss, such as increasing accelerator power, introducing excess reactivity and active reactivity control, the fission power will be declined with fuel depletion, which in turn makes it difficult to design an economical heat removal system. The reactivity loss rates can be reduced by increasing the TRU inventory [34], but there will be economic penalties associated with increased blanket size.

On the other hand, the burnup reactivity loss over an operating cycle is given as the product of the reactivity swing rate and irradiation cycle time. A low burnup reactivity loss can be achieved by design for a low specific power (i.e., high TRU inventory) or a short irradiation cycle time. The low specific-power approach requires a low power density and high TRU inventory, as well as a large number of irradiation cycles (and fuel management batches) to achieve the targeted high discharge burnup. The short irradiation-cycle approach, which permits a blanket with higher power density and specific power, requires more frequent refueling. The latter approach is adopted in this study because it employs a more compact (economical) blanket. The more frequent refueling may not adversely impact system availability given the likely need for periodic shut down for maintenance or replacement of accelerator, beam delivery and spallation target components. As a result, the present study focused on maximizing the discharge burnup under assumed design constraints discussed below; and the burnup reactivity loss is minimized by adjusting the cycle length.

The discharge burnup can be maximized by designing the system with maximum power density and fuel residence time and the minimum fuel volume fraction and fuel particle loading in the fuel. However, these design parameters are interrelated and limited by various design constraints. In the subcritical system, the TRU fraction in fuel is determined to maintain the desired sub-criticality level at the BOEC for the selected blanket configuration and fuel management scheme. This quantity is constrained by the maximum volumetric fraction of fuel particles (assumed here to be TRU-10Zr) in the dispersion fuel. In the previous studies [29,30], a fuel particle volume fraction limit of 50% was employed. However, the dispersion fuel will be easier to fabricate and likely have improved irradiation performance at lower fuel volume fractions [33]. Subsequently, the maximum volumetric fraction of fuel particles was assumed 25% in Reference 30, but in this study, it was relaxed to 45%.

A feasible long fuel lifetime design could be achieved by maintaining the fuel pin integrity that satisfies design constrains on the burnup limits for the fuel matrix and peak fast fluence limits for the cladding material. Typically, the irradiated fuel reached both limits at ~4-5 irradiation years. In the proposed dispersion fuel, the fission products are contained within the fuel particles that are mixed in the matrix. A higher burnup can be obtained in the dispersion fuel than the conventional metallic fuel, and thus the discharge burnup is not likely to constrain the design. Therefore, the fuel lifetime will be constrained only by the material damage to structures. For this analysis, a peak fast fluence limit of 4.0×10^{23} n/cm^2 is assumed based on data for low-swelling HT-9 stainless steel alloy developed in the ALMR program.

Finally, fuel heat load and heat transfer considerations are also the constraints that affect the power density of the transmutation blanket. In particular, the peak linear power is constrained by the need to limit the peak temperature at fuel centerline. As the power density increases, the minimum fuel volume fraction to satisfy the specified constraint on the peak linear power increases, and thus the maximum coolant volume fraction decreases. On the other hand, for a specified maximum coolant velocity, the minimum coolant volume fraction required for adequate cooling increases with increasing power density. Therefore, there exists an upper limit on the achievable power density.

3.3. Computational Methods and Models

For each blanket configuration and material volume fraction, equilibrium cycle analyses were performed. Cycle performance characteristics were calculated using the REBUS-3 code enhanced for ADS fuel cycle analysis [35,36]. Region-dependent multi-group cross sections used in the neutronics analyses were based on the ENDF/B-VII.0 data and were generated for a 33-group energy structure using the MC^2-3 code [14]. In addition to the equilibrium cycle analyses, the non-equilibrium cycle analysis was performed for the BOL core to evaluate the transition cycle performance of ADS system. The details of the two-stage fuel cycle options are discussed in Section 5.1.

The equilibrium cycle calculation was performed to analyze the performance of the second stage fuel cycle at equilibrium state. In the equilibrium cycle model of REBUS-3, the charged fuel contains HM recovered via recycling from the previous discharged ADS fuel cycles and is supplemented by the MA recovered from the first stage to make up for the HM consumed by fission. The isotopic composition of the external feed in equilibrium cycle is presented in Table 3.1. In the equilibrium composition evaluation, the nuclear material loss rate of 0.2% in the fresh fuel fabrication and 1.0% in the discharged fuel separation were assumed for evaluating the isotopic composition of the TRU recovered from the first stage. It was also assumed that 5% of rare-earth fission products would be carried over to the next cycle from the recycled fuel.

Table 3.1. Isotopic Composition of External Feed

Isotope	%	Isotope	%	Isotope	%
Np-237	29.6	Pu-241	2.6	Am-241	44.1
Am-242m	1.7	Am-243	16.5	Cm-242	1.9
Cm-243	0.1	Cm-244	3.3	Cm-245	0.2
Cm-246	0.0				

In this study, inhomogeneous fixed source problems were solved for the proposed system point design with the triangular-z finite difference option of the DIF3D code, using a generic distribution of spallation neutron source generated for a 1 GeV proton beam and a prototypic LBE target [37]. Depletion calculations were performed at a constant power level by increasing the source intensity over an operating cycle to compensate the burnup reactivity loss. In a REBUS-3 calculation for a fixed-source equilibrium cycle problem, the corresponding eigenvalue problem is solved first to prepare a good initial guess for the feed enrichment and the stage densities in each depletion zone [36].

3.4. System Point Design and Performance Characteristics

A point reference design of an 840 MWt sodium-cooled ADS blanket using a zirconium matrix MA dispersion fuel was developed based on the 840 MWt sodium-cooled ATW blanket design with zirconium matrix TRU dispersion fuel [28]. Using the core configuration of the ATW blanket design, parametric studies were carried out to achieve a higher fuel discharge burnup in ADS. The burnup reactivity loss was reduced with short irradiation cycle approach, and the optimum fuel volume fraction was determined to maximize the discharge burnup while satisfying the design constraints discussed in Section 3.2. The system point design is based on the equilibrium cycle performance; however, to evaluate the characteristics of ADS system, both the equilibrium and non-equilibrium cycle analyses were performed in this study.

In the equilibrium cycle, the MA-10Zr particle fraction in fuel was determined to attain the multiplication factor at BOEC equal to 0.97. The required fuel inventory in ADS is larger than ATW since the reactivity worth of MAs is less than that of the TRU fuel. In order to maintain the same compact core configuration of ATW with a higher fuel inventory, the fuel volume fraction should be maximized within the design criteria of 45% for the fuel particle volume fraction in dispersion fuel. The diameter of fuel pins in the ADS was increased from 0.74 cm to 0.77 cm, and the pin pitch-to-diameter ratio was reduced to 1.157. The assembly design parameters of ADS fuel blanket are summarized in Table 3.2.

The blanket layout of the ADS blanket point design is illustrated in Figure 3.1. The system is composed of 19 hexagonal assembly positions containing the LBE target/buffer, 132 fuel assemblies surrounding the target/buffer, 102 steel reflectors and 60 B_4C radial shields. The 132 fuel assemblies are divided into three enrichment zones (i.e., inner, middle and outer zones) to flatten the power distribution. The fuel management scheme and the fuel residence time were determined to satisfy the peak fast fluence limit. Each fuel assembly remained in the same position without shuffling or rotation. Higher fast flux occurs in the inner zone because the spallation neutron source is concentrated in the target. In order to satisfy the peak fast fluence limit, the fuel residence time was reduced for the inner zone. A six-month fuel residence time with capacity factor of 75% was used with 7-batch fuel management scheme for the inner zone, whereas an 8-batch scheme was used for the middle and outer zones.

Table 3.3 shows the equilibrium cycle performance of the sodium-cooled ADS system. In the equilibrium core, the heavy metal inventory at BOEC required to achieve the desired multiplication factor is 4208 kg. High fuel inventory was obtained by the increased fuel volume fraction of dispersion fuel. The fuel particle volume fraction of the charged fuel is 25.4%, 34.4%, and 38.2% in the inner, middle and outer zone, respectively. The large amount of fuel inventory reduces the average discharge burnup and the burnup reactivity loss. The average discharged

burnup is 19.6% in the ADS, and the burnup reactivity loss is 1.3% with a six-month cycle design. The highest fuel particle volume fraction is 38.2% in the outer zone which within the design criteria of 45% for the fuel particle volume fraction in dispersion fuel. The power distribution is flattened by enrichment zoning, and as a result, power peaking factors for each zone are practically the same. The power peaking factors are similar between BOEC and EOEC, but during burnup, power peaking is shifted from the middle to the inner zone due to the increased spallation neutron source. The peak fast fluence for the ADS system is currently 3.52×10^{23} n/cm^2, but could be further increased by either extending the cycle length or improving the capacity factor to attain a higher discharged burnup.

Table 3.2. Design Parameters of Sodium-Cooled ADS Blanket Designs

Parameter		ADS
Fuel particle form		MA-10Zr
Duct material		HT-9
Bond material		Na
Assembly pitch, cm		16.142
Duct outside flat-to-flat distance, cm		15.710
Duck thickness, cm		0.394
Number of fuel pins		271
Pin diameters, cm		0.770
Pin pitch-to-diameter ratio		1.157
Cladding thickness, cm		0.056
Fuel smeared density, %		85.0
Wire wrap diameter, cm		0.116
Active fuel height, cm		107.0
Volume fraction (Fabrication)	Fuel	0.347
	Na bond	0.256
	Structure	0.061
	Coolant	0.335
Number of fuel assemblies	Inner zone	42
	Middle zone	24
	Outer zone	66

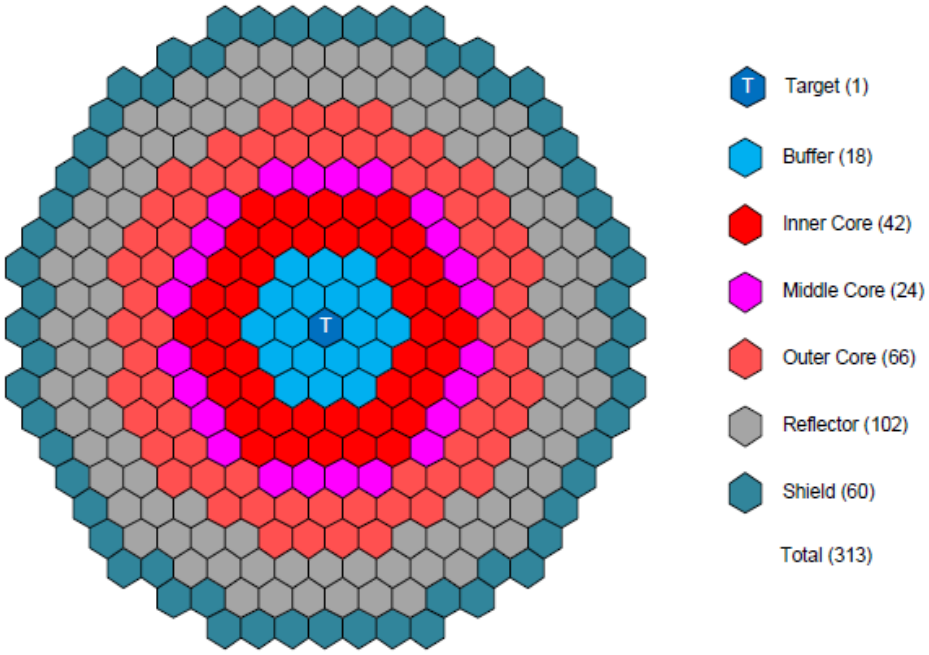

Figure 3.1. Sodium-Cooled ADS Blanket Configuration

Table 3.3. Equilibrium Cycle Performance of Sodium-Cooled ADS Blanket Design

Parameter		ADS
Thermal power, MW		840
Cycle length, EFPD		135
Capacity factor, %		75
BOEC heavy metal inventory, kg		4208
Fuel particle fraction, volume % in matrix	Inner zone Middle zone Outer zone	25.4 34.4 38.2
Multiplication factor	BOEC EOEC	0.97007 0.95726
Burnup reactivity loss, %Δk		1.3
Core-average power density, kw/l		247.6
Power peaking factor at BOEC/EOEC		1.55/1.58
Peak linear power, kW/m	Inner zone Middle zone Outer zone	37.8 37.2 37.1
Average discharge burnup, atom %		19.6
Peak fast fluence, 10^{23} n/cm^2		3.52
Net TRU consumption rate, kg/year		233
Equilibrium loading, kg/year	FR TRU Recycled HM Total HM	233 974 1206

Table 3.4 shows the non-equilibrium cycle performance of the sodium-cooled ADS system. In the start-up core, the volume fraction of fuel particles in dispersion fuel was further increased because only small amount of plutonium, which is of relatively high reactivity worth, is contained in the MA supplied by the first-stage FR due to the decay of Am-241. In order to meet the design limit on the volume fraction of fuel particles, additional fuel was introduced by replacing 54 reflectors with fuel assemblies. The resulting volume fractions of fuel particles in the charged fuel is 29.5%, 39.8%, and 44.2% in the inner, middle and outer zones, respectively. The highest volume fraction of fuel particles is 44.2% in the outer zone, which is within the design criteria of 45% for the volume fraction of fuel particles in dispersion fuel. The core inventory of heavy metal at BOL was increased from 4.2 MT to 7.6 MT in the modified core design.

Table 3.4. Transition Cycle Performance of Sodium-Cooled ADS Blanket Designs

Parameter		ADS
Thermal power, MW		840
Cycle length, EFPD		135
Capacity factor, %		75
Multiplication factor	BOC EOC	0.97012 0.97307
Burnup reactivity loss, %Δk		-0.30
Fuel particle fraction, volume % in matrix	Inner zone Middle zone Outer zone	29.5 39.8 44.2
BOL fuel loading, kg	Pu MA Total HM	1445 6110 7556

Table 3.5 presents the heavy metal mass flow rates in the equilibrium cycle of the sodium-cooled ADS. The charged fuel is primarily made of TRU recovered from the previously discharged ADS fuel and is supplemented by the MAs recovered from the first-stage FR. The negative consumption rate of Cm-242 is attributed to the short half-life of Am-242, which decays into Cm-242 (83%) and Pu-242 (17%) [38]. The MAs recovered from the fist-stage FR are consumed in ADS at a rate of 226.4 kg/year, and the net TRU consumption rate is 232.6 kg/year.

Table 3.5. Heavy Metal Mass Flow Rates (kg/year) in Equilibrium Cycle of Sodium-Cooled ADS System

Isotope	Charge	Discharge	Consumption	Feed	
				ADS TRU	FBR TRU
U-234	30.8	28.3	2.5	30.2	0.0
U-235	5.2	5.2	0.0	5.2	0.0
U-236	5.2	5.2	0.0	5.2	0.0
U-238	0.0	0.0	0.0	0.0	0.0
Np-237	182.0	113.7	68.3	114.0	67.8
Pu-236	0.0	0.0	0.0	0.0	0.0
Pu-238	201.5	192.4	9.1	199.3	0.0
Pu-239	52.8	52.8	0.0	52.8	0.0
Pu-240	89.0	83.1	5.8	87.5	0.0
Pu-241	19.9	15.1	4.9	14.2	6.1
Pu-242	68.0	68.0	0.0	68.0	0.0
Am-241	259.1	155.6	103.5	156.1	102.8
Am-242	22.9	19.0	3.9	18.9	4.1
Am-243	136.6	97.8	38.8	97.8	38.8
Cm-242	3.3	10.5	-7.2	1.6	4.6
Cm-243	0.9	0.8	0.1	0.8	0.1
Cm-244	98.2	96.3	1.8	91.9	7.8
Cm-245	19.5	19.1	0.5	19.1	0.5
Cm-246	11.3	11.3	0.0	11.3	0.0
Pu	431.3	411.4	19.9	421.8	6.1
MAs	733.8	524.1	209.8	511.5	226.4
Total HM	1206.3	974.1	232.2	973.8	232.6

4. Development of Minor Actinides and Long-lived Fission Products Target Design

In the second two-stage fuel cycle option, the MAs recovered from the discharged FR fuels are partially transmuted in FR through MA target assemblies in order to reduce the amount of MA to be sent to the second-stage ADS. A scoping design study was performed to develop the target designs for the transmutation of MA and LLFP in the LEUFBR. The design goal of the target assembly is to maximize the MA destruction while staying within the imposed thermal design constraints.

The major isotopes among the MAs in the used LEUFBR fuel are NP-237 and Am-241. These nuclides have relatively small fission-to-absorption cross section ratios in the fast energy range, but they have large thermal capture cross sections. Therefore, it would be a promising option to convert them first into fissile nuclides in moderated target assemblies and to fission the product fissile nuclides.

However, the moderation in the target assembly will result in an increased local power peaking in the neighboring fuel assemblies and in the target assemblies themselves when a significant amount of MAs is converted into fissile nuclides. To mitigate the local power peaking problem, the target assemblies were loaded in the core periphery and LLFP target pins were used as the thermal neutron filter to reduce the thermal neutron leakage from a target assembly to the neighboring fuel assemblies. The optimum moderator fraction in the target assembly was determined to maximize the MA transmutation performance while satisfying the imposed thermal design constraints.

Using the reference target design, the transmutation performance of LEUFBR was investigated by performing full-core depletion calculations using the DIF3D/REBUS-3 code [11-13]. The cross sections of moderated target assemblies were generated by combining the MC^2-3 [14] and MCNP6 [39] calculations. Fuel cycle analyses showed that the accumulated MAs and LLFPs (Tc-99, I-127 and I-129) of LEUFBR over the assumed plant lifetime of 60 years could be greatly reduced by employing MA target assemblies. At the equilibrium state, the use of MA target assemblies reduced the amount of MA to be sent to ADS by a factor of six compared to that of the fuel cycle without MA recycling in FR. As a result, the number of ADS could be reduced significantly in the second two-stage fuel cycle option.

4.1. Transmutation Characteristics of Minor Actinides

The main purpose of the proposed target assembly is to transmute the recovered MAs from the discharged fuels of the LEUFBR core. During the assumed plant lifetime of 60 years, 533 kg of MAs are accumulated in the LEUFBR fuel cycle, as shown in Figure 4.1. Figure 4.2 shows the isotopic composition of discharged MAs from LEUFBR. Np-237 and Am-241 are the main constituents of the discharged MAs from LEUFBR. The starting cycles of LEUFBR are mainly loaded with LEU fuel, so Np-237 is a predominant isotope in the discharged MAs. The Am-241 fraction increases with time since Am-241 production increases with increasing Pu loading.

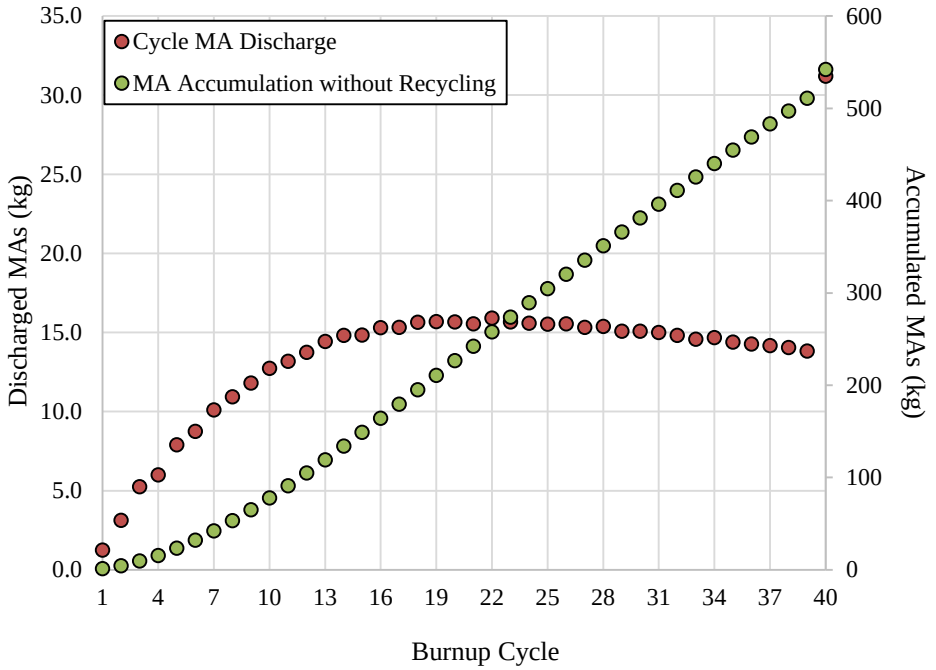

Figure 4.1. Discharged and Accumulated MAs at End of Each LEUFBR Cycle

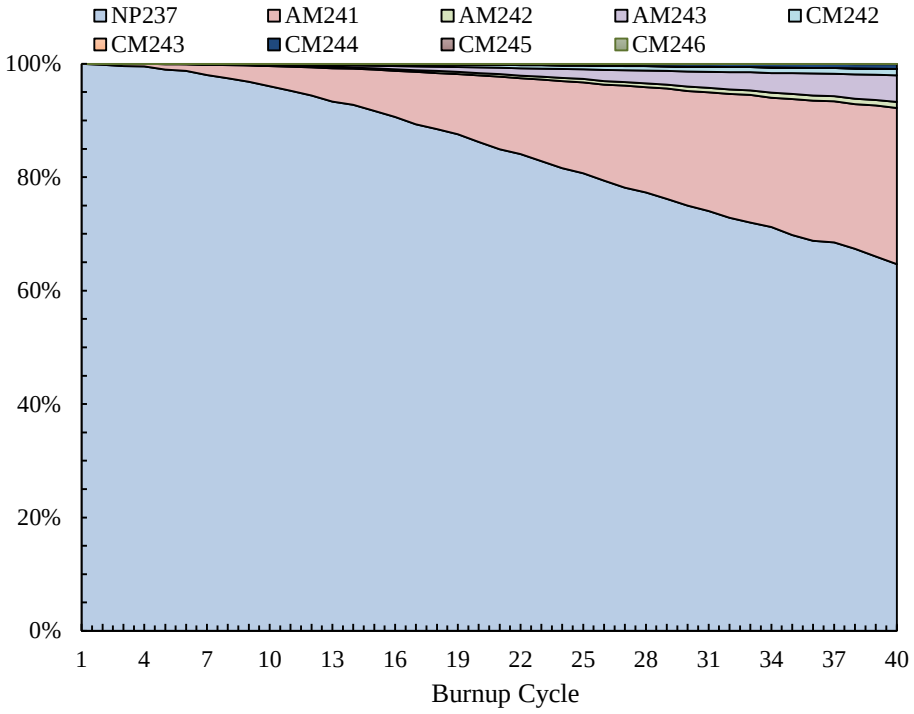

Figure 4.2. Isotopic Composition of MAs Discharged from Each LEUFBR Cycle (wt.%)

Averaged over the sixty-year lifetime, 97% of discharged MAs are comprised of Np-237 and Am-241 isotopes. As mentioned above, both Np-237 and Am-241 have relatively low fission-to-capture ratios in the fast energy region, but large thermal capture cross sections. This suggests that Np-237 and Am-241 could be incinerated effectively by first transmuting them

into fissile nuclides (or nuclides of high fission-to-capture ratio) by thermal neutron capture, as depicted in Figure 4.3. For example, reactions of neutron capture coverts Np-237 into Np-238, which in turn will decay into Pu-238. Pu-238 has a significantly higher fission-to-capture ratio compared to Np-237 in the fast energy range, as shown in Table 4.1 and Figure 4.4. Subsequent neutron capture in Pu-238 would lead to the production of fissile nuclide Pu-239. Similarly, neutron capture in Am-241 would lead to Am-242, which is a fissile nuclide. To create a thermal neutron environment within the fast spectrum system, the MAs can be placed into separate moderated target assemblies.

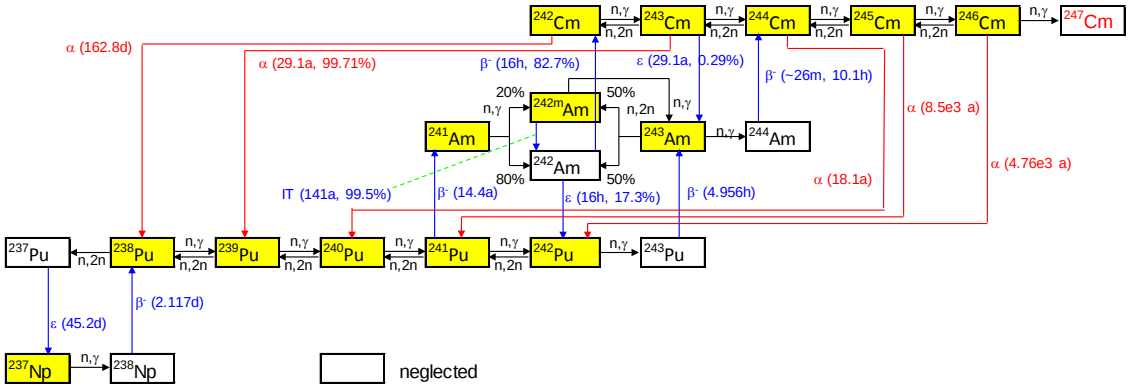

Figure 4.3. Burn Chains of Minor Actinides in LEUFBR

Table 4.1. Spectrum-Averaged Cross Sections in Thermal (PWR [40]) and Fast (LEUFBR) Systems

Isotope	Typical PWR Spectrum			LEUFBR Spectrum		
	σ_f	σ_c	σ_c/σ_f	σ_f	σ_c	σ_c/σ_f
U-235	38.8	8.7	0.22	1.62	0.42	0.26
U-238	0.10	0.86	8.35	0.04	0.21	5.53
Np-237	**0.52**	**33**	**63.5**	**0.35**	**1.26**	**3.56**
Pu-236	134	13.6	0.10	2.34	0.21	0.09
Pu-238	**2.4**	**27.7**	**11.5**	**1.05**	**0.54**	**0.52**
Pu-239	**102**	**58.7**	**0.58**	**1.63**	**0.32**	**0.20**
Pu-240	0.53	210.2	396.6	0.36	0.37	1.03
Pu-241	102.2	40.9	0.40	2.11	0.33	0.15
Pu-242	0.44	28.8	65.5	0.25	0.34	1.35
Am-241	**1.1**	**110**	**100.0**	**0.25**	**1.11**	**4.50**
Am-242	595	137	0.23	2.73	0.36	0.13
Am-243	0.44	49	111.4	0.19	1.14	6.05
Cm-242	1.14	4.5	3.95	0.16	0.20	1.30
Cm-243	88	14	0.16	2.51	0.43	0.17
Cm-244	1.0	16	16.0	0.43	0.56	1.31
Cm-245	116	17	0.15	2.50	0.45	0.18

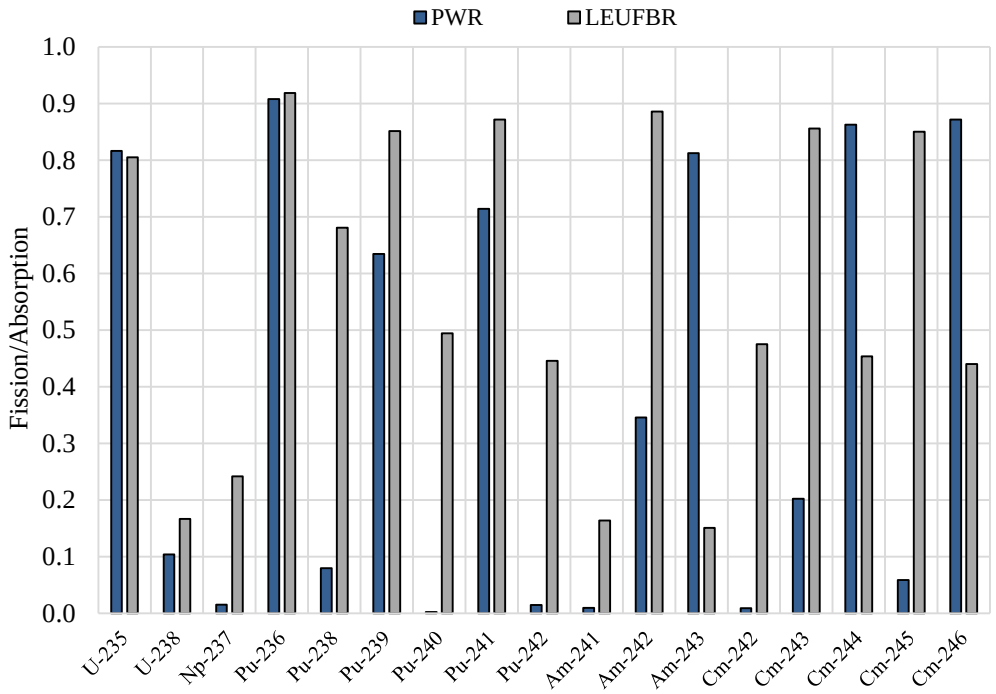

Figure 4.4. Fission-to Absorption Ratio in Thermal (PWR) and Fast (LEUFBR) Systems

4.2. Selection of Moderator and Fuel Materials

To transmute the Np-237 and Am-241 nuclides effectively, a proper moderating material and MA target composition must be selected. The two most important criteria for the moderating material are a high slowing-down power, which makes the number of collisions required to thermalize neutrons small, and a high slowing-down ratio, which yields a high thermal neutron flux. In considering the MA fuel composition, the important parameters to consider include the thermal conductivity, melting temperature, material density, fabrication cost, and compatibility with materials in the surrounding environment (sodium coolant).

Table 4.2 compares the slowing-down power and the slowing-down ratio for typical moderating materials. Zirconium-hydride has a high moderating capability and it has been extensively used in TRIGA reactors [41]. A series of experiments have also been conducted using zirconium-hydride as a moderator in Heat Transfer Reactor Experiment-3 (HTRE-3). Furthermore, zirconium-hydride has relative high thermal conductivity and decomposition temperature, which are important parameters to consider when placing it in the LEUFBR. For these reasons, zirconium-hydride was selected as the moderator for this study. Figure 4.5 shows the phase diagram of zirconium hydride for varying hydrogen content. The stoichiometry for zirconium hydride of 1.6 was selected. The delta phase of $ZrH_{1.6}$ is stable up to a temperature of at least 1000 °C.

The MA-containing metal alloy fuel was selected to take the advantage of the demonstrated performance of metal fuels. The MA fuel composition was chosen to be MA-40Zr under the assumption that it would have similar properties as the Pu-40Zr and Pu-MA-40Zr fuels. Metal fuel samples of Pu-40Zr, Pu-12Am-40Zr and Pu-10Am-10Np-40Zr were irradiated in the

Advanced Test Reactor (ATR) and included in the AFC irradiation test series to evaluate the effects caused by the existence of MAs. Recent experimental results showed that the major irradiation performance variables of TRU-Zr fuels are similar to that of U-Zr and U-Pu-Zr fuels. The formation of low melting phases in the multi-component alloy system is not a fuel performance issue for the use of TRU-bearing fuels as transmutation fuels [42]. In this study, a heterogeneous lattice consisting of MA-40Zr pins and $ZrH_{1.6}$ pins was selected from the fabrication, reprocessing and operation point of view. Some MA target pins are replaced by thermal neutron filter pins, composed of long-lived fission products (LLFPs), to reduce the thermal neutron leakage from the target assembly to the neighboring fuel assemblies as described in Section 4.5.

Table 4.2. Comparison of Key Parameters for Various Moderating Materials [43]

Material	Slowing-Down Power	Thermal Absorption Cross Section* (barns)	Slowing-Down Ratio
Graphite	0.06	0.0004	170
$ZrH_{1.94}$	1.54	0.030	51
$ZrD_{1.75}$	0.20	0.007	31
$YH_{1.89}$	1.22	0.054	23
$CeH_{2.12}$	1.03	0.032	32

* Absorption cross section at 0.0253 eV

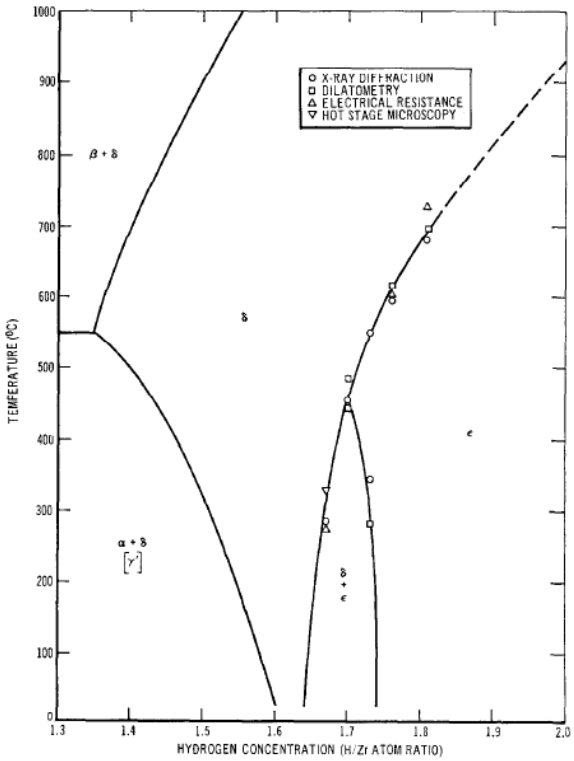

Figure 4.5. High Hydrogen Composition Region of Zirconium-Hydride Phase Diagram [44]

4.3. Design Constraints

The increased moderation in the MA target assembly results in an increased power peaking in the adjacent fuel assemblies and the moderated target assemblies themselves when a significant amount of MAs are converted into fissile nuclides. As a result, the moderator volume fraction in the target assembly is limited by the peak linear power limit on the adjacent fuel assemblies (drivers) and the moderated MA target assemblies. Since the linear power in the target assembly is proportional to the irradiation time (i.e., the core residence time of a target assembly), the target irradiation time is also constrained.

As presented in Section 2.2, two thermal design criteria were imposed for the driver fuel of LEUFBR core; one is on the fuel centerline temperature and the other is on the cladding inner wall temperature. Based on the single channel thermal-hydraulics analysis, it was found that the linear power limit due to the cladding inner wall temperature is lower than that of the other. Thus, the lower thermal limit due to the cladding inner wall temperature was selected for the MA target design. This constraint was imposed to limit the power-to-flow ratio and the peak linear power in the hottest fuel pin so that macroscopic eutectic liquefaction at the fuel-cladding interface cannot occur. For the driver fuel assembly, the liquefaction temperature changes as a function of plutonium fraction in the fuel. Base on a series of out-of-pile experiments [45], the threshold temperature for the liquefaction point was estimated to be ~685 °C. This temperature was determined with 14 wt.% Pu in U-Pu-10Zr fuel since the maximum estimated Pu fraction in the LEUFBR core is ~13.3 wt.% at the EOL core. By applying a 15 °C margin and 2-sigma hot channel factor uncertainties to the design limit, a maximum peak linear power of 54.8 kW/m was calculated for the LEUFBR core. The maximum allowable local power peaking is set to 1.40 based on this design limit and the peak linear power of neighboring fuel assemblies at cycle 16.

For the target assembly, the liquefaction temperature would change with the isotopic compositions of TRU fuel as it changes as a function of plutonium fraction in the U-Pu-10Zr fuel. However, almost no experimental information was available on the system containing Np, Am, Pu, Zr and Fe. Based on the phase diagram for the Np-Fe system proposed by J. K. Gibson [46], the eutectic temperature for Np-Fe system is between the corresponding temperatures for the U-Fe and Pu-Fe systems. Compared to the U-Pu-10Zr fuel, the increased Zr weight fraction in the target assemblies can compensate for the deteriorated thermal properties due to the presence of TRU. The threshold temperature for the liquefaction point of ~610 °C was used for the MA target assembly (MA-40Zr). The peak linear power limit of the target assembly was determined to be ~44 kW/m based on a single channel thermal-hydraulics analysis. For the finalized core design, detailed whole-core, sub-channel analyses were used in the evaluation of the peak cladding temperature in the core as discussed in Section 4.6.

4.4. Computational Methods and Models

The ANL suite of fast reactor analysis codes was used in the fuel cycle and thermal-hydraulics analyses. Using the 3-dimensional hexagonal-z geometry full core models, equilibrium and non-equilibrium cycle calculations were performed with the DIF3D/REBUS-3 code system [11-13]. Region-dependent, 33-group neutron cross section sets were generated

from the ENDF/B-VII.0 cross section library for the LEUFBR core compositions (excluding the MA target assembly) using the MC^2-3 [14] code.

Since the MC^2-3 code doesn't have the capability for generating thermal cross sections, the cross sections of the moderated MA target assemblies were generated by combining MCNP6 [39] and MC^2-3 calculations. For the MC^2-3 calculation, a one-dimensional model consisting of a homogeneous target assembly located between the outer core and reflector regions was used. A whole core model of MCNP6 was developed to generate target assembly cross sections. Figures 4.6 to 4.9 compare 33-group cross sections of Np-237 and Am-241 obtained with the MC^2-3 and MCNP6 codes. As can be seen in the figures, the cross sections from MCNP6 agree well with those in MC^2-3 except for the thermal group ($E < 0.414eV$). To correct the additional small deviations in epithermal region, the cross section obtained from MC^2-3 were replaced with MCNP6 cross sections for the 12 groups from 22 to 33.

A MCNP6 whole-core model was also built to determine the increase in the local power peaking in adjacent fuel assemblies. The composition used in the MCNP6 whole-core model was extracted from the REBUS-3 output of the LEUFBR. From the cycle-by-cycle REBUS-3 analysis, it was observed that the peak linear power of the neighboring fuel assemblies becomes the largest at the cycle 16. Therefore, the homogenized fuel compositions were obtained by taking the average of the compositions at the beginning and the end of the cycle 16.

In the calculation of the peak linear power, the power gradient across a homogenized fuel assembly is taken into account by the region-specific peak power densities of REBUS-3 depletion calculations. Therefore, we need to consider only the pin power increase in a heterogeneous assembly configuration due to the local distribution of the thermal flux leaking from the moderated target assembly. In order to estimate the increase in the local power peaking, two whole-core MCNP6 models shown in Figures 4.10 and 4.11 were developed: one with no target assembly and the other with moderated target assembly. The fission energy of each pin cell was calculated using the F7 tally function of MCNP6. The power peaking factor of each fuel pin is determined by dividing the fission energy in each fuel pin by the average value over the fuel pins in the corresponding assembly. The power peaking factor of an assembly is obtained by the maximum value of the pin power peaking factors in the assembly. The local power peaking increase in a neighboring fuel assembly due to the moderated target assembly is determined by the ratio of the assembly power peaking factor with the MA target assembly to the averaged pin power of the same assembly in the base case with no MA target assembly.

For the finalized design, detailed steady-state thermal-hydraulic analyses were performed to evaluate the pin temperature distribution in the LEUFBR core. Heating rates for thermal-hydraulic calculations were determined by coupled neutron and gamma heating calculations. For these heating calculations, region-dependent 33-group neutron cross sections (ISOTXS), 21-group gamma cross sections (GAMISO), and gamma production cross sections and heating factors (PMATRX) were generated based on a two-dimensional full core RZ model using the MC^2-3 code [14]. The coupled neutron and gamma heating calculations were done in several steps. The neutron flux was first calculated using the triangular-z finite difference option of the DIF3D code [11] and the ISOTXS cross section set. Using the calculated neutron flux and the PMATRX data set, the photon source distribution induced by neutron reactions was computed

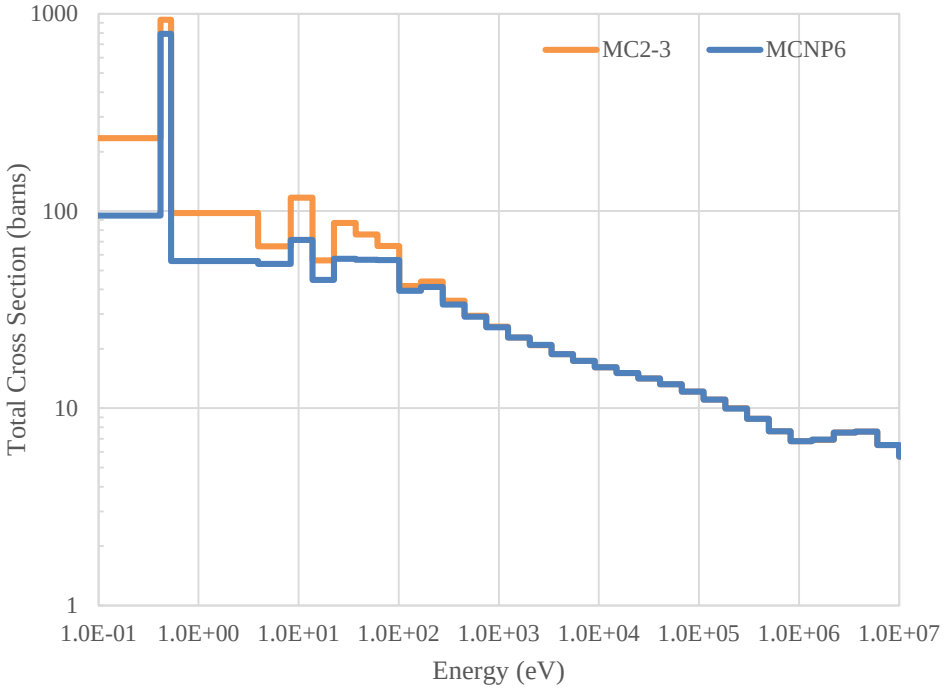

Figure 4.6. Total Cross Sections of Np-237 Calculated by MC^2-3 and MCNP6

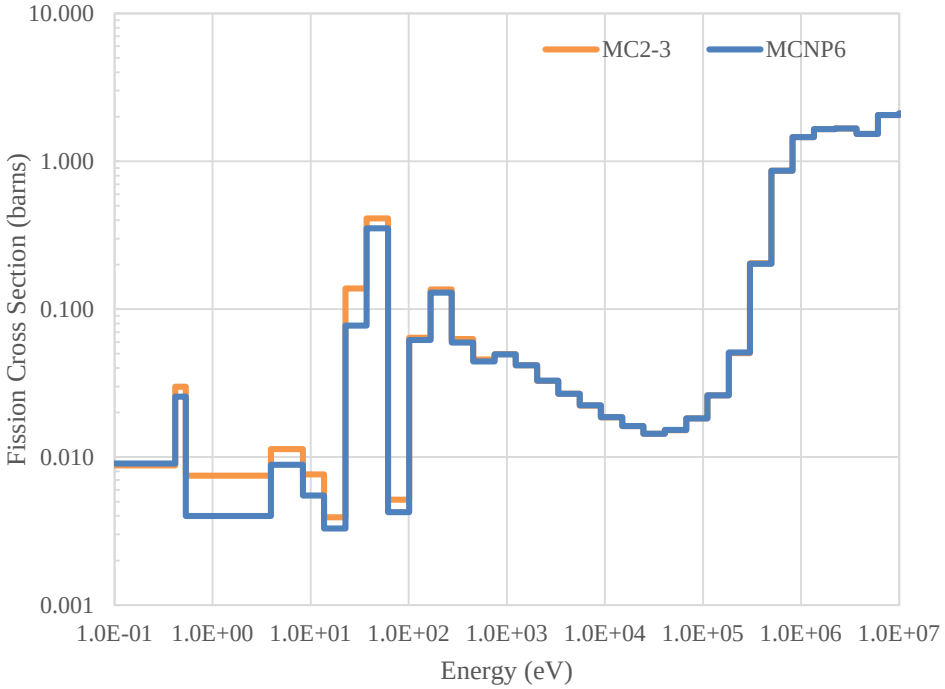

Figure 4.7. Fission Cross Sections of Np-237 Calculated by MC^2-3 and MCNP6

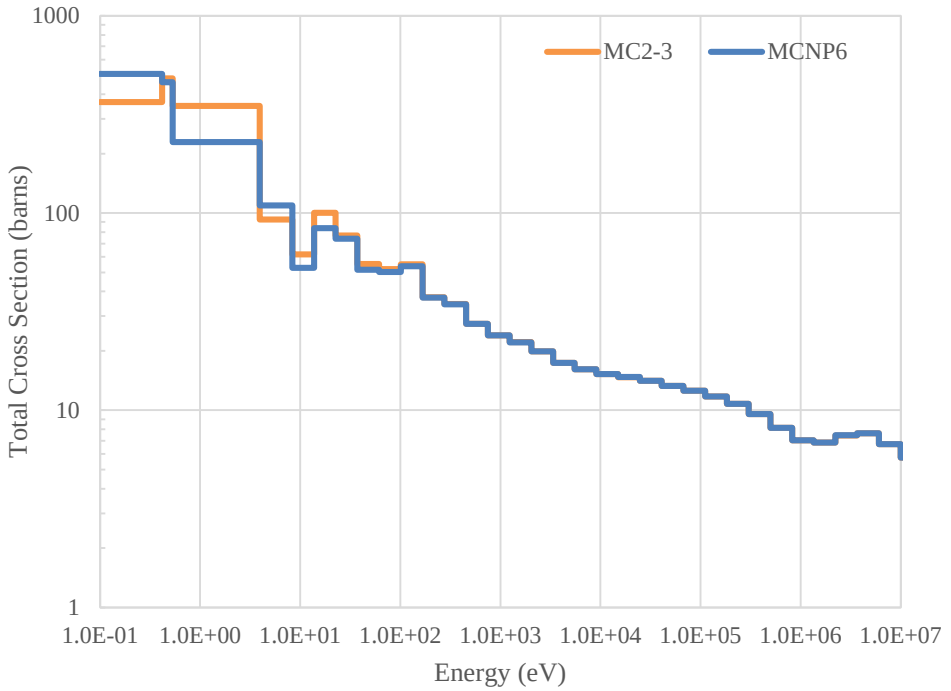

Figure 4.8. Total Cross Sections of Am-241 Calculated by MC^2-3 and MCNP6

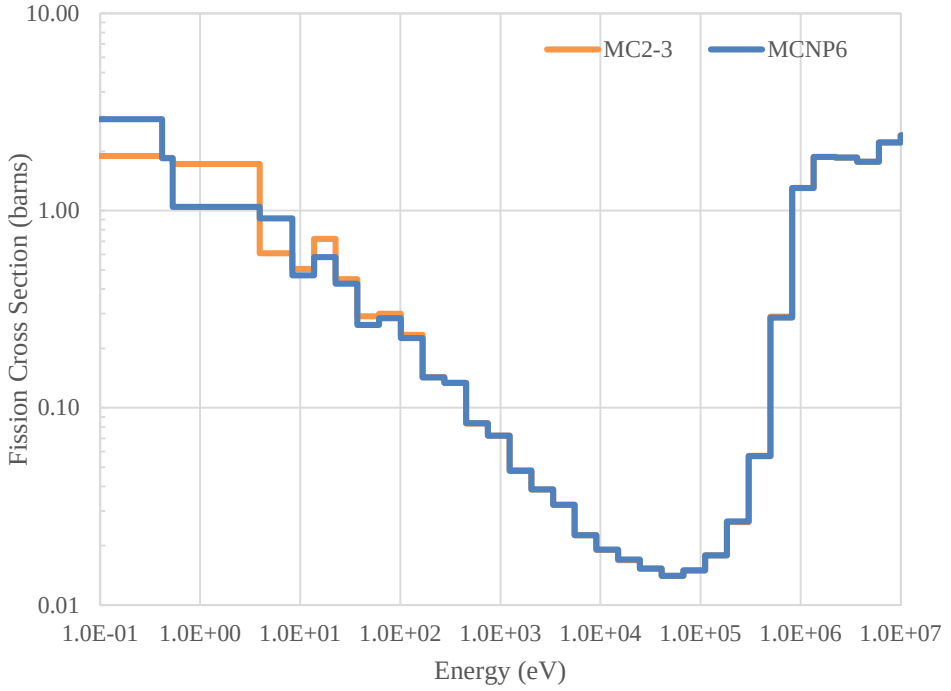

Figure 4.9. Fission Cross Sections of Am-241 Calculated by MC^2-3 and MCNP6

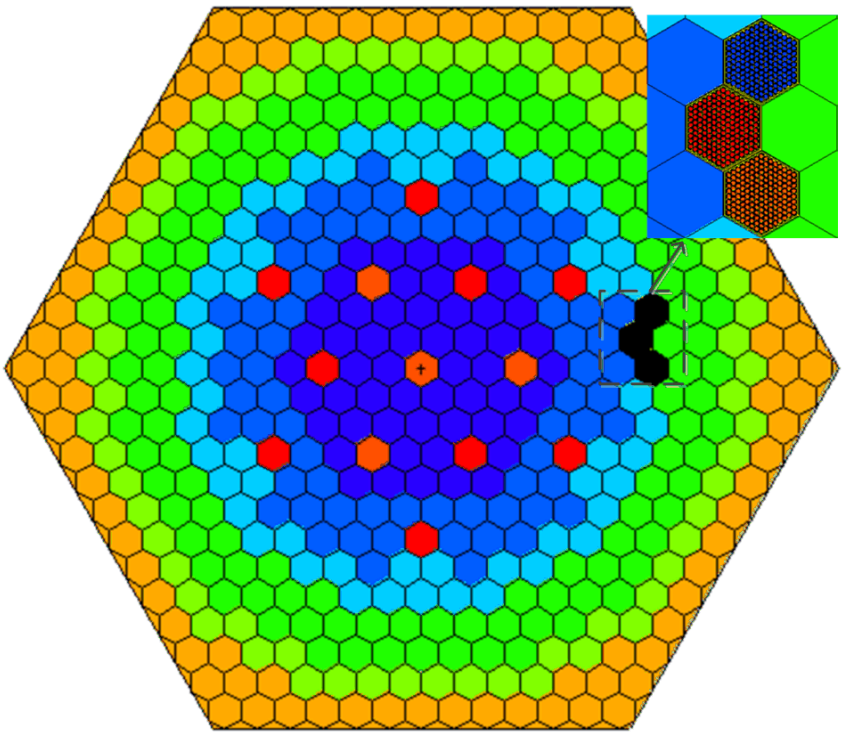

Figure 4.10. Whole-Core MCNP6 Model for Base Case with No Target Assembly

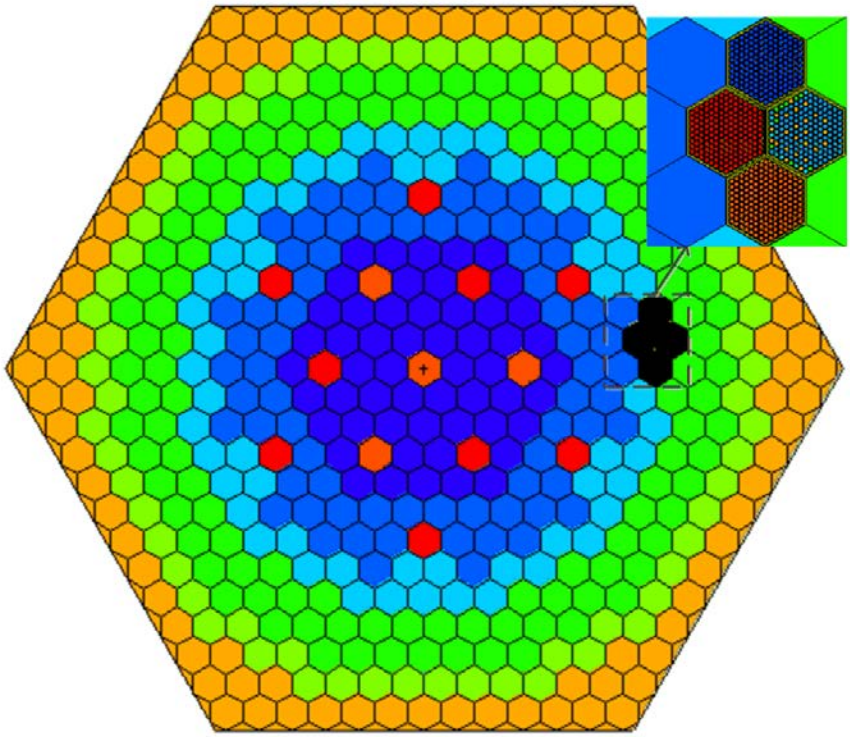

Figure 4.11. Whole-Core MCNP6 Model with Moderated Target Assembly

with the GAMSOR code [47]. With this calculated gamma source distribution, the gamma flux was calculated by solving a fixed source problem using the DIF3D code and the GAMISO cross section set. Finally, using the calculated neutron and gamma fluxes and the heating factors called KERMA (Kinetic Energy Release in Materials) factors provided in the PMATRX dataset, the neutron, gamma, and total heating rate distributions were calculated using the SUMMAR module of DIF3D. These heating rate distributions were normalized such that the total heating rate (i.e., the sum of neutron and gamma heating rates) is equal to the rated power.

Using the pin power distributions, whole-core temperature calculations were performed using the sub-channel analysis code SE2-ANL [21]. The SE2-ANL code is a modified version of the multi-assembly, steady-state sub-channel analysis code SUPERENERGY-2 [22]. The coolant inlet and bulk outlet temperatures were set to 355 ºC and 510 ºC, respectively. The average flow rate was determined such that the average temperature rise in coolant across the core is 155 ºC. Sodium coolant flow was distributed to the assemblies with the overall goal of equalizing the accrual of pin cladding damage and thus pin reliability.

4.5. Target Assembly Design Studies

Using the selected MA-40Zr fuel and $ZrH_{1.6}$ moderator, parametric studies were performed to determine the optimal fuel to moderator ratio in the target assembly. The MA target to moderator ratio was varied by adjusting the numbers of target and moderator pins. Four different pin designs of diameters from 5.99 mm to 9.5 mm were used with fixed assembly dimensions. Figure 4.12 shows the effective one-group capture cross sections of MAs (i.e., the transmutation rate per unit MA nuclide and flux) as a function of the moderator to MA target volume ratio for four different target pin designs. As expected, the effective one-group capture cross section of MA increases monotonically with increasing moderator volume fraction. The target pin size affects the one-group cross section through the change in the spatial self-shielding effect, but this effect is relatively small and becomes noticeable only when the moderator to MA target volume ratio is larger than 3.0. Since the gain of small pin size through the reduced self-shielding effect is small, a relatively larger pin size of 9.5 mm diameter was selected to increase the MA loading per pin, which would increase the absolute transmutation rate. Under the same assembly dimensions with the drive assembly, this yields a target assembly of 169 pins.

Figure 4.13 shows the absolute capture reaction rate and one-group capture cross section of the target assembly with target and moderator pins of 9.5 mm diameter as a function of the moderator to target volume ratio. The capture rate and one-group capture cross section were normalized to the corresponding values of the target assembly with no moderator pin. It can be observed from the one-group capture cross section that the relative transmutation rate increases with increasing moderator volume fraction. On the other hand, the increased moderator volume fraction results in a reduced MA loading and hence a reduced absolute transmutation rate. It is noted that the effectiveness of moderator (i.e., the slope of one-group cross section) decreases when the moderator to fuel volume ratio is larger than 2.0. These results suggest that a trade-off between the relative and absolute transmutation rates needs to be made depending on the imposed design constraints. Since the MA production rate is relatively low in the LEUFBR core starting from uranium fuel, there exist more than sufficient spaces for target assemblies in the core that can accommodate the MA production in the LEUFBR. As a result, a higher MA

burnup, which is favorable to reducing the reprocessing loss of MA, can be achieved by loading multiple target assemblies with a smaller amount of MA. Therefore, the moderator volume in the target assembly was maximized within the peak linear power limit of target pins.

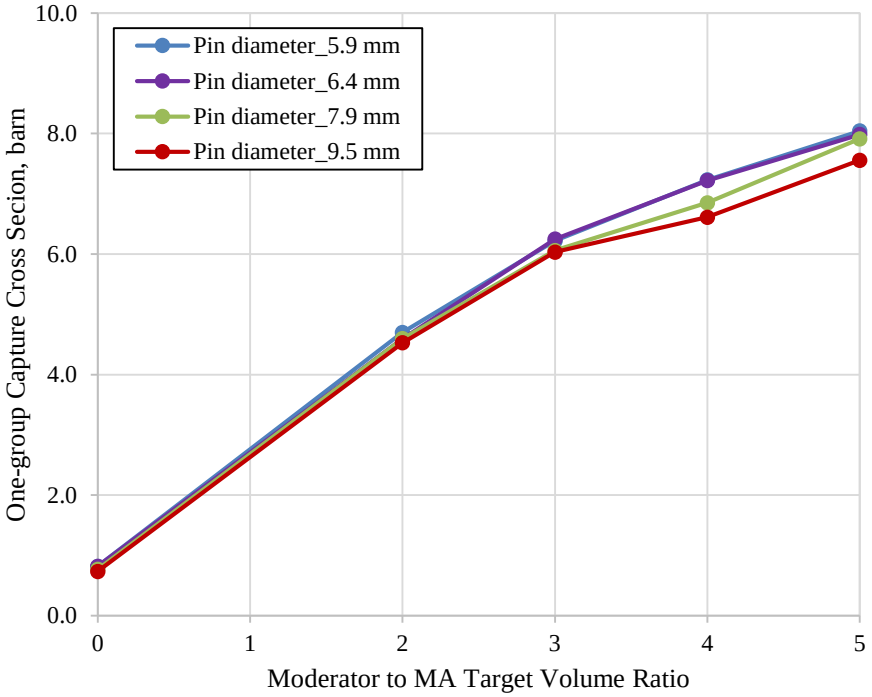

Figure 4.12. One-Group Capture Cross Sections of MAs versus Moderator Volume Fraction for Four Target Pin Designs

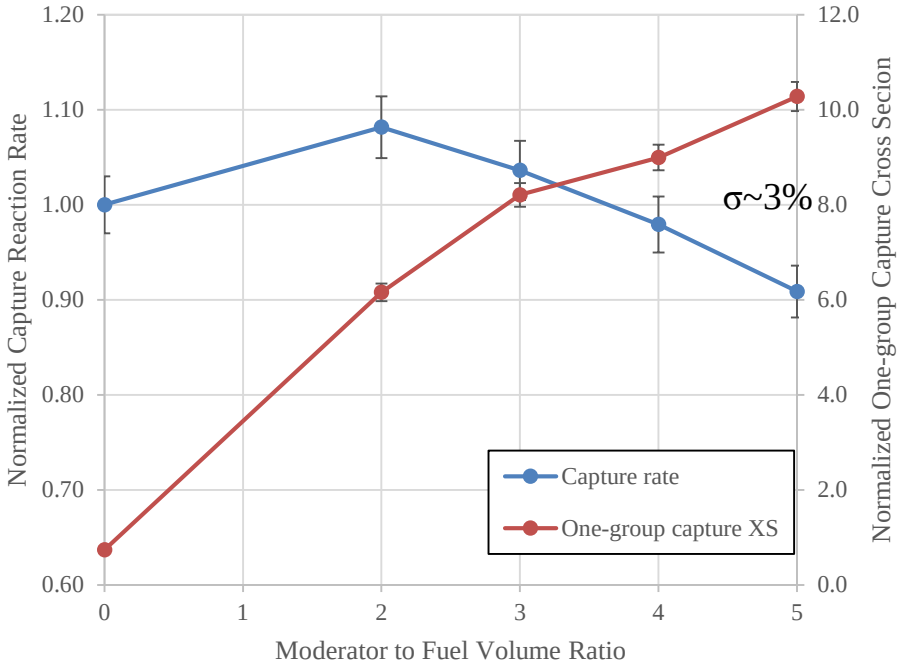

Figure 4.13. Capture Rate and One-group Capture Cross Section of MAs versus Moderator Volume Fraction

As noted above, the transmutation rate per unit MA loading increases with increasing moderator to target volume ratio. On the other hand, the increased moderator to target volume ratio increases the local power peaking in the nearby fuel assemblies and the target assembly itself when a significant amount of MAs are converted into fissile nuclides. As a result, the moderator volume fraction in the target assembly is limited by the peak linear power limit on the driver and target assemblies. Since the linear power in the target assembly is proportional to the irradiation time (i.e., the core residence time of a target assembly), the target irradiation time is also constrained.

In order to investigate the core residence time of target assembly, a full-core depletion calculation was performed using the REBUS-3 code with the cross sections generated using the MC^2-3 and MCNP6 codes for various target assembly designs. The peak linear power of target pins was evaluated using the node-averaged power densities from the DIF3D calculation with homogenized assemblies and the local power peaking factors from the MCNP6 calculations with heterogeneous assembly configurations. The local power peaking factors in the adjacent fuel assembly was also evaluated. The core configuration for this calculation was extracted from the output of REBUS-3 fuel cycle analysis of the LEUFBR core. Since the maximum peak linear power of the neighboring fuel assemblies occurs at the cycle 16, the compositions of the cycle 16 were adopted for evaluating the power peaking. Using the linear power limit of 54.8 kW/m and the peak linear power of the adjacent fuel assembly determined from the REBUS-3 calculation, a maximum allowable local power peaking in the adjacent fuel assembly was determined to be 1.40.

Figure 4.14 shows the peak linear power in the target assembly after one cycle irradiation as a function of the moderator volume fraction in the target assembly. Using the above peak linear power limit of 44 kW/m, the upper limit of the moderator volume fraction that allows at least one cycle irradiation is around 40%. For the target assembly designs with a smaller moderator volume fraction, the number of irradiation cycles can be increased so that the peak linear power at the end of irradiation approaches to the design limit. However, the transmutation rate per cycle increases with moderator volume fraction in the target assembly. To maximize the transmutation performance, a target assembly design with a moderator volume fraction of 39.2% was selected in this study, which satisfies the design limit imposed on the peak linear power in the target assembly.

Figure 4.15 shows the reference configuration of target assembly. The target assembly contains 169 pins of 9.5 mm diameter and has the same assembly dimensions as the driver fuel assembly. Twenty-four MA target pins, one hundred and twenty-seven moderator pins, nine technetium pins and nine calcium iodide pins are almost evenly distributed in the target assembly. The red, blue, orange and yellow pins represent the MAs, zirconium hydride, technetium and calcium iodide pins, respectively. The number of LLFP pins was determined based on the available amount of recovered LLFP from discharged fuels of LEUFBR and the loading management scheme of MA target assemblies. As can be seen in the Figure 4.15, some of the MAs pins and different types of thermal neutron filter pins must be placed at the driver and target assembly interface to reduce the leakage of moderated neutrons to the core. Some of the MAs pins are distributed in the target assembly to make use of the moderated neutrons from the driver fuel assemblies. The local power peaking factors for the target assembly and the

adjacent fuel assembly of this design are 1.37 and 1.36, which satisfy the local power peaking limit estimated based on the fuel/cladding eutectic temperature.

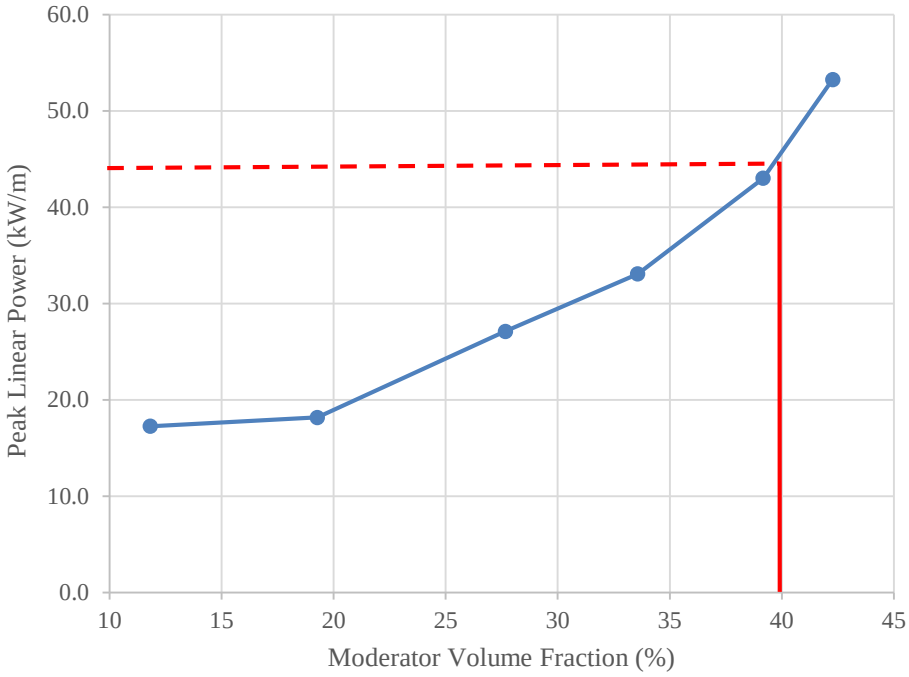

Figure 4.14. Peak Linear Power after One Irradiation Cycle versus Moderator Volume Fraction

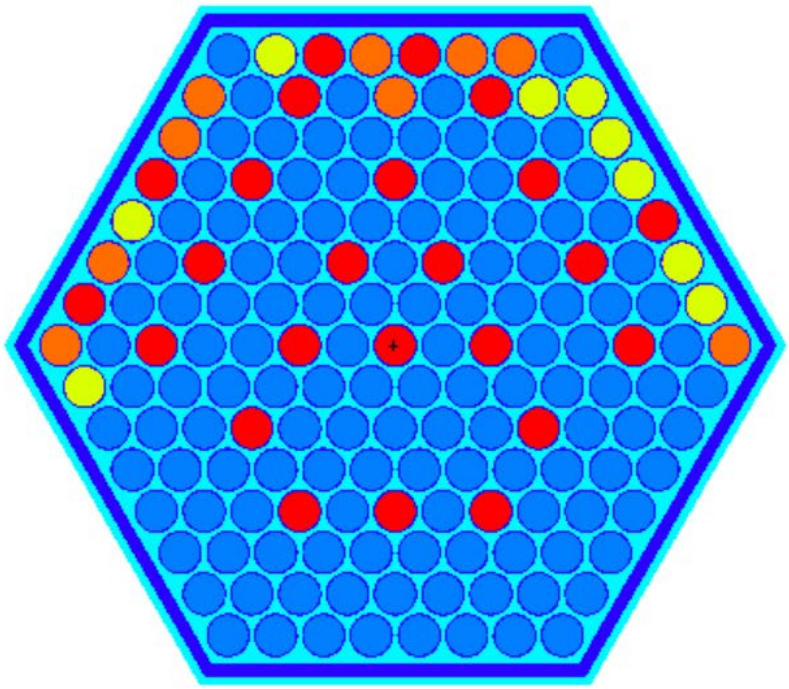

Figure 4.15. Target Assembly Layout (red: MAs, blue: $ZrH_{1.6}$, orange: Tc and yellow: CaI_2)

4.6. Sub-channel Thermal-hydraulics Analysis

To assess the power peaking effects induced by the moderated target assembly, two heating calculations were performed: one with no target assembly and the other with moderated target assemblies. The core configurations for the DIF3D models were extracted from the output of the REBUS-3 fuel cycle analysis of LEUFBR. As discussed in Section 4.4, the BOC and EOC configurations of the cycle 16 were analyzed. The pin power distributions of the case with the moderated target assemblies were calculated by superimposing the local pin power factors in the target and adjacent fuel assemblies determined from a MCNP6 calculation with heterogeneous assembly geometries, on the reconstructed pin power distributions from the DIF3D calculations with homogenized assemblies.

Figure 4.16 gives the LEUFBR core configuration with two target assemblies loaded in the reflector zone and the associated assembly numbers to be used in presenting the calculation results later. Figure 4.17 shows the assembly power distributions at BOC and EOC of the cycle 16. The left hand side (LHS) figure is for the core without the target assembly and the right hand side (RHS) figure is for the core with the target assemblies, which were loaded at BOC of the cycle 16. It is observed that the moderated target assemblies reduce the power production

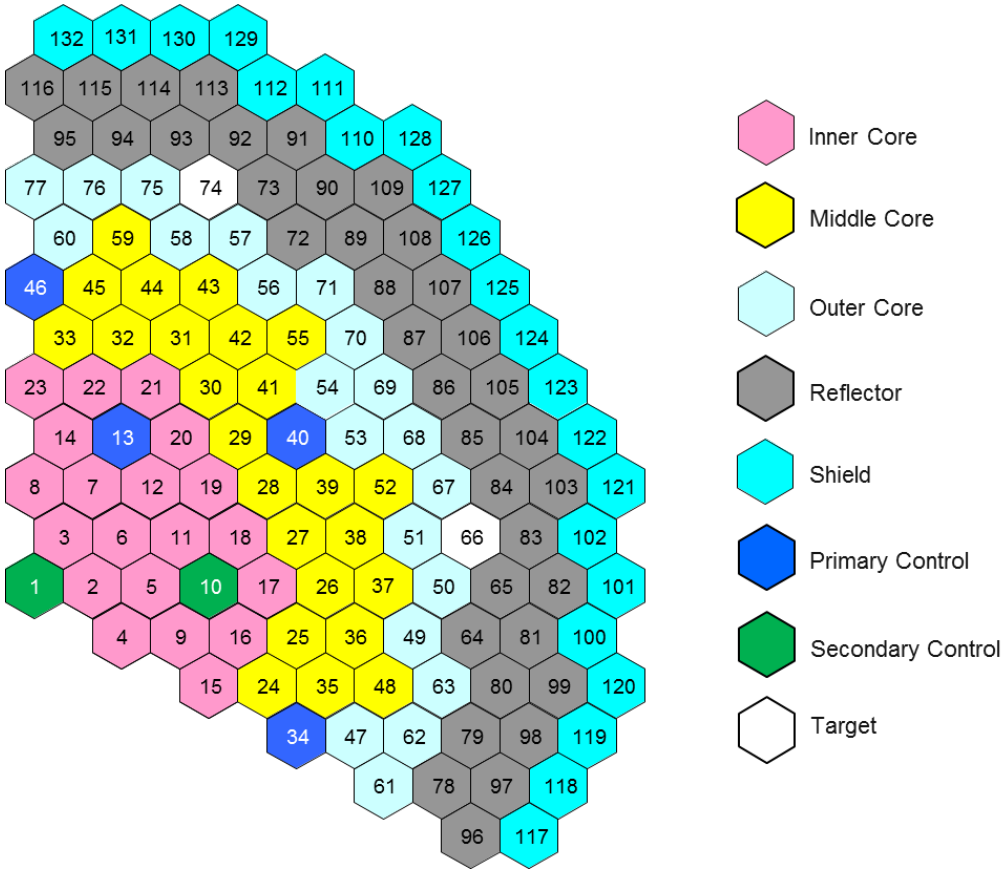

Figure 4.16. Assembly Numbering of LEUFBR Core (1/3 Core)

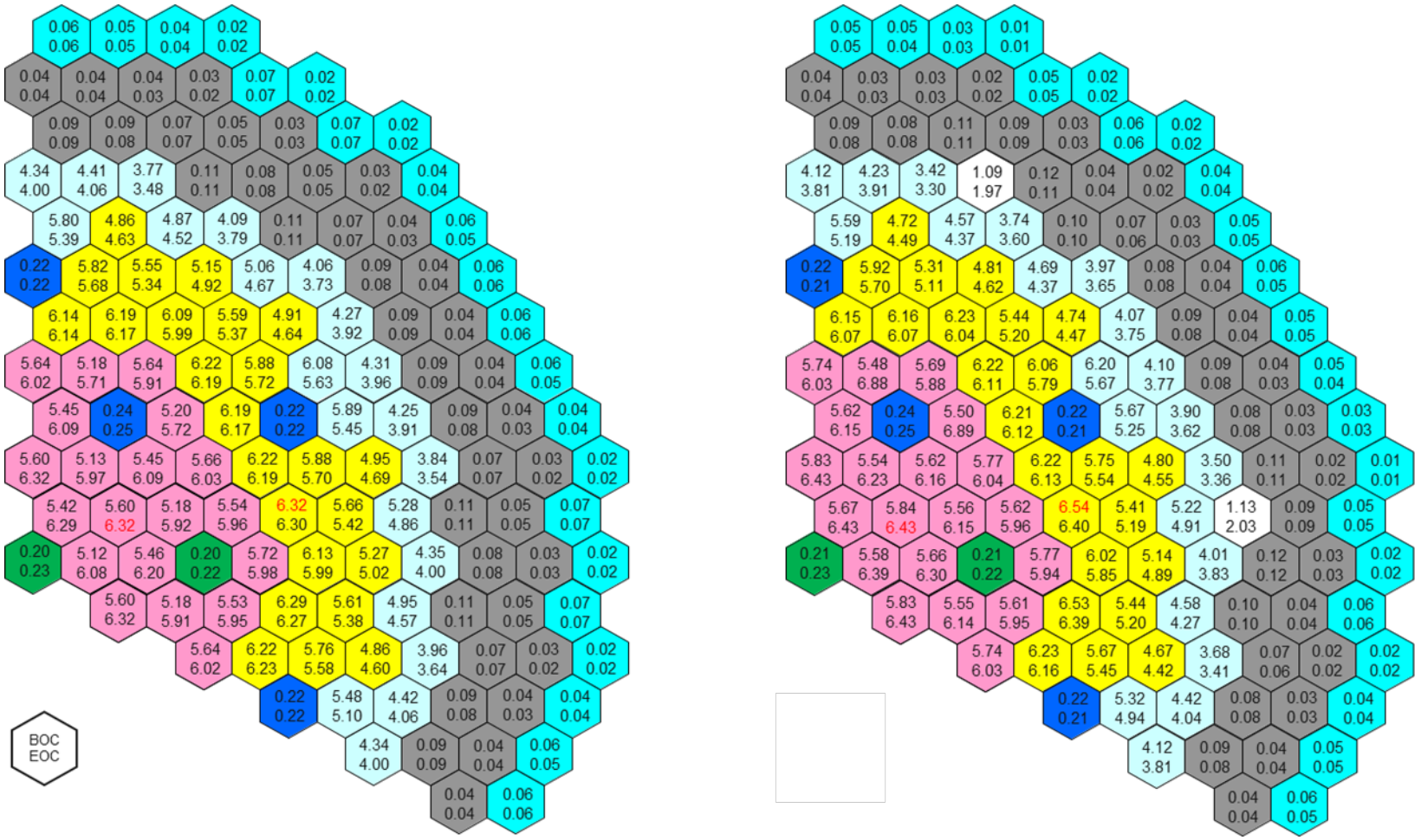

Figure 4.17. Power Distributions (MWt) in LEUFBR Core without (Left) and with Target Assemblies (Right)

in the assemblies near the target assemblies (within 3 or 4 rows of assemblies from the target assemblies) and increase the power production in the assemblies far from the target assemblies. This power shift mitigates the local power peaking effects induced by the moderated target assemblies. The combined effects of the increased pin peaking factor and the decrease of total assembly power result in a decrease in the peak linear power in the fuel assemblies adjacent to target assemblies. In the target assemblies, the power production increases from BOC to EOC because of the fissile material build-up in the MA target pins. In addition, the fission reactions occurred in the target assemblies produced more gamma rays than in the case without target assemblies. The gamma rays were then transported to the nearby reflectors, where the gamma heating performs as the dominant heat source. Therefore, slightly increased power levels in reflectors were observed as shown in Figure 4.17.

Figure 4.18 compares the radial flux distributions around a target assembly (i.e., assembly 66) for the two core configurations. It can be seen that the target assemblies reduce the fast flux in its neighboring fuel assemblies, ~15% in the next assembly. The fast neutrons leaking from the next fuel assembly are moderated in the target assembly by zirconium hydride moderator pins. Because of the thermal neutron filter pins, most of the moderated neutrons are absorbed in the target assembly and only a small fraction can be transported back to the adjacent fuel assemblies. Consequently, the moderated target assemblies become a fast neutron sink and lead to a flux depression in the neighboring fuel assemblies.

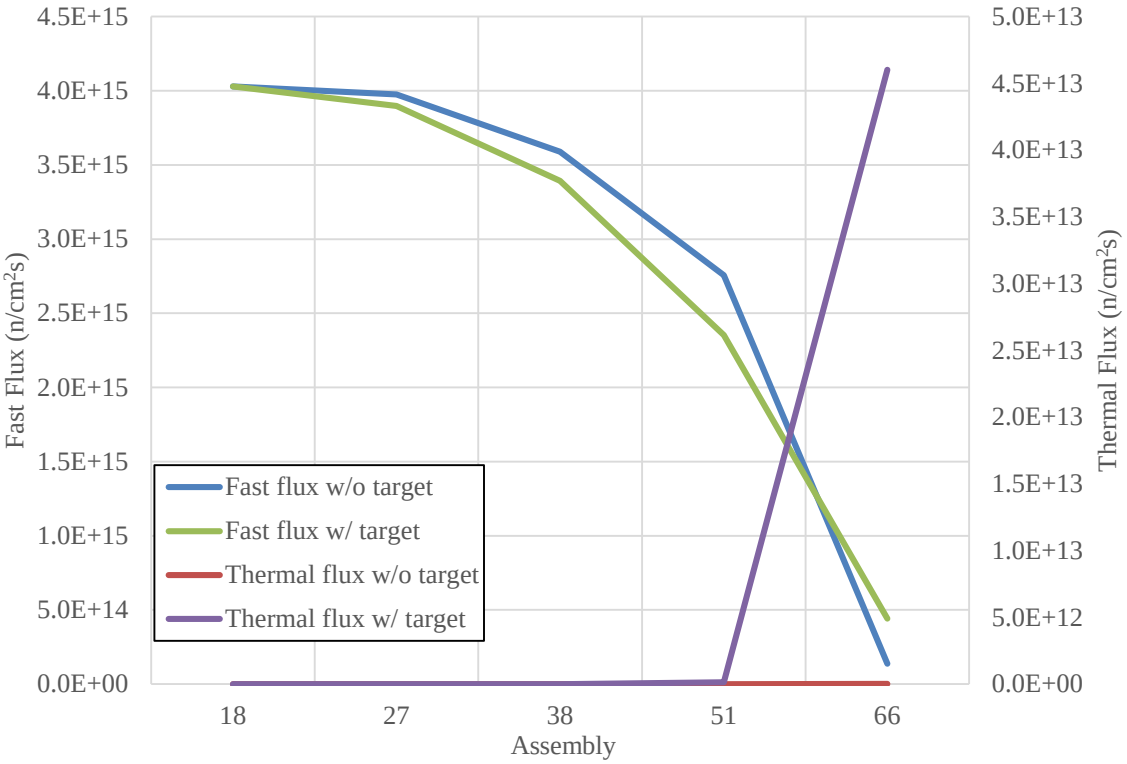

Figure 4.18. Radial Flux Distributions in LEUFBR Core with and without Target Assembly

Orifice zoning of assemblies and flow allocation to the assemblies in each orifice zone were iteratively determined with the overall goal of equalizing the accrual of fuel pin damage and thus pin reliability. The fuel assembles were grouped into five orifice zones, considering the

assembly power levels and the fuel management scheme. The non-fueled assemblies were group into four orifice zones. The assembly flow rates in non-fueled orifice zones were determined to be proportional to the assembly power to yield a uniform coolant outlet temperature. A separate orifice zone was assigned to the target assemblies. The assembly flow rates in individual orifice zones were iteratively determined such that the peak 2-sigma cladding mid-wall temperatures of individual fuel assemblies were equalized over the cycle. Hot channel factors for PRISM design were used for 2-sigma cladding and fuel temperature calculations. Figure 4.19 shows the resulting orifice zones and assembly flow rates of the LEUFBR core.

Figure 4.20 shows the maximum 2-sigma cladding inner wall temperatures of LEUFBR core for the core configurations of the cycle 16 without and with the target assemblies. In both cases, the maximum 2-sigma cladding inner wall temperature occurs at the outer core assemblies in the eighth row at BOC. The temperature of LEUFBR core without target assemblies moves to the middle core assemblies in the sixth row at EOC, while it moves to the inner core assemblies in the second row at EOC for LEUFBR core with the target assemblies. The overall maximum 2-sigma cladding inner wall temperatures during a cycle is 648.4 ºC in the case with no target assembly and 649.2 ºC in the case with the moderated target assemblies. These peak temperatures satisfy the imposed design limit of 650 ºC.

Figure 4.21 shows the minimum 2-sigma margins to the fuel melt for each assembly for the cases without and with the target assemblies. In both cases, the minimum 2-sigma margin to the fuel melt among all the assemblies occurs in the outer core assemblies in the eighth row at BOC, and it moves to the middle core assemblies in the sixth row at EOC. The minimum 2-sigma margin to fuel melt is 151.6 ºC in the case with no target assembly and 142.4 ºC in the case with target assemblies. These results indicate that the peak fuel temperature in both cases has a significant margin of ~150 ºC to the fuel melting temperature (~1100 ºC).

Figure 4.22 shows the pin-bundle pressure drops of fuel and target assemblies. The height of pin bundle is set as 381.6 cm, which includes the height of active core, fission gas plenum, lower shield and end plug. The maximum pressure drop across the pin bundle is about 0.43 MPa in the case with no target assembly and about 0.45 MPa in the case with target assemblies. The pin-bundle pressure drops of LEUFBR are slightly higher than the pressure drops in the ABR design, from which the LEUFBR core design started. The maximum pin-bundle pressure drop of ABR is 0.38 MPa [3,4]. The thicker pin design of LEUFBR core results in a decreased flow area in the fuel assembly and hence the flow velocity is increased. In addition, the increased core height in LEUFBR also contributes to the higher pin bundle pressure drops.

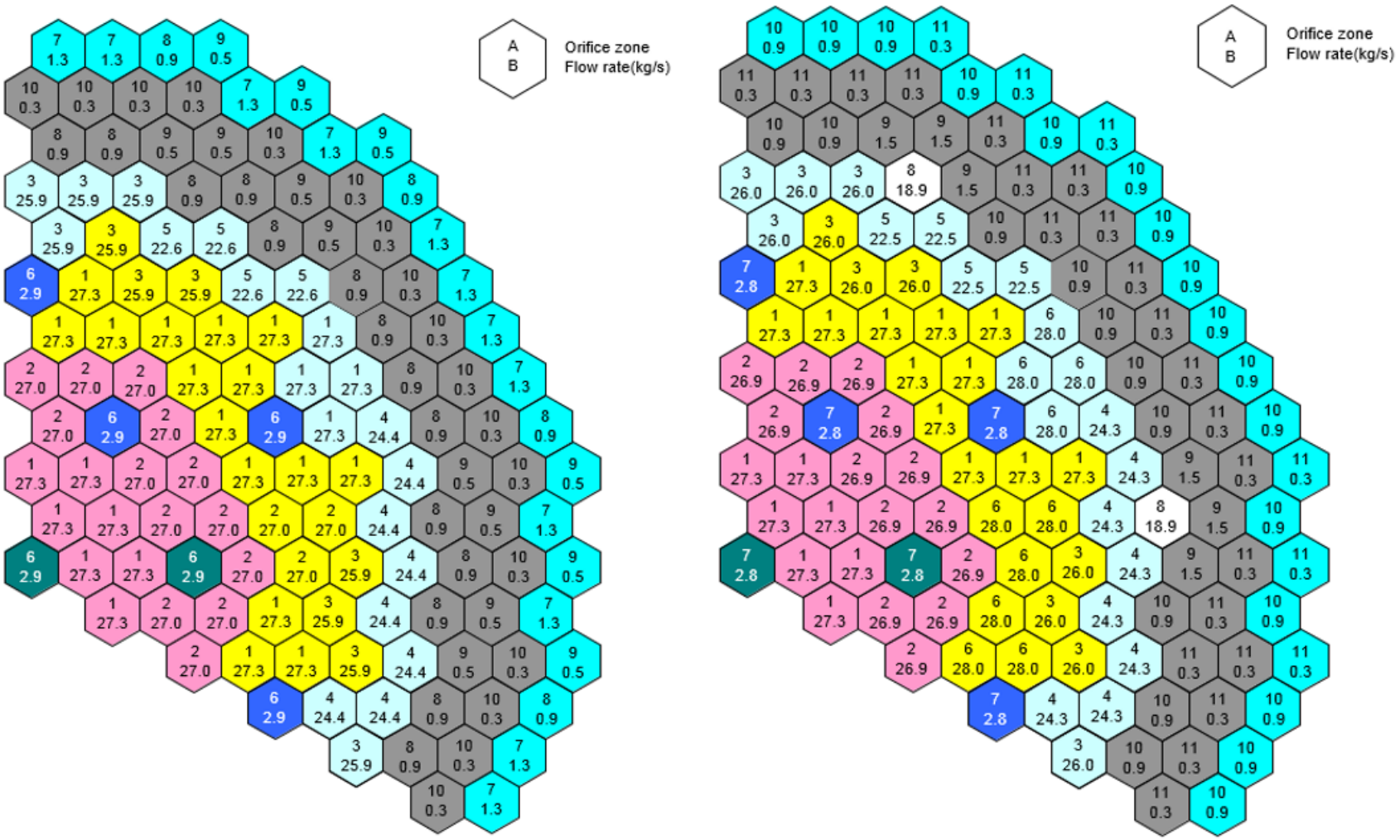

Figure 4.19. Orifice Zones and Assembly Flow Rates (kg/s) of LEUFBR Core without (Left) and with Target Assemblies (Right)

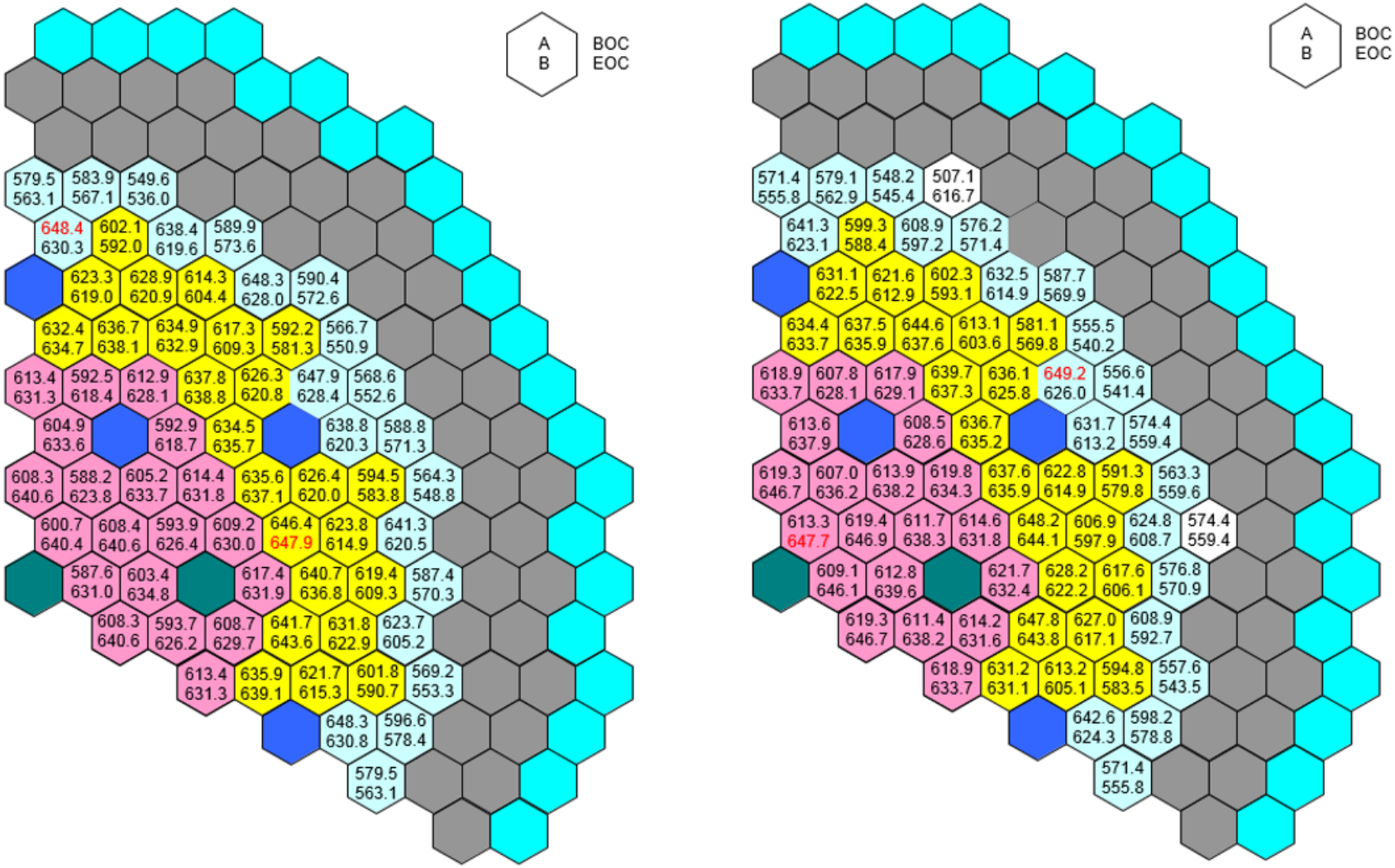

Figure 4.20. Maximum 2-sigma Cladding Inner Wall Temperatures (ºC) of LEUFBR Core without (Left) and with Target Assemblies (Right)

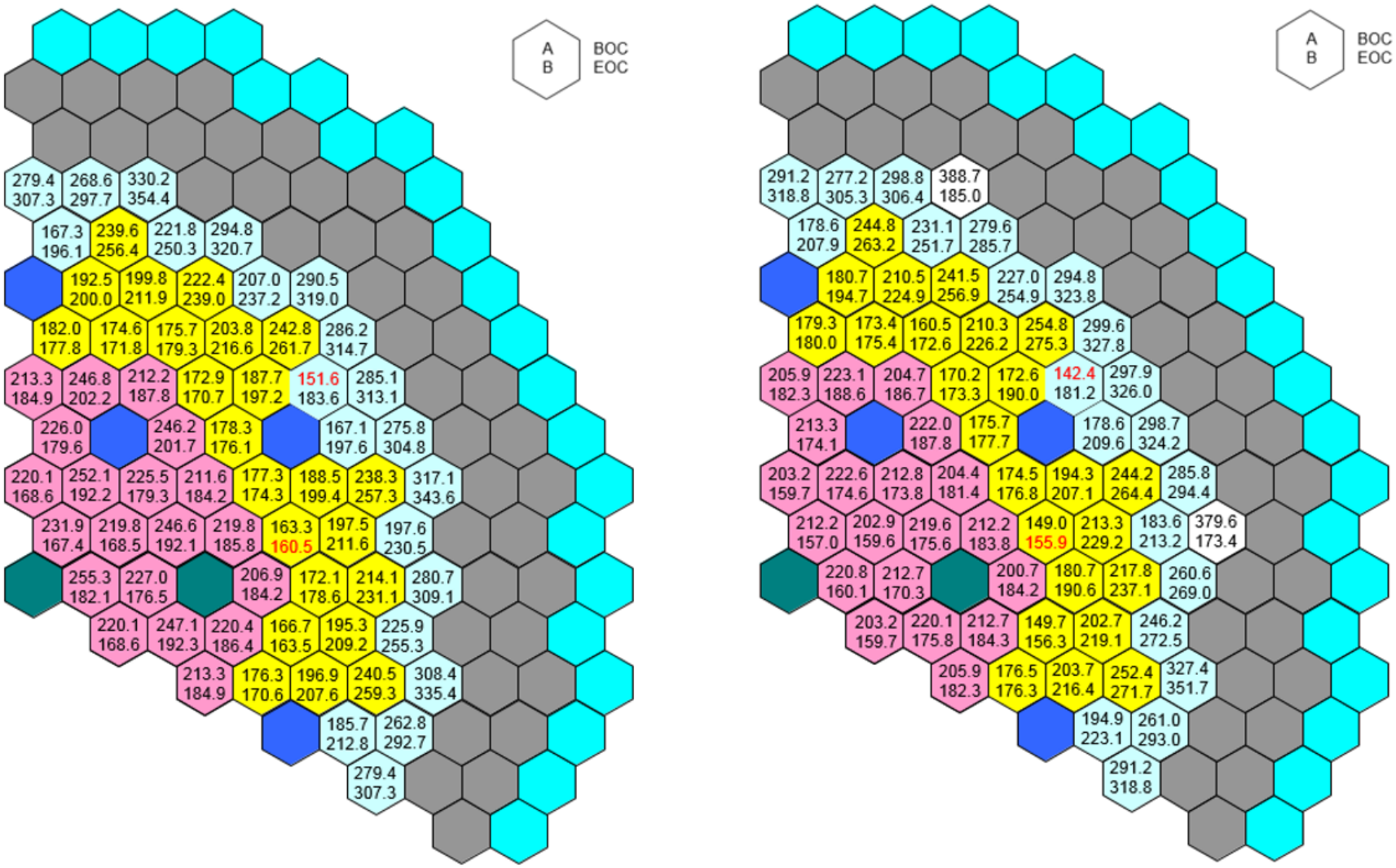

Figure 4.21. Maximum 2-sigma Margins to Fuel Melt (ºC) of LEUFBR Core without (Left) and with Target Assemblies (Right)

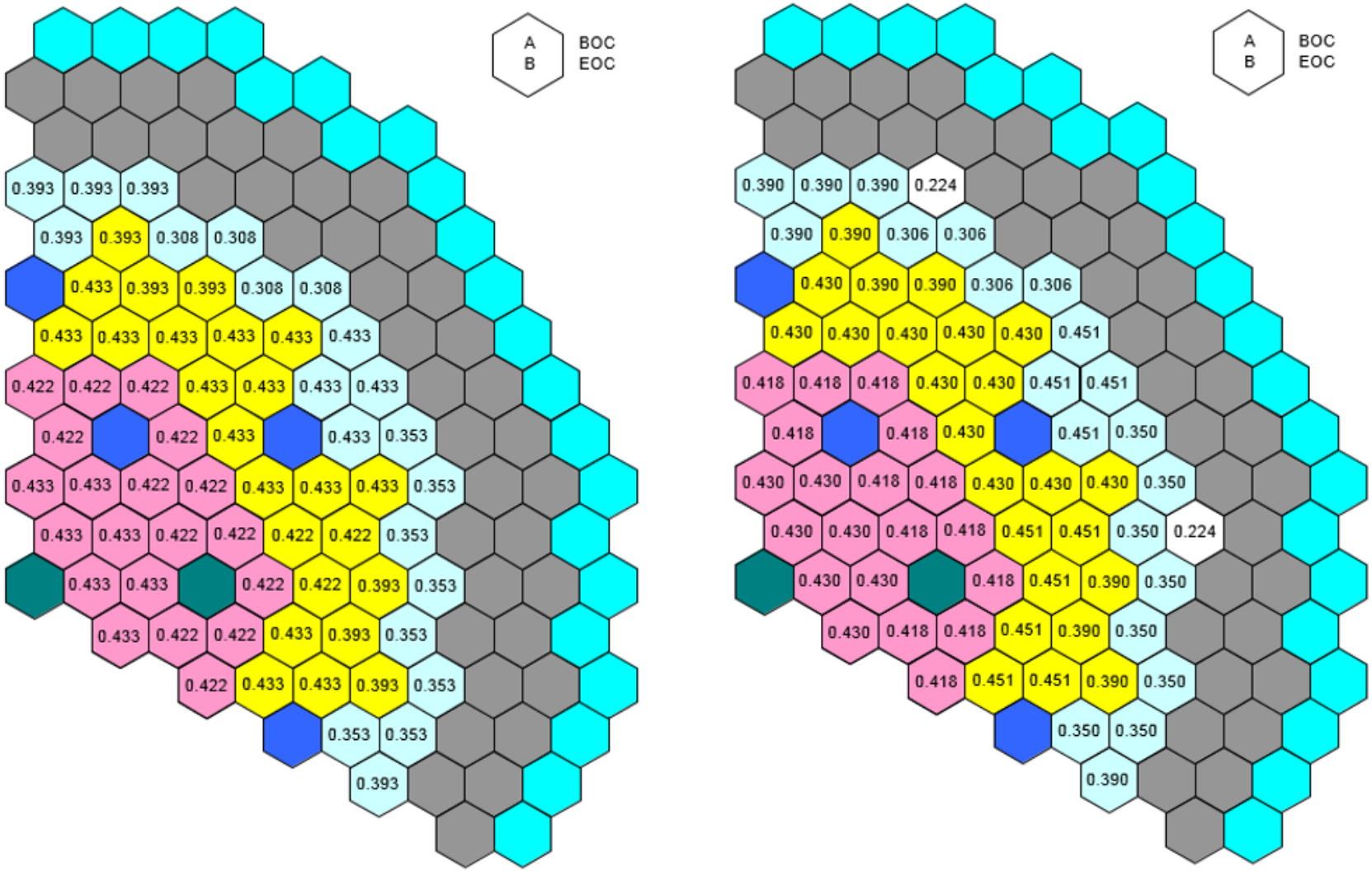

Figure 4.22. Average Pin Bundle Pressure Drop (MPa) of LEUFBR Core without (Left) and with Target Assemblies (Right)

4.7. Transmutation Performance of LEUFBR with Target Assemblies

The transmutation capability of LEUFBR was investigated using the LEUFBR core design and the target assembly design discussed in Section 4.5. A full-core depletion calculation was performed to evaluate the efficiency of MA transmutation in the LEUFBR core. Using the cross sections generated with the MC^2-3 and MCNP6 codes, an equilibrium cycle calculations were performed to analyze the performance of the target assembly at the equilibrium state. In addition, an explicit cycle-by-cycle calculation was performed for an assumed plant lifetime of 60 years to study the overall MA transmutation performance of the LEUFBR core.

The bred fissile and remaining MA nuclides in target assemblies can be recycled in the LEUFBR or sent to the second-stage ADS. In this study, it was assumed that the bred Pu and MAs in target assemblies would be recycled into the LEUFBR and the remaining MAs would be sent to the second-stage ADS if the total amount of recovered MA were larger than the capacity of target assemblies. It was also assumed that Pu and MA are recovered in two separate production streams. The recovered Pu from target assemblies is mixed with the recovered U and Pu from the discharged fuel and recycled into the driver fuel assemblies. The recovered MA from the discharged fuel of both driver fuel and target assemblies was recycled in the target assemblies.

In order to minimize the local power peaking problem induced by moderated target assemblies, the target assemblies were loaded in the reflector region. The loading of target assemblies in the reflector region utilizes the neutrons leaking out of the core and minimizes the perturbation in the core performances. The core residence time of target assemblies was one burn cycle, which was constrained by the peak cladding inner wall temperature. Based on the results from the equilibrium cycle analysis of LEUFBR, a loading scheme of six target assemblies was selected to minimize the buildup of MAs in the LEUFBR core at the equilibrium state. As discussed in Section 4.6, the LEUFBR core with six moderated target assemblies satisfied all the imposed thermal design limits. To confirm that the other properties are not affected noticeably either, the core reactivity coefficients and kinetics parameters as well as the reactivity control requirements and shutdown margins were evaluated for the equilibrium core loaded with six target assemblies. The results showed that the presence of target assemblies would not have a significant impact on the performance of LEUFBR. Minimal differences were observed in fuel density coefficient and the sodium void worth due to the change in fuel composition. The integral reactivity parameters for the quasi-static reactivity model showed that the passive safety features remained unchanged.

Table 4.3 shows the TRU mass flow of driver fuel and target assemblies. At the equilibrium state, a total amount of 17.9 kg of MA was loaded in the target assemblies, whereas 19.7 kg of MA was recovered from the reprocessing facility. The amount of MAs to be sent to the ADS was 1.8 kg. After one cycle irradiation, the remaining MA and the Pu generated in the target assemblies were 9.2 kg and 3.2 kg, respectively. A transmutation rate of 48.6% and an absolute transmutation amount of 8.8 kg were obtained with six target assemblies. It was found that the total transmutation amount of MA is saturating with increasing number of target assemblies. The MA transmutation rate with twelve target assemblies was roughly 8.8 kg/cycle, in which higher mass actinides were increased due to the successive neutron captures.

Table 4.3. TRU Mass Flow per Cycle in Driver Fuel and Target Assemblies at Equilibrium State of LEUFBR

Isotope	Discharged Drivers		Target Assemblies			
			BOEC		EOEC	
	Mass, kg	Fraction, %	Mass, kg	Fraction, %	Mass, kg	Fraction, %
Np-237	2.99	28.6	3.75	20.9	0.84	6.8
Pu-236	- -	- -	- -	- -	0.00	0.0
Pu-238	- -	- -	- -	- -	2.23	18.0
Pu-239	- -	- -	- -	- -	0.36	2.9
Pu-240	- -	- -	- -	- -	0.14	1.1
Pu-241	- -	- -	- -	- -	0.18	1.4
Pu-242	- -	- -	- -	- -	0.29	2.3
Am-241	4.62	44.2	4.40	24.6	0.05	0.4
Am-242	0.18	1.7	0.17	1.0	0.00	0.0
Am-243	1.97	18.8	2.34	13.1	0.73	5.9
Cm-242	0.20	1.9	0.24	1.4	0.52	4.2
Cm-243	0.01	0.1	0.04	0.2	0.04	0.3
Cm-244	0.46	4.4	5.15	28.8	5.18	41.9
Cm-245	0.03	0.3	0.32	1.8	0.31	2.5
Cm-246	0.00	0.0	1.47	8.2	1.49	12.1
MAs	10.5		17.9		9.2	
TRU	10.5		17.9		12.3	

The results from the equilibrium cycle analysis showed that the use of moderated target assemblies could effectively reduce the amount of MA to be sent to ADS. Using the same loading scheme of six target assemblies, non-equilibrium cycle-by-cycle analyses were performed to study the overall MA transmutation performance of the LEUFBR core over the assumed plant lifetime of 60 years. It was assumed that a target assembly would be fabricated only when the recovered amount of MAs is sufficient to fabricate at least one assembly. Based on the available amount of recovered MA, the target assemblies were loaded in the core from the 9-th cycle. After one irradiation cycle in the core, six target assemblies were discharged and sent to the reprocessing plant. Considering the reprocessing and fabrication times, it was assumed that the MA in the target and driver fuel assemblies discharged at the end of n-th cycle would be recycled to the core at the beginning of (n+2)-th cycle. Since the amount of recovered MA varied with burn cycles, some MA pins were replaced with LLFP pins when the available MA was less than the MA loading in the reference design of target assembly. Total one hundred and ninety-two target assemblies were loaded in the core over an assumed plant lifetime of 60 years.

Figure 4.23 presents the accumulated MA of LEUFBR core over each cycle. Without MA recycling in LEUFBR, 533.0 kg of MAs and 395.7 kg of LLFPs (technetium and iodine) were accumulated for the assumed plant lifetime of 60 years. With the use of 192 target assemblies, overall transmutation fractions of 88.6% and 36.1% were obtained for MAs and LLFPs,

respectively. It can be seen that the MA produced in each cycle can be consumed in six target assemblies from cycle 9 to cycle 38. The inventory of MA left at the end of plant lifetime is the MAs remaining in the target assemblies discharged at the end of cycles 39 and 40, which have not been recycled. On the other hand, the LLFPs were produced more in the core than consumed in six target assemblies, and thus they accumulated with burnup cycles. These results indicate that the MAs can be more effectively transmuted than the LLFPs by implementing moderated target assemblies. This is due to the relatively large transmutation cross sections of MAs than those of LLFPs. The MA and LLFP inventories at the end of plant lifetime are 61.0 kg and 253.0 kg, respectively, and they need to be burned in ADS.

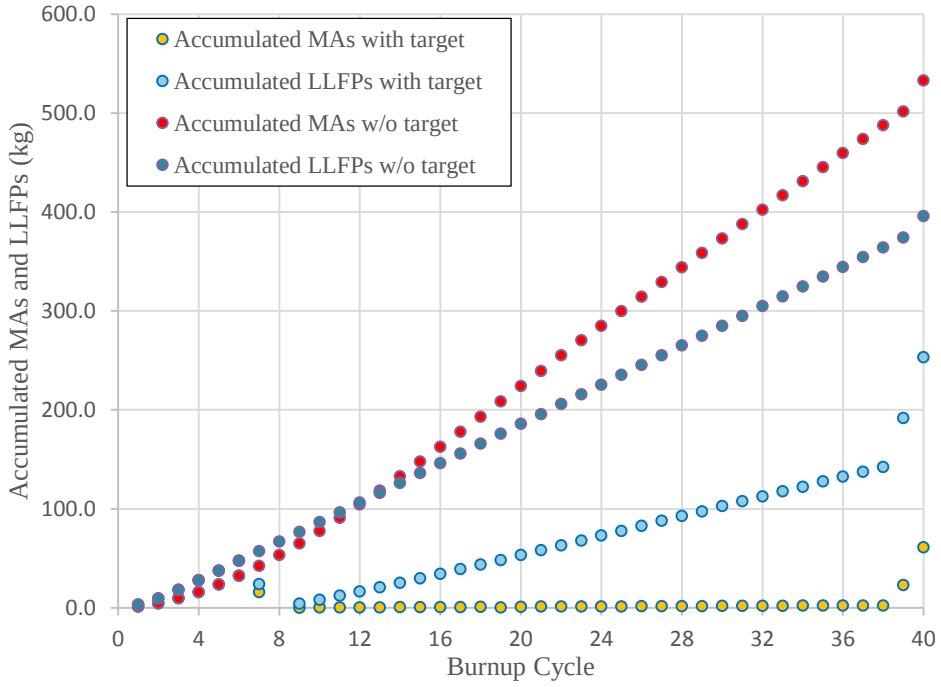

Figure 4.23. Accumulated MAs and LLFPs vs. Burn Cycle of LEUFBR Core

5. Fuel Cycle Performance of Three Fuel Cycle Options

Using the FR, ADS and MA target assembly designs discussed in Sections 2, 3 and 4, the fuel cycle performances of the two proposed two-stage fuel cycle options are evaluated. One is the two-stage fuel cycle option of continuous recycle of plutonium in a FR and subsequent burning of MAs in ADS. The other option is the two-stage fuel cycle option with MA target assemblies employed in FR to reduce the amount of MAs to be sent to the second-stage ADS. For comparison, a single-stage fuel cycle option that employs homogeneous recycling of TRU in the FR was considered as well.

The performance characteristics of these three fuel cycle options were evaluated against the Fuel Cycle Evaluation Metrics of the Fuel Cycle Options Campaign. For each fuel cycle option, the fuel cycle data package was prepared for the equilibrium state as the evaluations considered in the nuclear fuel cycle E&S report [2]. The mass flow data was evaluated for a 100 GWe-yr electricity production based on the equilibrium cycle calculation. For fair comparison of the amount of fuel materials used and wastes produced in each fuel cycle option, the same nuclear loss rates of 0.2% in the fresh fuel fabrication and 1% in the discharged fuel separation were assumed. The reactor and fuel information of each fuel cycle is provided in Appendix C.

5.1. Two-stage Fast Spectrum Fuel Cycle Options Based on FR and ADS

The performance characteristics were evaluated for the two fuel cycle options proposed in this study. One is a two-stage fuel cycle option of continuous recycle of plutonium in a FR and subsequent burning of MAs in ADS. The first-stage FR starts with LEU fuel. Pu and uranium are co-extracted from the discharged fuel and recycled into FR, and the recovered MAs are sent to the second-stage ADS. At the equilibrium cycle, the reactor will operate with the recovered plutonium and natural uranium only without supporting LEU. The other is a two-stage FR/ADS fuel cycle option with MA targets in the FR. In the second option, the recovered MAs are not directly sent to ADS, but partially incinerated in the FR in order to reduce the amount of MAs to be sent to the ADS.

5.1.1. First Two-Stage FR/ADS Fuel Cycle Option

The first proposed two-stage fuel cycle option of continuous recycle of plutonium in the FR and subsequent burning of MAs in ADS is illustrated schematically in Figures 5.1 to 5.3. In the first stage, the FR is categorized as the uranium-fueled core (i.e., LEUFBR) and the Pu-fueled core based on the external fuel feed at BOL. The LEUFBR is operated for the assumed plant lifetime of 60 years starting from an initial uranium core, and the accumulated uranium and Pu including the core inventory at EOL are used to start the Pu-fueled FR. The fuel volume fraction of Pu-fueled FR was reduced to 35.1% to minimize the TRU generation while maintaining the fissile break-even with external feed of natural uranium only. A two-year transition time from a LEUFBR to a Pu-fueled FR was assumed to account for the fuel separation, fabrication and reloading. For both FR cores, Pu and U are co-extracted from the discharged fuel and recycled back into the reactor. The recovered MAs are sent to the second-stage ADS. The initial HM inventory of ADS is extracted from the discharged fuel of LEUFBR. The discharged fuel of ADS is reprocessed, and all the recovered HMs is recycled into the ADS along with the MAs recovered from the first-stage FR.

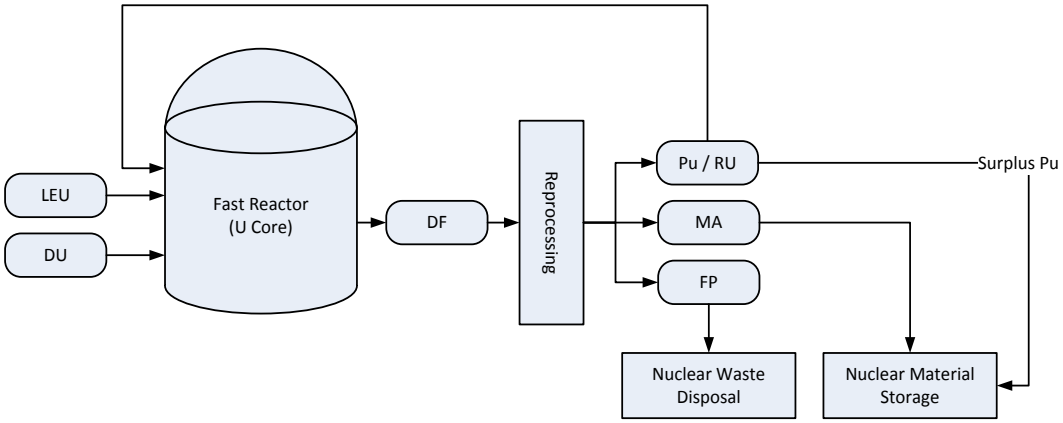

Legend:

LEU = Low-Enriched Uranium DU = Depleted Uranium DF = Discharged Fuel

RU = Recovered Uranium MA = Minor Actinides FP = Fission Products

Figure 5.1. Schematic Illustration of First Two-Stage FR/ADS Fuel Cycle Option (U Core, LEUFBR, before Starting ADS)

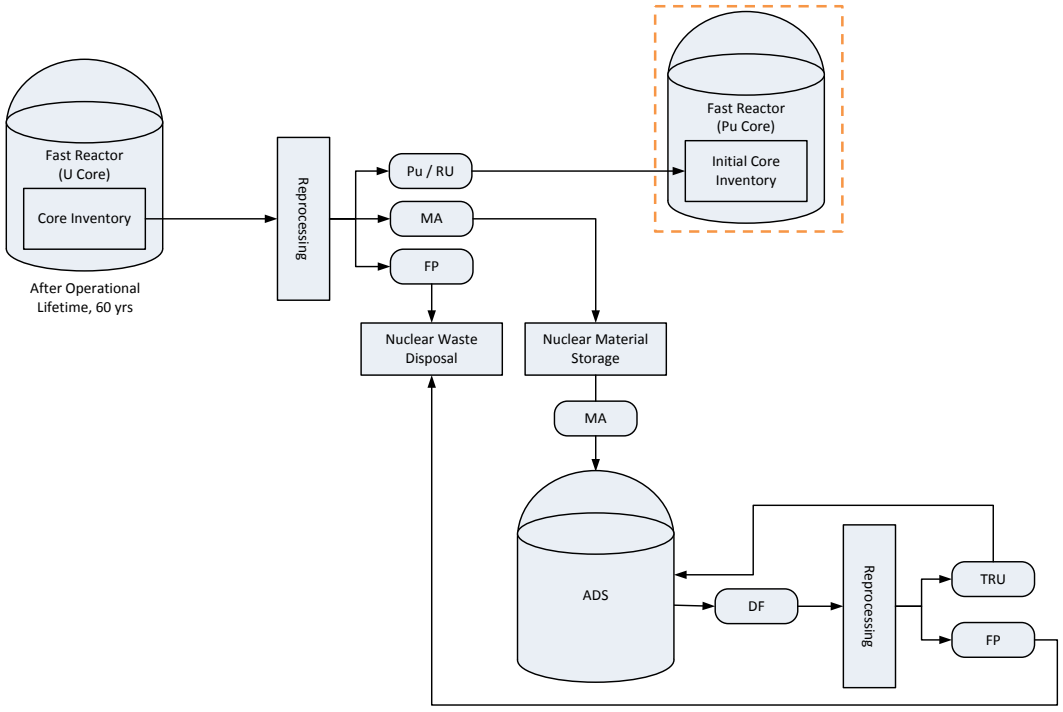

Figure 5.2. Schematic Illustration of Transition between U/Pu-fueled FRs in First Two-Stage FR/ADS Fuel Cycle Option

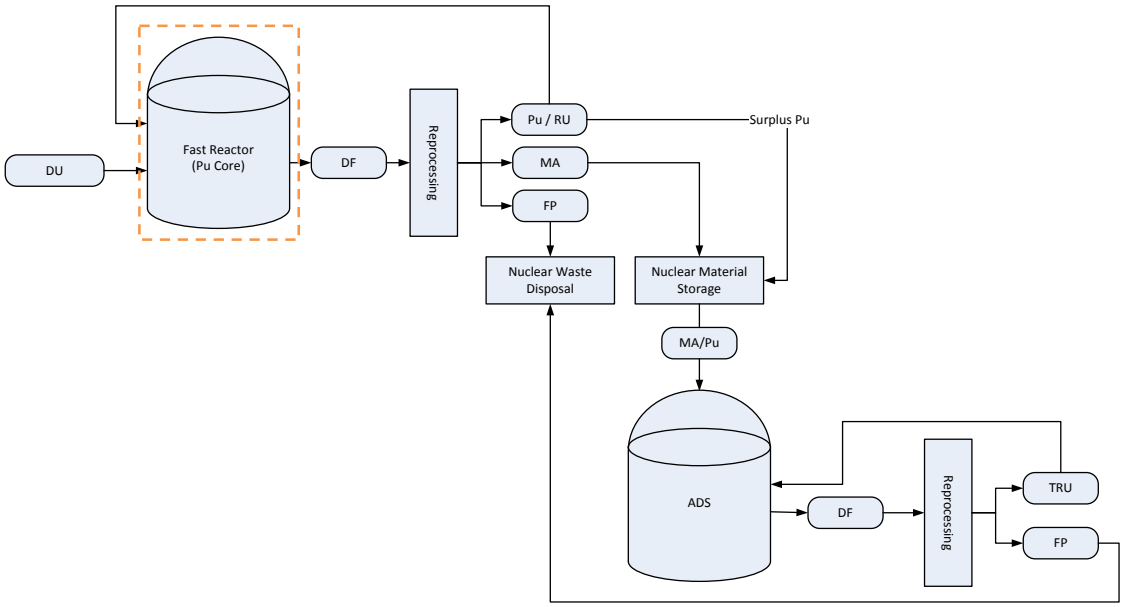

Figure 5.3. Schematic Illustration of First Two-Stage FR/ADS Fuel Cycle Option (Equilibrium State)

The performance characteristics of the first proposed two-stage fuel cycle option are summarized in Table 5.1. The MA generation rate in the Pu-fueled FR is 6.5 kg/year while the TRU consumption rate of the ADS is 232.6 kg/year. The number of Pu-fueled FRs to be supported by one ADS was estimated to be 37 based on the mass balance of MA at the equilibrium state. With an assumed separation loss of 1% and a fabrication loss of 0.2%, the Pu-fueled FR produces only negligible amount of surplus Pu (0.2 kg/year) for an equilibrium cycle. This surplus Pu would be burned with MA in the ADS. The Pu-fueled FR reaches the break-even core after 19 burn cycles (28.5 years). For the succeeding cycles, the required fresh fuel to maintain the targeted cycle length (18 months) can be fabricated only with the recycled fuel and natural uranium. The amount of Pu required to start a Pu-fueled FR is 3.5 MT, while each reference LEUFBR (LEU-fueled FR with a fuel volume fraction of 39.4% and 35.3%) produces 3.7 MT of Pu over its assumed lifetime of 60 years. As a result, 35 LEUFBRs are required to support 37 Pu-fueled FRs from the Pu mass balance.

In order to present the fuel cycle performance in the general form, the mass flow data was evaluated for a 100 GWe-yr electricity production based on the equilibrium cycle calculation. Electricity sharing between the first-stage Pu-fueled FR and the second-stage ADS was determined based on the mass balance between the recovered MA and surplus Pu mass in the first stage and the consumed TRU mass in the second stage. TRU was recovered in the first-stage FR at a rate of 18 kg/GWe-yr, and TRU was consumed by fission in the second-stage ADS at a rate of 958 kg/GWe-yr. In order to balance the consumed TRU in ADS and the recovered TRU from FRs, the electricity sharing between FR and ADS is 98.1% to 1.9% for this fuel cycle option.

Table 5.1. Comparison of Two-Stage Fuel Cycle Performance Parameters

Parameter		U-fueled FR	Pu-fueled FR	ADS
Reactor power, MWt		1000	1000	840
Fuel form		U-10Zr/ U-Pu-10Zr	U-Pu-10Zr	MA-10Zr dispersion
Cycle length, months		18	18	6
Capacity factor, %		90	90	75
Specific power, MW/MT		42.5	47.6	203.7
Number of batches		3/3/4	3/3/4	7/8/8
Average fuel residence time, year		4.98	4.98	3.79
Fuel inventory in core, MT		22.8	20.4	4.2
Charge fuel mass per batch, MT		7.2	6.4	0.6
Charge fuel mass fraction, %	U Pu MAs	100/87.2* 0/12.8 0	86.7 13.3 0	3.4 35.8 60.8
Surplus Pu plus EOL Pu inventory, MT		3.7	---	---
Pu inventory at (BOEC+2)-th cycle feed, MT		---	3.5	---
Discharged MAs from FR, kg/year		---	6.5	---
TRU consumption in ADS, kg/year		---	---	232.6
Number of systems		35	37	1

* BOL/EOL

Table 5.2 shows the mass flow data at equilibrium state estimated for a 100 GWe-yr electricity generation using the fuel cycle performance parameters. In this table, the signs of (-) and (+) present the feed to and the product form each system, and the masses in each column show the mass flow per each technology to support each stage. At the equilibrium state, the FR is fueled with 1005.0 MT of U and 153.9 MT of Pu, whereas 904.3 MT of U, 154.2 MT of Pu, 1.7 MT of MA are recovered from the reprocessing facility. During the reprocessing/separating and fresh fuel fabrication processes, 10.7 MT and 2.3 MT of nuclear materials are lost to the waste stream, respectively. The masses in the last column indicate the required (-) or produced (+) nuclear material per year needed to generate 100 GWe-yr of electricity. Results show that approximately 102.8 MT of natural uranium would be required for sustaining this two-stage fuel cycle option. Since the Pu and MA are continuously recycled, this fuel cycle option does not release Pu or MA except for the loss from the fuel fabrication and separation. For the overall fuel cycle, there are 90.5 MT of FPs and 13.1 MT of HM sent to the repository.

Compared to the two-stage fuel cycle option based on PWR and ADS [26], the two-stage, fast-spectrum fuel cycle option significantly improves the uranium resource utilization and reduces the loss of HM to the waste stream. For a total energy generation of 100 GWe-yr, the required natural uranium is reduced from 14,027 MT to 103 MT, and the amount of HM to be sent to the geological repository is reduced from 26.0 to 13.1 MT.

The direct use of LEU as the startup fuel of FR also enhances the uranium resource utilization relative to the option to generate the startup Pu fuel in current light water reactors (LWRs). If the TRU recovered from 10-year cooled LWR-used fuel of 50 MWd/kg burnup is

used as the FR startup fuel, a total amount of 4.3 MT of TRU is required to feed a FR until it reaches a self-sustaining equilibrium cycle. This requires 303.5 MT of LWR used fuel to be processed. Assuming a U-235 enrichment of 4.2% and an enrichment tail of 0.2%, 2,375.6 MT of natural uranium is required to fabricate 303.5 MT of LWR fuel. Normalized to the amount of electricity generation, the direct use of LEU in FR enhances the uranium resource utilization by a factor of ~1.5. It is noted that if the comparison is limited to the new uranium resources from the present moment, existing LWR used fuel requires no new uranium resource.

Table 5.2. Mass Flow Data of the First Proposed Two-stage FR/ADS Option (Metric Ton per 100 GWe-yr at Equilibrium State)

Stage		1			2			Sum
Technology		Fuel	NPPT[a]	Rep/Sep[b]	Fuel	NPPT	Rep/Sep	
Electricity, GWe-yr		98.1			1.9			100.0
Feed or product of nuclear materials (MT)								
Natural resource	NU	-102.8						-102.8
	Th							
Products from fuel or NPPT technology	DU							
	U	+1,005.0	-1,005.0		+0.3	-0.3		0.0
	Pu	+153.9	-153.9		+3.2	-3.2		0.0
	MA				+5.5	-5.5		0.0
	DF		+1,159.7	-1,159.7		+9.0	-9.0	0.0
Products from Rep/Sep technology	RU	-904.3		+904.3	-0.3		+0.3	0.0
	Pu	-154.2		+154.2	-3.1		+3.0	0.0
	MA			+1.7	-5.6		+3.9	0.0
	FP			+88.7			+1.7	+90.5
Loss[c]		+2.3		+10.7	+0.0		+0.1	+13.1

[a] NPPT = Nuclear Power Plant / Transmutation
[b] Rep/Sep = Reprocessing / Separation
[c] Loss of U, Pu and MAs

5.1.2. Second Two-Stage FR/ADS Fuel Cycle Option with MA Targets in FR

The performance characteristics of the second fuel cycle option of the two proposed two-stage FR/ADS fast spectrum fuel cycles are presented in this subsection. As shown in Figure 5.4, the first stage is a sodium-cooled FR fuel cycle similar to the counterpart of the first proposed FR/ADS fuel cycle option discussed in Section 5.1.1. Pu and uranium are co-extracted from the discharged fuel and recycled in the first stage, but the recovered MAs are not sent to the second stage directly. The recovered MAs are made into target assemblies and incinerated in the first-stage FR. As discussed in Section 4, the recovered MA can be effectively converted into fissile nuclides in moderated target assemblies by utilizing their large capture cross sections in the thermal energy region. The total amount of MA to be sent to ADS for this fuel cycle option with moderated MA target assemblies is about one-sixth of that for the first proposed fuel cycle option discussed in Section 5.1.1.

The fuel cycle performance of this two-stage fuel cycle option was evaluated with the reference FR core and ADS blanket designs. The equilibrium cycle analyses for the first-stage FR were discussed in Section 4.7. Using the MAs recovered from the first stage, the equilibrium cycle calculation was performed for the second-stage ADS. In the equilibrium cycle model of

REBUS-3, the HM recovered from discharged ADS fuels was used as the primary HM feed and the MAs recovered from target assemblies and the surplus Pu of the first-stage FR were used as the external feed to make up for the TRU consumed by fission. The isotopic composition of the recovered TRU at equilibrium cycle is presented in Table 5.3. It is noted that the fraction of the high mass actinides were increased in the external feed stream. This is mainly due to the successive neutron captures of actinides in moderated target assemblies. A significant difference is observed in the fraction of Cm-244 which is mainly produced by the (n,γ) reaction of Am-243 via β decay of Am-244.

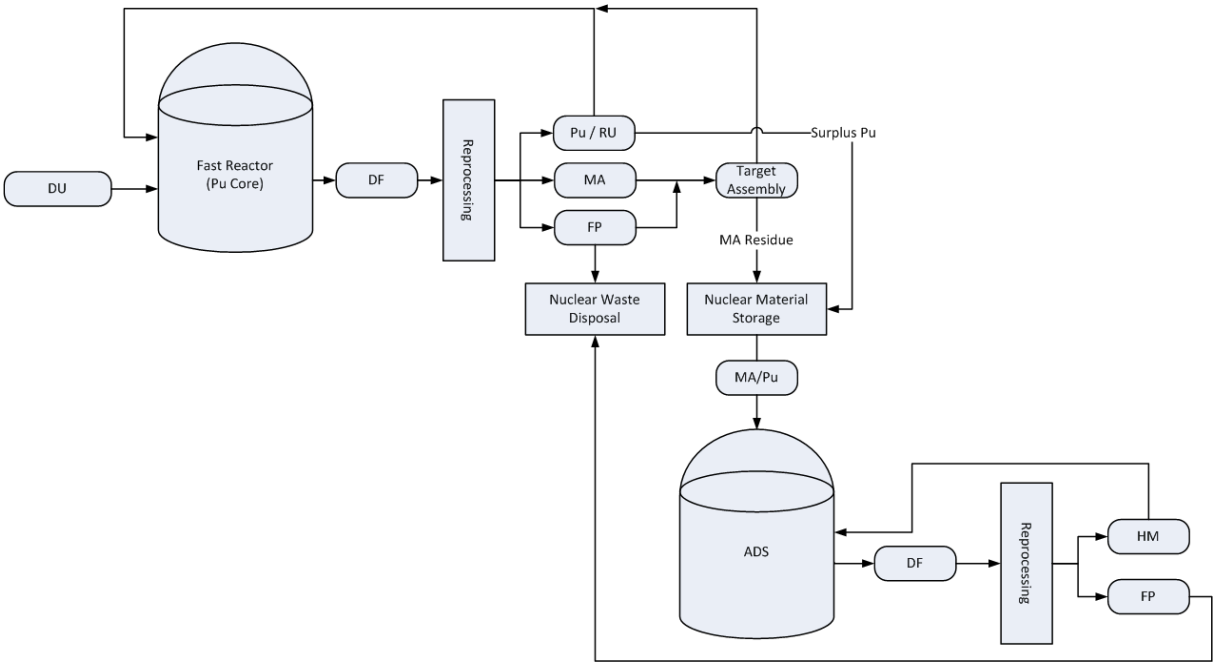

Figure 5.4. Schematic Illustration of the Second Proposed Two-stage FR/ADS Option (Equilibrium State)

Table 5.3. Isotopic Composition of External Feed for Second-Stage ADS

Isotope	%	Isotope	%	Isotope	%
Np-237	6.8	Pu-236	0.0	Pu-238	18.0
Pu-239	2.9	Pu-240	1.1	Pu-241	1.4
Pu-242	2.3	Am-241	0.4	Am-242m	0.0
Am-243	5.9	Cm-242	4.2	Cm-243	0.3
Cm-244	41.9	Cm-245	2.5	Cm-246	12.1

Table 5.4 presents the equilibrium cycle performance of the sodium-cooled ADS system of the second two-stage fuel cycle option. In the equilibrium core, the HM inventory at BOEC required to achieve the desired multiplication factor of 0.97 is 3062 kg. The volume fractions of fuel particles in the charged fuel are 19.4%, 26.2%, and 29.1% in the inner, middle and outer core zones, respectively. Compared to the second-stage ADS of the first fuel cycle option without target assemblies, the heavy metal inventory at BOEC is reduced from 4208 kg to 3062 kg because of the increased amount of plutonium due to target assemblies. The reduced amount

of fuel inventory increases the average discharge burnup to 25.4% from 19.4%. The peak fast fluence for the ADS system is 3.98×10^{23} n/cm^2, which is within the design constraint. The burnup reactivity loss is 3.2% with a six-month cycle design. The power distribution is flattened by enrichment zoning, and as a result, power peaking factors for each zone are practically the same. The power peaking factors are similar between BOEC and EOEC, but during burnup, power peaking is shifted from the outer to the inner zone due to the increased spallation neutron source to maintain the same power level.

Table 5.4. Equilibrium Cycle Performance of Sodium-Cooled ADS Blanket Designs

Parameter		ADS
Thermal power, MW		840
Cycle length, EFPD		135
Capacity factor, %		75
BOEC heavy metal inventory, kg		3062
Fuel particle fraction, volume % in matrix	Inner zone Middle zone Outer zone	19.4 26.2 29.1
Multiplication factor	BOEC EOEC	0.97065 0.93894
Burnup reactivity loss, %Δk		3.2
Core-average power density, kw/l		247.6
Power peaking factor at BOEC/EOEC		1.51/1.51
Peak linear power, kW/m	Inner zone Middle zone Outer zone	36.1 34.4 35.0
Average discharge burnup, atom %		25.4
Peak fast fluence, 10^{23} n/cm^2		3.98
Net TRU consumption rate, kg/year		256
Equilibrium loading, kg/year	FR TRU Recycled HM Total HM	256 664 920

Using the performance parameters of LEUFBR and ADS, the mass flow data at the equilibrium state for the second proposed two-stage fuel cycle option were assessed for a nuclear fleet of 100 GWe-yr electricity production. TRU are recovered in the first-stage FRs at a rate of 3 kg/GWe-yr, and they are consumed by fission in the second-stage ADSs at a rate of 1045 kg/GWe-yr. Based on the TRU production and consumption rates, the electricity sharing between FRs and ADSs in the nuclear fleet was estimated to be 99.7% to 0.3%. The decrease in demand for ADS results from the reduced amount of MA from the first-stage FR.

Table 5.5 shows the mass flow data at equilibrium state estimated for a 100 GWe-yr electricity generation. In this table, the signs of (-) and (+) present the feed to and the product form each system, and masses in each column show the mass flow per each technology to support each stage. At the equilibrium state, the FR is fueled with 1045.7 MT of U, 159.2 MT of Pu and 3.3 MT of MA, whereas 944.6 MT of U, 159.5 MT of Pu, 3.6 MT of MA are recovered from the reprocessing facility. During the reprocessing/separating and fresh fuel fabrication

processes, 11.2 MT and 2.4 MT of nuclear materials are lost to the waste stream, respectively. The masses in the last column indicate the required (-) or produced (+) nuclear material per year needed to generate100 GWe-yr of electricity. Results show that approximately 103.2 MT of natural uranium would be required for sustaining the second proposed two-stage fuel cycle option. Since the Pu and MA are continuously recycled, this fuel cycle option does not release Pu or MA except for the loss from the fuel fabrication and separation. For the overall fuel cycle, there are 88.9 MT of FPs and 13.6 MT of HM sent to the repository.

Table 5.5. Mass Flow Data of Second Proposed Two-stage FR/ADS Option (Metric Ton per 100 GWe-yr at Equilibrium State)

Stage		1			2			Sum
Technology		Fuel	NPPT	Rep/Sep	Fuel	NPPT	Rep/Sep	
Electricity, GWe-yr		99.7			0.3			100.0
Feed or product of nuclear materials (MT)								
Natural resource	NU	-103.2						-103.2
	Th							
Products from fuel or NPPT technology	DU							
	U	+1,045.7	-1,045.7		+0.0	-0.0		0.0
	Pu	+159.2	-159.2		+0.4	-0.4		0.0
	MA	+3.3	-3.3		+0.6	-0.6		0.0
	DF		+1,209.0	-1,209.0		+1.0	-1.0	0.0
Products from Rep/Sep technology	RU	-944.6		+944.6	-0.0		+0.0	0.0
	Pu	-159.5		+159.5	-0.3		+0.3	0.0
	MA	-3.3		+3.6	-0.7		+0.4	0.0
	FP	-1.6		+90.2			+0.3	+88.9
Loss		+2.4		+11.2	+0.0		+0.0	+13.6

5.2. Single-Stage Fast Reactor Option with Homogeneous Recycle of TRU in FR

For comparison purposes, a single-stage fuel cycle option with homogeneous recycling of TRU (Pu and MAs) in LEUFBR was evaluated in addition to the two-stage options of recycling of MA in separate target assemblies and ADS. As illustrated in Figure 5.5, in the homogeneous recycling option, TRU is recycled in the driver fuel assemblies without partitioning into Pu and MA streams, which could reduce the proliferation risk. In sodium-cooled fast reactors with oxide fuel, the concentration of MAs in the fuel needs to be limited not to affect the core characteristics. In general, the reactivity coefficients (e.g. void reactivity and Doppler reactivity effects) deteriorate with increasing MA content. Thus, safety implications should be examined carefully as the MAs increases in the core. A recent study [48] has suggested that 5% of MA content in the HM could be set as a preliminary limit for the medium and small size fast reactor.

The equilibrium cycle calculations were performed to analyze the performance of this fuel cycle option at the equilibrium state. Again, using the fuel cycle performance parameters of LEUFBR core, the mass flow data was assessed for a nuclear fleet of 100 GWe-year electricity production. Table 5.6 shows the mass flow data at equilibrium state estimated for a 100 GWe-yr electricity generation. In the table, the signs of (-) and (+) present the feed to and the product form each system, and masses in each column show the mass flow per each technology to support each stage. At the equilibrium state, the FR is fueled with 1003.0 MT of U and 161.9

MT of TRU, whereas 902.4 MT of U and 162.2 MT of TRU are recovered from the reprocessing facility. During the reprocessing/separating and fresh fuel fabrication processes, 10.8 MT and 2.3 MT of nuclear materials are lost to the waste stream, respectively. The masses in the last column indicate the required (-) or produced (+) nuclear material per year needed to generate100 GWe-yr of electricity. Results show that approximately 102.6 MT of natural uranium would be required for sustaining this fuel cycle option. Since the Pu and MA are continuously recycled, this fuel cycle option does not release Pu or MA except for the loss from the fuel fabrication and separation. For the overall fuel cycle, there are 90.4 MT of FPs and 13.1 MT of HM sent to the repository.

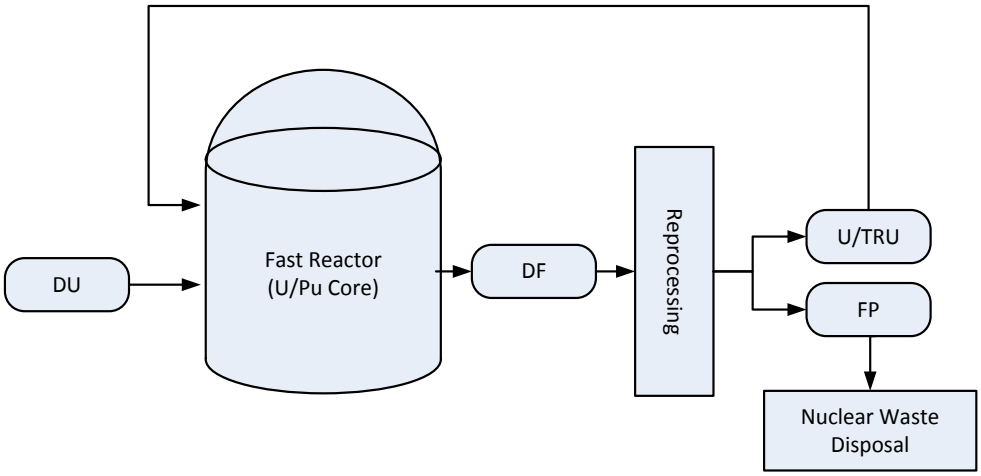

Figure 5.5. Schematic Illustration of the Single-stage Fuel Cycle Option

Table 5.6. Mass Flow Data of Single-stage Fuel Cycle Option (Metric Ton per 100 GWe-yr at Equilibrium State)

Stage		1			Sum
Technology		Fuel	NPPT	Rep/Sep	
Electricity, GWe-yr		100.0			100.0
Feed or product of nuclear materials (MT)					
Natural resource	NU	-102.6			-102.6
	Th				
Products from fuel or NPPT technology	DU				
	U	+1,003.0	-1,003.0		0.0
	TRU	+161.9	-161.9		0.0
	DF		+1,165.8	-1,165.8	0.0
Products from Rep/Sep technology	RU	-902.4		+902.4	0.0
	TRU	-162.2		+162.2	0.0
	FP			+90.4	+90.4
Loss		+2.3		+10.8	+13.1

The transitional cycle characteristics of homogenous recycling in the LEUFBR core were also evaluated by an explicit cycle-by-cycle analysis over an assumed plant lifetime of 60 years. The same fuel management scheme used in the equilibrium core was employed for this TRU-

recycling core. Since the pyroprocessing of metal fuel would not require a long cooling time of spent fuel, it was assumed that the recovered TRU from the discharged fuels at the end of *n*-th cycle could be recycled into the core at the beginning of (*n*+2)-th cycle. The reprocessing loss rate of 0.1% is assumed in the mass flow evaluation. With this fuel management scheme, the U, Pu as well as MAs are co-extracted from the discharged fuel and recycled into FR from the third cycle. The evolution of recycled fuel composition during operating cycles is provided in Figure 5.6. It can be noted that the Pu and MA content increases monotonically with burnup cycles. The Pu and MA content in the recycled fuel are 13.6% and 0.5%, respectively, in the last cycle of the assumed 60-year plant lifetime.

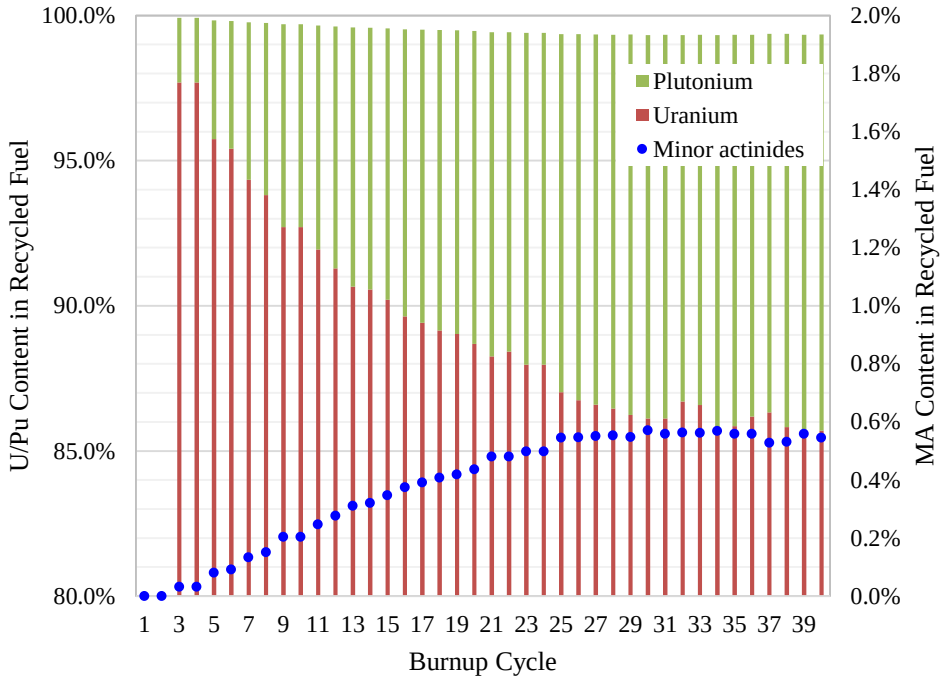

Figure 5.6. Evolution of Recycled Fuel Composition vs. Burn Cycle of LEUFBR Core

5.3. Comparative Study on Three Fuel Cycle Options

The fuel cycle performance parameters of three fuel cycle options have been evaluated in Sections 5.1 and 5.2. The considered fuel cycle options were two two-stage fuel cycle options (consisting of first-stage FR with and without MA target assemblies and second-stage ADS) and a single-stage fuel cycle option of homogeneous recycle of TRU in FR. The results from the equilibrium cycle analysis showed that the three fuel cycle options could achieve high reductions in the actinide inventory because of the continuous recycle of the Pu and MA. The three fuel cycle options do not release Pu or MA to the geological repository except for the loss from the fuel fabrication and separation. For the fuel cycle options with closed fuel cycle, the reprocessing loss and the fission products dominate the nuclear waste management performance.

To evaluate the nuclear waste management performance of the three fuel cycle options, radiotoxicity values were estimated using the International Commission on Radiation Protection data [49] and the ORIGEN2 [50] code. Based on the mass flow data and one-group

cross sections obtained from REBUS-3 calculations, the detailed composition of discharged fuel was obtained through modeling of the irradiation with ORIGEN2. This composition was then decayed during the one-year cooling time and recycled elements (99% of the U and Pu) were removed to estimate the radioactivity of the high level waste for each fuel cycle option. The potential radiological risk of the waste was also shown by calculating the inhalation and ingestion toxicity and the decay heat of nuclear waste at 10, 100 and 100,000 years after fuel discharge. In the evaluation, the mass of radioactive waste was analyzed with a normalized quantity per unit of electricity generation (t/GWe-yr) and only high-level wastes were considered. The high-level wastes considered for these fuel cycle options include the fabrication and reprocessing losses, and the fission products. The depleted uranium and the activation products were not considered in this evaluation.

Table 5.7 presents the nuclear waste management parameters of three fuel cycle options. The total radioactivity in terms of the inhalation and ingestion toxicity and the decay heat showed similar trend for the first proposed two-stage fuel cycle option and the single-stage fuel cycle option. Since all the actinides are recycled in these fuel cycle options, the level of radiotoxicity in each transmutation scenario is correlated to the fuel inventory. The second proposed two-stage fuel cycle option contains about 5% more radioactivity than the other two options due to the increased fuel inventory. Since the LLFPs (Tc-99, I-127 and I-129) were loaded and recycled in the target assemblies, the waste management parameters were also evaluated by considering the FR with transmutation of LLFPs. The calculation results showed that Tc-99 plays a significant role in the long-term activity. If all the Tc-99 is continuously recycled, the activity value and decay heat at 100,000 year after fuel discharge are reduced by 55% and 7%, respectively.

The calculated activity for all the fuel cycle options identified in Table 5.7 shows behavior similar to that of the EG24 in nuclear fuel cycle E&S report. In the EG24 evaluation group, TRU is continuously recycled and the entire fission product is sent to disposal together with the reprocessing loss. The transmutation scenario of continuous recycling of TRU have been considered as an option which constantly provides the lowest values of inhalation and ingestion toxicity and the decay heat [51]. These results from the equilibrium cycle analysis showed that the three fuel cycle options are capable of achieving the transmutation goal. They could reduce the nuclear waste generation significantly compared to the currently employed once-through fuel cycle.

In addition to the nuclear waste management performance, the resource utilization in each fuel cycle was examined. Since the high internal conversion in the FR, no uranium enrichment was required for the FR in each fuel cycle at the equilibrium state. Table 5.8 summarizes the performance characteristics of fuel cycle options. For the three fuel cycle options, the mass flow data was similar and about 100 MT of natural uranium would be required for producing 100 GWe electricity per year. A slightly increase in the natural uranium requirement of the second proposed FR/ADS two-stage fuel cycle option was due to the absorption of fission neutrons by non-fuel material. The capture reaction rate of non-fuel material in the target assemblies was increased by a factor of 2.6 relative to that in the reflector with same number of assemblies. Note that the high content of zirconium presented in the target assemblies resulted in an increased fuel requirement in the fuel cycle with target assemblies.

Table 5.7. Comparison of Nuclear Waste Management Parameters for Proposed Fuel Cycle Options

		Activity, Curies/GWe-yr			Toxicity inhalation, Sv/GWe-yr		
Years after disposal		10 yr	100 yr	100,000 yr	10 yr	100 yr	100,000 yr
FR/ADS two-stage fuel cycle	FR	6.82E+06	7.74E+05	4.72E+02	2.65E+10	1.67E+10	1.69E+08
	ADS	1.50E+05	1.80E+04	1.66E+01	2.01E+10	6.94E+09	6.50E+06
	Total	**6.97E+06**	**7.92E+05**	**4.89E+02**	**4.66E+10**	**2.36E+10**	**1.75E+08**
FR/ADS two-stage fuel cycle with MA targets	FR[a]	7.31E+06	8.30E+05	5.10E+02	4.25E+10	2.15E+10	1.76E+08
	Activity due to Tc-99	3.91E+02	3.91E+02	2.83E+02	1.88E+05	1.88E+05	1.36E+05
	Contribution of Tc-99	0%	0%	**55**%	0%	0%	0%
	FR_transmutation of Tc-99	7.31E+06	8.30E+05	2.27E+02	4.24E+10	2.15E+10	1.76E+08
	ADS	2.28E+04	2.53E+03	1.71E+00	2.47E+09	3.68E+08	5.23E+05
	Total[b]	**7.33E+06**	**8.33E+05**	**2.29E+02**	**4.49E+10**	**2.19E+10**	**1.76E+08**
Homogeneous recycling of TRU in FR		**6.97E+06**	**7.92E+05**	**4.89E+02**	**4.68E+10**	**2.41E+10**	**1.75E+08**

[a] No transmutation of LLFP in FR

[b] Sum of parameters of FR with transmutation of Tc-99 and ADS

		Toxicity ingestion, Sv/GWe-yr			Decay Heat, W/GWe-yr			Mass,
Years after disposal		10 yr	100 yr	100,000 yr	10 yr	100 yr	100,000 yr	t/GWe-yr
FR/ADS two-stage fuel cycle	FR	2.09E+09	2.73E+08	3.91E+05	1.82E+04	2.09E+03	1.78E+00	1.04
	ADS	8.38E+07	1.94E+07	5.98E+04	6.09E+02	1.01E+02	1.97E-01	0.02
	Total	**2.18E+09**	**2.93E+08**	**4.50E+05**	**1.88E+04**	**2.19E+03**	**1.98E+00**	**1.06**
FR/ADS two-stage fuel cycle with MA targets	FR	2.27E+09	3.00E+08	4.45E+05	1.97E+04	2.27E+03	1.98E+00	1.11
	Activity due to Tc-99	9.27E+03	9.26E+03	6.69E+03	1.96E-01	1.96E-01	1.42E-01	0.02
	Contribution of Tc-99	0%	0%	2%	0%	0%	7%	
	FR_transmutation of Tc-99	2.27E+09	3.00E+08	4.39E+05	1.97E+04	2.27E+03	1.84E+00	1.11
	ADS	1.16E+07	1.51E+06	3.21E+03	9.51E+01	9.70E+00	1.14E-02	0.00
	Total	**2.28E+09**	**3.02E+08**	**4.42E+05**	**1.98E+04**	**2.28E+03**	**1.85E+00**	**1.11**
Homogeneous recycling of TRU in FR		**2.18E+09**	**2.94E+08**	**4.55E+05**	**1.88E+04**	**2.20E+03**	**1.99E+00**	**1.06**

For the driver fuel assemblies, the average discharge burnup was determined to be approximately 70 GWd/t and the TRU fraction of HM inventory in the two two-stage fuel cycle options was 14.2% while that increased to 14.8% in the single-stage fuel cycle option with homogeneous recycling of TRU in FR. Since LLFP pins were used as the thermal neutron filters in the target assemblies, a transmutation fraction of 14.5% in LLFPs is attained in the fuel cycle with MA target assemblies in FR. The accumulated LLFPs to be send to repository could be further reduced by loading multiple targets with a larger amount of LLFPs. The reduced amount of accumulated Tc-99 will result in a significantly reduce of activity value at 100,000 year after fuel discharge.

Table 5.8. Comparison on Equilibrium Cycle Performance

TRU recycle option			Pu in FR/ MA in ADS	With MA targets in FR	Homo. Recycle of TRU in FR
Electricity sharing of ADS in FR/ADS nuclear fleet, %			1.9	0.3	0
Mass flow (MT) per 100 GWe-yr	Natural U resource required		102.8	103.2	102.6
	Separation/fabrication loss of U		11.1	11.6	11.1
	Separation/fabrication loss of TRU		2.0	2.0	2.0
Core performance parameters	Average discharge burnup, GWd/t	Fuel/Target in FR	72.7	70.5/278.1	73.7
		Fuel in ADS	177.5	231.0	- -
	TRU fraction of HM inventory, %	Fuel/Target in FR	14.2	14.2/100	14.8
		Fuel in ADS	96.4	98.2	- -

The TRU can be recycled with different approaches. The second option shown in the Table 5.8 is known as the heterogeneous recycling option that concentrates the MA in a moderated target assembly. As explained above, the third option in the Table 5.8 is so called homogeneous recycling which incorporates the MA as a minority part of the nuclear fuel. For detailed comparison of two recycling options, the capture cross sections and the transmutation rates of equilibrium cycle were extracted from the REBUS-3 fuel cycle analyses and compared in Table 5.9. At the equilibrium state, the total transmutation rate (sum of capture and fission reaction rates) of MA was similar in both recycling options. As shown in Table 5.9, the MA inventory in the homogeneous and heterogeneous recycling options were 102.1 kg and 32.3 kg, respectively. In the driver fuel assemblies, the cross sections were comparable for both cases but the transmutation rate was larger in the homogeneous recycling option than that in the heterogeneous recycling option due to the larger amount of MA inventory. On the other hand, the one-group microscopic capture cross section in the moderated target assembly was about eight times larger than that in the fuel region while the total flux level in target assembly is two orders of magnitude lower than that in the fuel region. Considering the high concentrated MA and the enhanced capture cross sections in the target assembly, the transmutation rate in the target assemblies is only slightly less than that in the fuel region of homogeneous recycling option. For the heterogeneous recycling option, the transmutation rate could be further improved by increasing the MA loading in the target assemblies.

Table 5.9. Transmutation Data of Homogeneous and Heterogeneous Recycling Options

Recycle option	Homogeneous	Heterogeneous	
	Driver	Driver	Target
MA inventory, kg	102.1	18.8	13.5
One-group capture XS of MAs, barn	2.81	2.97	21.9
One-group fission XS of MAs, barn	0.91	0.79	6.5
Total flux, neutron-cm/sec	1.23E+22	1.18E+22	1.84E+20
Fast flux fraction, %	66.6	67.1	33.4
Capture reaction rate of MAs, 1/sec	1.87E+17	8.29E+16	1.47E+17
Fission reaction rate of MAs, 1/sec	4.09E+16	1.89E+16	7.06E+15

6. Conclusions

For effective utilization of uranium resource and reduction of nuclear wastes to be sent to geological repository, two two-stage fast spectrum fuel cycle options were proposed based on the intrinsic nuclear characteristics of FRs. One is a two-stage fuel cycle option of continuous recycle of plutonium in FR and subsequent burning of MAs in ADS. The other is a two-stage FR/ADS fuel cycle option with MA targets employed in FR to reduce the amount of MAs to be sent to the second-stage ADS. For comparison, a single-stage fast reactor fuel cycle with homogeneous recycling of TRU was considered as well. To evaluate the proposed two-stage fuel cycle options, design studies were performed to develop reference designs for a 1000 MWt sodium-cooled fast reactor core, named LEUFBR (LEU-fueled fissile break-even reactor), an 840 MWt sodium-cooled ADS blanket, and a moderated MA target assembly. The LEUFBR starts with LEU fuel, and at the equilibrium cycle, the reactor will operate with the recovered Pu and natural uranium only without supporting LEU. Pu and uranium are co-extracted from the discharged fuel and recycled in the reactor. The recovered MAs are directly sent to the second-stage ADS in the first option, but in the second option, they are partially incinerated in the FR to reduce the amount of MAs to be sent to the ADS. The 1000 MWt LEUFBR core design was employed as the FR of the single-stage fuel cycle option as well.

Starting from a metal fuel core design of 1000 MWt ABR, a compact core configuration was developed for LEUFBR by increasing the active core height and replacing six primary control assemblies with fuel assemblies. A reference core design was developed through detailed neutronics and thermal-fluidic analyses. The analysis results indicate that the fissile break-even core would be feasible while satisfying the imposed thermal and material related design constraints. A fuel volume fraction of 39.4% was selected to maximize the natural resource utilization for the initial LEU cores. The U-235 enrichment of the LEU startup core was 13.6% and a fissile break-even core was reached after 14 cycles. For the subsequent cycles, the required fresh fuel could be fabricated only with the recycled uranium and Pu and an external feed of depleted uranium. After an assumed plant lifetime of 60 years, the recovered U and Pu from the U-fueled FR are used to start a new Pu-fueled FR. The fuel volume fraction of Pu-fueled FR was reduced to 35.1% to minimize the surplus TRU generation by maintaining a fissile break-even core. The evaluated reactivity coefficients provided sufficient negative feedbacks, and the control systems provided more than adequate shutdown margins. In addition, the integral coefficients for the quasi-static reactivity balance analysis indicated that both the uranium and Pu cores have passive safety features.

A preliminary 840 MWt sodium-cooled ADS blanket design was developed utilizing non-uranium metallic dispersion fuel in which MA-10Zr fuel particles are dispersed in a zirconium metal matrix. In this study, similar design goals and analysis techniques were adopted from the previous analyses for 840 MWt ATW blanket designs with LBE and sodium coolants. In the equilibrium fuel cycle, the charged fuel contains TRU recovered from the discharged ADS fuel, supplemented by the MA recovered from the Pu-fueled FRs.

A target assembly design was developed using the MA-40Zr target and $ZrH_{1.6}$ moderator. To maximize the MA transmutation rate, the moderator volume fraction was increase to its maximum value of 39.2% within the imposed thermal design limits on the cladding inner wall temperature of target pins. Long-lived fission product pins were employed as thermal neutron

filters to reduce the local power peaking in the adjacent fuel assemblies due to the thermal neutron leakage from the moderated target assembly. At the equilibrium state, the use of MA target assemblies reduces the amount of MA to be sent to ADS by a factor of six compared to that of the fuel cycle without MA recycling in FR. The results of sub-channel thermal-hydraulic analyses confirmed that all the fuel and target assemblies satisfied the imposed thermal design limits on the peak 2-sigma cladding inner wall and fuel centerline temperatures.

In the first two-stage fuel cycle option, one ADS supports 35 U-fueled or 37 Pu-fueled FRs in such a way that the TRU consumption in ADS is balanced by the recovered MA and surplus Pu in FRs. The MA and surplus Pu were recovered in the first-stage FR at a rate of 18 kg/GWe-yr, and they consumed by fission in the second-stage ADSs at a rate of 958 kg/GWe-yr. Based on these TRU production and consumption rates, the electricity sharing between FRs and ADSs in a nuclear fleet was estimated to be 98.1% to 1.9%. In a nuclear fleet of 100 GWe-yr electricity production, approximately 102.8 MT of natural uranium would be required for sustaining the first proposed two-stage fuel cycle option. Since the Pu and MA are continuously recycled, this fuel cycle option does not release Pu or MA except for the loss from the fuel fabrication and separation. For the overall fuel cycle, there are 90.5 MT of FPs and 13.1 MT of HM sent to the repository.

For the second two-stage fuel cycle option, the recovered MA are not directly sent to ADS but partially incinerated in the FR via moderated MA target assemblies. The production rate of MA and surplus Pu in the first-stage FRs was reduced to 3 kg/GWe-yr and the TRU consumption rate in the second-stage ADS was 1045 kg/GWe-yr. The electricity sharing between FRs and ADSs was estimated to be 99.7% to 0.3%. In a nuclear fleet of 100 GWe-yr electricity production, about 103.2 MT of natural uranium is required to support this two-stage fuel cycle option and there are 88.9 MT of FPs and 13.6 MT of HM sent to the repository.

In the single-stage fast reactor cycle with homogeneous recycling of TRU, the mass flow data to produce 100 GWe-yr electricity were similar to those of the two proposed two-stage fuel cycle options. The MA content of fuel at the end of the assumed plant lifetime of 60 years was less than 1%. Since the amount of MAs generated in the LEUFBR core was relatively small, the presence of the small amount of MAs should not affect the core characteristic of the LEUFBR core.

All the three fuel cycles considered can be operated with natural or depleted uranium only at the equilibrium state, since all the uranium, plutonium and MAs are continuously recycled. Relative to the single-stage fast reactor with TRU fuel, the FRs in the two-stage fuel cycle options may have potential benefits from the fuel fabrication and reprocessing points of views [52]. In the two-stage fuel cycles where TRU elements are partitioned into Pu and MA streams, the normal fuel fabrication methods can be applied to the most of the fuel assemblies since all the MA are concentrated in a few ADSs or in a few target assemblies. On the other hand, the single-stage fuel cycle option may have economic advantage over the two-stage fuel cycle options. Moreover, co-extraction of Pu and MA would reduce the proliferation risk.

In summary, the two proposed two-stage fuel cycle options (consisting of first-stage FR with and without MA target assemblies and second-stage ADS) and the single-stage fast reactor option with homogeneous recycling of TRU showed similar performances in terms of natural

uranium utilization and waste generation. The results from the equilibrium cycle analysis showed that the three fuel cycle options could achieve high reductions in waste generation because of the continuous recycle of the Pu and MA. In addition, the mass flow data showed that the proposed two-stage fast spectrum fuel cycle options increase the efficiency of natural uranium utilization and reduce the nuclear waste generation compared to the conventional two-stage fuel cycle options based on thermal and fast spectrum systems.

References

1. U.S. Department of Energy, *Nuclear Energy Research and Development Roadmap*, Report to Congress (2010).
2. R. Wigeland et al., "Nuclear Fuel Cycle Evaluation and Screening - Final Report," FCRDFCO-2014-000106, US DOE (2014).
3. W. S. Yang, T. K. Kim, and R. N. Hill, "Performance Characteristics of Metal and Oxide Fuel Cores for a 1000 MWt Advanced Burner Reactor," Proc. of Workshop on Advanced Reactors With Innovative Fuels ARWIF-2008, Fukui, Japan, February 20-22, 2008.
4. T. K. Kim, W. S. Yang, C. Grandy, and R. N. Hill, "Core Design Studies for a 1000 MWt Advanced Burner Reactor," Annals of Nuclear Energy, 36, 331-336 (2009).
5. R. N. Hill and H. S. Khalil, "Physics Studies for Sodium Cooled ATW Blanket," *Proceedings of the IAEA Technical Committee Meeting on Core Physics and Engineering Aspects of Emerging Nuclear Energy Systems for Energy Generation and Transmutation*, Argonne National Laboratory (2000).
6. G. L. Hofman, L. C. Walters, and T. H. Bauer, "Metallic Fast Reactor Fuels," *Progress in Nuclear Energy*, **31**, 83 (1997).
7. R. D. Leggett and L. C. Walters, "Status of LMR Fuel Development in the United States of America," *Journal of Nuclear Materials*, **204**, 23 (1993).
8. D. C. Wade and E. K. Fujita, "Trends versus Reactor Size of Passive Reactivity Shutdown and Control Performance," *Nucl. Sci. Eng.*, **103**, 182 (1989).
9. D. C. Wade and R. N. Hill, "The Design Rationale for the IFR," *Prog. Nuclear Energy*, **31**, 13 (1997).
10. H. C. Tsai, "Fuel/Cladding Compatibility in Irradiated Metallic Fuel Pins at Elevated Temperatures," *Proc. 1990 International Fast Reactor Safety Meeting*, Snowbird, UT, August 12-16, 1990.
11. K. L. Derstine, "DIF3D: A Code to Solve One-, Two-, and Three-Dimensional Finite Difference Diffusion Theory Problem," ANL-82-64, Argonne National Laboratory (1984).
12. R. D. Lawrence, "The DIF3D Nodal Neutronics Option for Two- and Three-Dimensional Diffusion Theory Calculations in Hexagonal Geometry," ANL-83-1, Argonne National Laboratory (1983).
13. B. J. Toppel, "A User's Guide to the REBUS-3 Fuel Cycle Analysis Capability," ANL-83-2, Argonne National Laboratory (1983).
14. C. H. Lee and W. S. Yang, "MC^2-3: Multigroup Cross Section Generation Code for Fast System Analysis," ANL/NE-11-41, Argonne National Laboratory (2011).
15. H. Henryson II, B. J. Toppel, and C. G. Stenberg, "MC^2-2: A Code to Calculate Fast Neutron Spectra and Multi-group Cross Sections," ANL-8144, Argonne National Laboratory (1976).

16. W. M. Stacey, Jr., et al, "A New Space-Dependent Fast Neutron Multigroup Cross Section Preparation Capability," *Trans. Am. Nucl. Soc.*, **15**, 292 (1972).

17. W. S. Yang, Private Communication, Argonne National Laboratory, July 2005.

18. M. A. Smith, C. Adams, W. S. Yang, and E. E. Lewis, "VARI3D & PERSENT: Perturbation and Sensitivity Analysis," ANL/NE-13/8, Argonne National Laboratory, June 15, 2013

19. G. Palmiotti, E. E. Lewis, and C. B. Carrico, "VARIANT: Variational Anisotropic Nodal Transport for Multi-Dimensional Cartesian and Hexagonal Geometry Calculations," ANL-95/40, Argonne National Laboratory (1995).

20. A. E. Waltar and A. B. Reynolds, *Fast Breeder Reactors*, Pergamon Press (1981).

21. W. S. Yang and A. M. Yacout, "Assessment of the SE2-ANL Code Using EBR-II Temperature Measurements," *Proc. 7th International Meeting on Nuclear Reactor Thermal Hydraulics*, NUREG/CP-0142, Saratoga Springs, New York, September 10-15, 1995, Vol. **3**, pp. 2394-2409, US Nuclear Regulatory Commission (1995).

22. K. L. Basehore and N. E. Todreas, "SUPERENERGY-2: A Multiassembly, Steady-State Computer Code for LMFBR Core Thermal-Hydraulic Analysis," PNL-3379, Pacific Northwest Laboratory (1980).

23. T. K. Kim and W. S. Yang, "Design Sensitivity Studies of 1000 MWt Reference ABR Core Concepts to Achieve Low and High Conversion Ratios," ANL-AFCI-200, Argonne National Laboratory (2007).

24. R. E. Alcouffe, F. W. Brinkley, D. R. Marr, and R. D. O'Dell, "User's Guide for TWODANT: A Code Package for Two-Dimensional, Diffusion-Accelerated, Neutral-Particle Transport," LA-10049-M, Los Alamos National Laboratory (1990).

25. T. K. Kim, W. S. Yang, and R. N. Hill, "Fuel Cycle Strategies for Advanced Burner Test Reactor," ANL-AFCI-174, Argonne National Laboratory (2006).

26. W. S. Yang, T. K. Kim, and T. A. Taiwo, "Performance Evaluation of Two-Stage Fuel Cycle Based on PWR and ADS," *Proc. of ICAPP 2013*, Jeju Island, Korea, April 14-18, 2013.

27. W. S. Yang, D. G. Naberejnev, and H. S. Khalil, "Physics Design Optimization of an LBE Cooled ATW Blanket," *Trans. Am. Nucl. Soc*., **83**, 328-330 (2000).

28. W. S. Yang and H. S. Khalil, "Reduction of Burnup Reactivity Loss in Accelerator Driven Transmutation Systems," *Proc. of the 4th Topical Meeting on Nuclear Applications of Accelerator Technology*, Washington DC (2000).

29. W. S. Yang and H. Khalil "Blanket Design Studies of a Lead-Bismuth Eutectic Cooled Accelerator Transmutation of Waste System," *Nuclear Technology*, **135**, 162-182 (2001).

30. W. S. Yang, "Blanket Design Studies for Maximizing the Discharge Burnup of Liquid Metal Cooled ATW Systems," *Annals of Nuclear Energy*, **29**, 509-523 (2002).

31. "A Roadmap for Developing Accelerator Transmutation of Waste (ATW) Technology – A Report to Congress," DOE/RW-0519, Department of Energy (October 1999).

32. E. L. Gluecker, "U.S. Advanced Liquid Metal Reactor (ALMR)," Progress in Nuclear Energy, 31, 43-62 (1997).

33. D. C. Crawford, S. L. Hayes, and M. K. Meyer, "Current U.S. Plans for Development of Fuels for Accelerator Transmutation of Waste," *Proceedings of the IAEA Technical Committee Meeting on Core Physics and Engineering Aspects of Emerging Nuclear Energy Systems for Energy Generation and Transmutation*, Argonne National Laboratory (2000).

34. R. N. Hill, D. C. Wade, J. R. Liaw, and E. K. Fujita, "Physics Studies of Weapons Plutonium Disposition in the Integral Fast Reactor Closed Fuel Cycle," *Nuclear Science and Engineering*, **121**, 17-31 (1995).

35. W. S. Yang and H. S. Khalil, "Analysis of the ATW Fuel Cycle Using the REBUS-3 Code System," *Trans. Am. Nucl. Soc*., **81**, 277-279 (1999).

36. W. S. Yang and B. J. Toppel, "REBUS-3 Code Enhancements for ADS Fuel Cycle Analyses," ANL-AAA-016, Argonne National Laboratory, June 2002.

37. "Comparison Calculations for an Accelerator-driven Minor Actinide Burner," NEA/NSC/DOC (2001)13, Nuclear Energy Agency, Organization for Economic Cooperation and Development (2001).

38. R. M. Ferrer, M. Asgari, S. E. Bays, and B. Forget, "Fast Reactor Alternative Studies: Effects of Transuranic Groupings on Metal and Oxide Sodium Fast Reactor Designs," INL/EXT-07-13236, Idaho National Lab, September 2007.

39. "MCNP6™ USER'S MANUAL, Code Version 6.1.1beta," LA-CP-14-00745, Rev. 0, Los Alamos National Laboratory (2014).

40. A. E. Waltar, D. R. Todd, and P. V. Tsvetkov, *Fast Spectrum Reactors*, Springer (2012).

41. H. Golfier et al., "Parametrical Analysis of Tc-99 and I-129 Transmutation in Reactor," *Proc. Int. Conf. Future Nuclear Systems (GLOBAL '99),* Jackson Hole, Wyoming, August 29 – September 3, 1999 (1999).

42. W. M Mueller, J. P. Blackledge, and G. G. Libowitz, *Metal Hydrides*, Academic Press, New York, 1968.

43. K. Moore and W. Young, "Phase Studies of the Zr-H System at High Hydrogen Concentrations," *J. Nuclear Materials*, **27**, 316-324 (1968).

44. "Status of Minor Actinide Fuel Development," IAEA Nuclear Energy Series NF-T-4.6 (2010).

45. O. Inagaki, K. Nakamura, T. Ogata, "Progress in understanding of Fuel-Cladding Chemical Interaction in Metal Fuel," *International Conference on Fast Reactors and Related Fuel Cycles*, Paris, France, March 4-7, 2013.

46. J. K Gibson, R. J. Haire, E. C. Beahm, M. M. Gensini, A. Maeda, and T. Ogawa, "The neptunium - iron phase diagram," *J. Nuclear Materials*, **211**, 215-222 (1994).

47. R. N. Hill, "Coupled Neutron-Gamma Heating Calculations," Private Communication, Argonne National Laboratory, February 2, 1988.

48. "Homogeneous versus Heterogeneous Recycling of Transuranics in Fast Nuclear Reactors," NEA No. 7077, Nuclear Energy Agency, Organization for Economic Cooperation and Development (2012).

49. Eckerman K, Harrison J, Menzel HG, and Clement CH, "Compendium of Dose Coefficients Based on ICRP Publication 60," ICRP: 2012 (ICRP Publication 119. Ann. ICRP 41).

50. "ORIGEN2 V2.2: Isotope Generation and Depletion Code – Matrix Exponential Method, " USA: Oak Ridge National Laboratory; June 2002 (CCC-371).

51. N. E. Stauff, T. K. Kim, and T. A. Taiwo, "Variations in Nuclear Waste Management Performance of Various Fuel-cycle Options," *J. Nucl. Sci. Technol.*, http://dx.doi.org/10.1080/00223131.2015.1032380.

52. R. Wigeland, T. Taiwo, and M. Todosow, "Investigation of Benefits from U/TRU Recycle – Quantification and Comparison to U/Pu Recycle," *Proc. of Global 2015*, Paris France, September 20-24, 2015.

Appendix A: REBUS-3 Code Modification – Feed Enrichment Search for Partial Reloading

The original REBUS-3 code has the capability of searching the feed enrichment such that the multiplication factor at a specified time point becomes the desired value specified by the user. This capability applies to non-equilibrium cycle problems as well as equilibrium cycle problems. For a problem with the feed enrichment search option, however, only fresh fuel can be introduced in the reactor at the beginning of problem. As a result, in order to determine the feed enrichment of fresh assemblies for a non-equilibrium cycle problem with partial reloading, a multi-cycle problem should be run starting from the first cycle loaded with all fresh fuel up to the cycle of interest. This makes the feed enrichment search for non-equilibrium cycle problems unnecessarily complicated and time consuming. In particular, the cycle-by-cycle transitional core analysis for LEUFBR requires tremendous efforts. Therefore, the LEUFBR analysis necessitated to implement a feed enrichment search capability of REBUS-3 for partial reloading for the efficient design process.

The enrichment search capability for partial reloading has been added to REBUS-3 to permit its application to a wide range of fuel management strategies. The feed enrichment of fresh fuel can now be determined without performing the previous burn cycle analyses for an arbitrary core composed of fresh and burned fuel assemblies. In the following, the code modification is briefly described, and then the user information for running the new version is provided. Several enrichment search problems are also illustrated including the new enrichment search option for partial reloading.

A.1. Program Modification and User Information

The input processing module FCI002 and the computational module FCC004 were modified to add an enrichment search capability for partial reloading. In order to minimize the code modifications, the use of the existing logics was maximized with extended ranges of input parameters specified in the dataset A.BURN. The new enrichment search option for partial reloading is invoked by providing a negative number for the number of previous burn cycles in columns 7-12 of the type 03 card of the dataset A.BURN. The compositions of fresh and burned fuel are specified as usual on the type 13 and 14 cards of the dataset A.NIP3. The atom densities of all active isotopes should be set to 1.0 in defining the materials used to make up secondary compositions for fresh fuel, as discussed in the type 11 card of the file description of A.BURN. On the contrary, the atom densities of burned fuel should be actual values in the unit of atoms/barn·cm.

The number of previous burn cycles for burned fuel is used to determine the time to discharge the corresponding fuel out of the reactor. It is specified differently depending on the way to specify the fuel management scheme. When the data for fuel management path are provided on the type 11 cards of the dataset A.BURN, the number of previous burn cycles of burned fuel is specified in columns 13-18 as usual. On the contrary, when the type 35 cards of A.BURN are used to specify the fuel management paths, a new way was defined since the number of previous burn cycles is not used for the general fuel management paths specified on the type 35 cards of A.BURN. In this case, the number of previous burn cycles is specified by

providing the negative value of it for a starting stage number with the corresponding ending stage number of 1.

As described above, the atom densities of active isotopes in each material should be 1.0 for fresh fuel. This is required to retrieve from the region densities the volume fraction of the materials containing active isotopes in the corresponding secondary composition. It is called the active volume fraction in each stage of the corresponding material type. However, since the burned fuel is specified with the actual densities, the active volume fraction of each burned fuel cannot be retrieved from the region densities. As a result, it needs to be specified separately. In order to specify the active volume fraction of each burn fuel, a new card of type 46 was newly defined in the dataset A.BURN. This card provides the list of the fuel management paths involving the secondary compositions of the same active volume fraction.

Several subroutines were modified and two new subroutines were written to implement these changes. The subroutine CTLCDS of the FCI002 module was modified to initialize the associated parameters when the number of previous burn cycles specified on the type 03 card of the dataset A.BURN is negative. In order to determine the number of previous burn cycle of each burned fuel by processing the type 35 cards of A.BURN, the subroutines CHECKR, CHK37, PATHS, and SIZE of the FCI002 module were modified. In order to determine the active volume fraction of each burned fuel by processing the type 46 cards of A.BURN, the subroutines BRNCDS, EXCYCL, and ACT were modified and two new subroutines BRN46 and CHK46 were added to the FCI002 module. Finally, in order to fix the error in the dimensions of the arrays IDEM and SUP, the subroutines REFAB and REPROC of the FCC004 module were modified. The new description of type 03, 35, and 46 are provided in the Appendix B. The details of the input preparation are discussed in the sample problems described in the next section.

A.2. Sample Problem

A simple fast reactor core was devised to illustrate the various enrichment search options and to test the new enrichment search option for partial reloading. Figure A.1 shows the planar view of the one-sixth core employed in the analyses. Each driver or blanket assembly has a lower and an upper reflector. The flux calculations were performed with the hexagonal-z model using the nodal diffusion theory. The fueled region of each assembly was treated as a single burn region. The depletion calculation utilizes burnup chains for nuclides ranging from U-234 to Cm-246. Using this simple configuration, the feed enrichment search was performed for various fuel management strategies with an operating cycle length of 465 days and three-batch refueling strategy. No reprocessing plant was modeled, and two external feed streams were employed: one for the driver fuel and the other for blanket fuel.

In order to test the functionality of the modified version of REBUS-3, the enrichment search was first performed for equilibrium cycle problems, which is not affected by the code modifications. Then the enrichment search was performed for non-equilibrium cycle problems that approximately represent one of the equilibrium cycle problems. For the equilibrium cycle problems, two fuel management strategies were investigated. The first one is the scattered loading without fuel shuffling; it is assumed that each fuel assembly is composed of all stages of fuel in equal volume fraction. In the second scheme, the fuels are shuffled at the end of each

burn cycle by carrying out a specified move sequence repeatedly. As the non-equilibrium cycle problems, two multi-cycle problems were analyzed: one starting from a core loaded with all fresh fuel and the other starting from a core configuration obtained from the second equilibrium cycle problem. The first one is not affected by the code modifications when the type 11 cards of the dataset A.BURN are used to specify the fuel management scheme. Two calculations were performed for each problem by specifying the fuel management scheme using the type 11 and the type 35 cards of A.BURN.

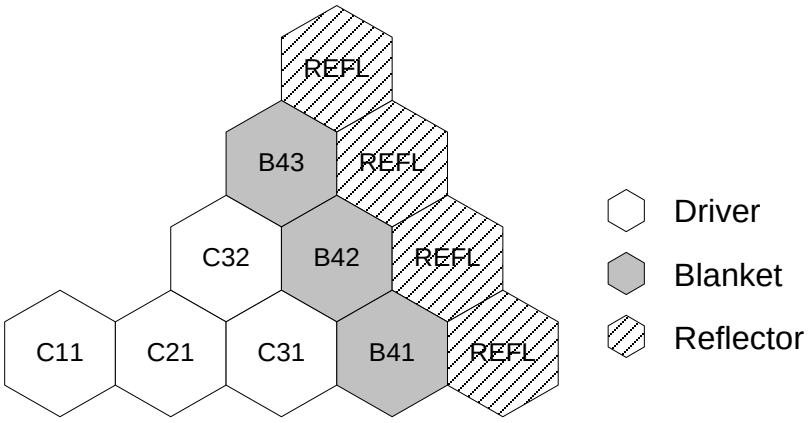

Figure A.1. Planar Layout of Sample Problem

A.2.1. Equilibrium Cycle Problems

The feed enrichment search for the equilibrium cycle was performed for two fuel management strategies. One is the scattered loading without shuffling, and the other is a repetitive fuel management scheme where fuels are shuffled in a specified move sequence.

Scattered Loading

The feed enrichment of an equilibrium cycle was first searched for the scattered loading without shuffling. On the type 13 cards of the dataset A.NIP3, two active materials MDRIVE and MRBLKT are defined by setting the active atom densities to 1.0. These materials are respectively used to define secondary compositions SCDRV and SCRBL on the type 14 cards of A.NIP3. Using these secondary compositions, three primary compositions PCDRV1, PCDRV2, and PCRBL are defined on the type 14 cards of A.NIP3. The type 15 cards of A.NIP3 assign these primary compositions to burn regions. In the type 15 cards of A.NIP3, each driver and blanket assembly in Figure1 is divided into three regions; the fueled region is suffixed with B, and the lower and upper reflectors are suffixed with A and C, respectively.

The type 11 cards of the dataset A.BURN define three fuel management paths for the scattered loading. Since the primary composition is used to define each path, additional paths are internally defined for the primary compositions PCDRV2 and PCRBL that are assigned to more than one region. Each secondary composition assigned to a region resides in the same region for all three stages. Thus, the fuel in each region is composed of all three stages of fuel in equal volume fraction. At the end of each cycle, one third of fuel is discharged from each region and fresh fuel is reloaded.

The feed enrichment was determined such that the k-eff at the end of equilibrium cycle (EOEC) is 1.002 as specified on the type 04 card of A.BURN. The modified version produced the same results with the existing version as expected. The required feed enrichment to satisfy this criticality constraint was 27.50%. The resulting k-eff at the beginning of equilibrium cycle (BOEC) and EOEC were 1.02001 and 1.00254, respectively.

Reloading with Fuel Shuffling

The feed enrichment of an equilibrium cycle was searched for a repetitive fuel management scheme. In this problem, fuels are shuffled at the end of each cycle by carrying out the specified move sequence repeatedly. Compared with the input data for the scattered loading case, only the type 11 cards of the dataset A.BURN are different. The type 11 cards shown in Figure A.2 define three fuel management paths. PATH1 defines a stationary path where the fuel resides in the region C11B for all three stages. (Because of the one-sixth core model employed, the volume of the region C11B is different from any other region volume, and hence the fuel in this region cannot be moved into any other region.) On the contrary, PATH2 and PATH3 define sequences of fuel movements. For example, PATH1 shows that at EOEC thrice times burned fuel is discharged from the region C32B, twice burned fuel is moved from C31B to C32B, once burned fuel is moved from C21B to C31B, and fresh fuel is loaded into the region C21B. Figure A.2 shows the number of previous burn cycles at BOEC for each driver and blanket assembly except for the center assembly that is composed of all three stages of fuel in equal volume fractions.

```
11   PATH1  0 1 SCDRV  C11B  2 SCDRV C11B
11   PATH1  0 3 SCDRV  C11B
11   PATH2  0 1 SCDRV  C21B  2 SCDRV C31B
11   PATH2  0 3 SCDRV  C32B
11   PATH3  0 1 SCRBL  B41B  2 SCRBL B42B
11   PATH3  0 3 SCRBL  B43B
```

Figure A.2. Type 11 Cards of A.BURN for the Equilibrium Cycle with Fuel Shuffling

The feed enrichment of fresh fuel was determined by imposing the same criticality condition applied to the scattered loading case. As expected, the modified version produced the same results with the existing version. The required feed enrichment to satisfy the imposed criticality constraint was 27.33%. The resulting k-eff at BOEC and EOEC were 1.01976 and 1.00197, respectively. The feed enrichment is slightly lower than that of the scattered loading case, since more fresh fuel is loaded near the core center. The region C21B is loaded with fresh fuel in the fuel shuffling case, but only one third of the fuel is replaced with fresh fuel in the scattered loading case.

A.2.2. Non-equilibrium Cycle Problems

The enrichment search was performed for non-equilibrium cycle problems that approximately represent the equilibrium state shown in Figure A.3. In order to search the feed enrichment for this core configuration using the current version, at least three burn cycles need to be analyzed starting from a core loaded with all fresh fuel. If the fuel management scheme is specified using the type 11 cards of A.BURN, this analysis can be formed unaffected by the

code modifications. Thus, a three-cycle problem starting from a core loaded with all fresh fuel was first studied by specifying the fuel management scheme using the type 11 cards of A.BURN. Then the same calculation was repeated by specifying the fuel management scheme using the type 35 cards to test the modifications related with the type 35 cards. Finally, to test the enrichment search option for the partial reloading, the feed enrichment was searched for a core configuration obtained from the equilibrium cycle problem with fuel shuffling. Two calculations were performed separately by specifying the fuel management scheme using the type 11 and the type 35 cards of A.BURN.

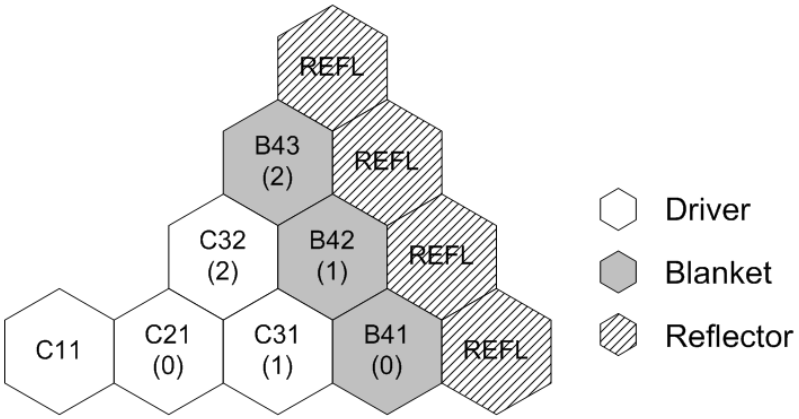

Figure A.3. Number of Previous Burn Cycles of Each Assembly at BOEC in the Equilibrium Cycle Problem with Fuel Shuffling

Three-Cycle Problem Starting from a Core Loaded with All Fresh Fuel

As mentioned above, in the current version, only fresh fuel can be introduced in the reactor at the beginning of problem. As a result, in order to determine the feed enrichment of fresh assemblies for the core configuration shown in Figure A.3, at least three burn cycles need to be analyzed starting from the first cycle loaded with all fresh fuel. Thus, a three-cycle non-equilibrium problem was studied using the same sequence of fuel movement as in the equilibrium cycle problem with fuel shuffling.

In order to represent the burned states of individual assemblies, the same sequence of fuel movement to an equilibrium cycle needs to be specified differently in a non-equilibrium cycle problem. For the equilibrium cycle, three fuel management paths were defined to specify the fuel shuffling sequence as shown in Figure A.3. On the other hand, for the non-equilibrium cycle, four additional paths need to be defined to represent the burned states of individual regions as in the type 11 cards of the dataset A.BURN shown in Figure A.4. For example, PATH3 specifies that once burned fuel initially loaded into the region C21B resides in the region C31B. The reactor configuration for each of three cycles obtained by applying these fuel management paths is shown in Table A.1. In this table, to show the fuel movement explicitly, different names are employed for the same secondary composition.

The feed enrichment was determined such that the k-eff at the end of each cycle is 1.002 as in equilibrium cycle problems. The modified code produced the same results with the existing version as expected. The required feed enrichment and the k-eff at the beginning and the end

of cycle are summarized in Table A.2. Compared with the equilibrium cycle problem with fuel shuffling, the feed enrichment for the first cycle is reduced by ~2.4% since all the fuels loaded into the reactor is fresh. On the other hand, the enrichments for the second and third cycles are increased slightly since less fresh fuels are loaded. (In the equilibrium cycle, one third of the fuel in the region C11B is replaced with fresh fuel.) It can be seen from the results in Table A.2 that the feed enrichment converges approximately to the value of the equilibrium cycle problem.

```
11   PATH1   0 1 SCDRV  C11B  2 SCDRV C11B
11   PATH1   0 3 SCDRV  C11B
11   PATH2   0 1 SCDRV  C21B  2 SCDRV C31B
11   PATH2   0 3 SCDRV  C32B
11   PATH3   1 1 SCDRV  C21B  2 SCDRV C31B
11   PATH3   1 3 SCDRV  C32B
11   PATH4   2 1 SCDRV  C21B  2 SCDRV C31B
11   PATH4   2 3 SCDRV  C32B
11   PATH5   0 1 SCRBL  B41B  2 SCRBL B42B
11   PATH5   0 3 SCRBL  B43B
11   PATH6   1 1 SCRBL  B41B  2 SCRBL B42B
11   PATH6   1 3 SCRBL  B43B
11   PATH7   2 1 SCRBL  B41B  2 SCRBL B42B
11   PATH7   2 3 SCRBL  B43B
```

Figure A.4. Type 11 Cards of A.BURN for the Non-equilibrium Three-Cycle Problem Starting from a Core Loaded with All Fresh Fuel

Table A.1. Reactor Configuration of the Non-equilibrium Three-Cycle Problem Starting from a Core Loaded with All Fresh Fuel

Burn Cycle	Material Contained in Each Region						
	C11B	C21B	C31B	C32B	C41B	C42B	C43B
1	Driver1 (0)	Driver2 (0)	Driver3 (0)	Driver4 (0)	Blanket1 (0)	Blanket2 (0)	Blanket3 (0)
2	Driver1 (1)	Driver4 (0)	Driver2 (1)	Driver3 (1)	Blanket3 (0)	Blanket1 (1)	Blanket2 (1)
3	Driver1 (2)	Driver3 (0)	Driver4 (1)	Driver2 (2)	Blanket2 (0)	Blanket3 (1)	Blanket1 (2)

* The numbers in parentheses are the number of previous burn cycles.

In order to test the modifications in the subroutines REPROC and REFAB, the same calculation was repeated by specifying the fuel management scheme using the type 35 cards of A.BURN. When the type 35 cards are employed, the fuel management paths are specified as shown in Figure A.5. Since the paths specified with the type 35 cards are not repetitive, additional paths need to be defined for the fresh fuels to be loaded at cycles 2 and 3. For example, as indicated in Table A.1, the fresh fuel loaded into the region C32B at the beginning of cycle 1 is discharged at the end of cycle 1, and then the fuel in the region C31B is moved into the region C32B and the fuel in C21B is moved into C31B. Thus, a new fuel needs to be loaded into the region C21B. The new path PATH4A defines the move sequence for this newly charged fuel into the region C21B at the cycle 2. PATH4 shows that the fuel in the region C32B is discharged at the end of cycle 1.

Table A.2. Feed Enrichment and Multiplication Factor of Each Cycle in the Non-equilibrium Three-Cycle Problem Starting from a Core Loaded with All Fresh Fuel

Burn Cycle	Feed Enrichment (%)	k-eff at BOC	k-eff at EOC
1	26.69	1.02038	1.00219
2	27.63	1.01966	1.00170
3	27.96	1.01970	1.00200

```
35   PATH1   PCDRV1  C11B  1 3
35   PATH2   PCDRV2  C21B  1 1 C31B  2 2 C32B  3 3
35   PATH3   PCDRV2  C31B  1 1 C32B  2 2
35   PATH4   PCDRV2  C32B  1 1
35   PATH5   PCRBL1  B41B  1 1 B42B  2 2 B43B  3 3
35   PATH6   PCRBL1  B42B  1 1 B43B  2 2
35   PATH7   PCRBL1  B43B  1 1
35   PATH3A  PCDRV2  C21B  3 3
35   PATH4A  PCDRV2  C21B  2 2 C31B  3 3
35   PATH6A  PCRBL1  B41B  3 3
35   PATH7A  PCRBL1  B41B  2 2 B42B  3 3
```

Figure A.5. Type 35 Cards of A.BURN for the Non-equilibrium Three-Cycle Problem Starting from a Core Loaded with All Fresh Fuel

Three-Cycle Problem Starting from a Core Loaded with Fresh and Burned Fuels

In order to test the enrichment search option for the partial reloading, a three-cycle non-equilibrium problem was studied starting from the core configuration shown in Figure A.3. The burned fuel compositions obtained from the equilibrium cycle problem with fuel shuffling were loaded into the regions C31B, C32B, B42B, and B43B, and the feed enrichment was searched for the fresh fuels to be loaded into regions C11B, C21B, and C41B. The reactor configuration for each of three cycles is shown in Table A.3. Note that this problem only approximates the equilibrium cycle problem with fuel shuffling; in the equilibrium cycle problem, one third of the fuel in the region C11B is replaced with fresh fuel at the end of each cycle.

On the type 13 cards of the dataset A.NIP3, four additional materials MTDRV2, MTDRV3, MTRBL2, and MTRBL3 are defined using the active isotope densities obtained from the equilibrium cycle analysis; MTDRV2 and MTDRV3 represent respectively the compositions of once and twice burned driver assemblies, and MTRBL2 and MTRBL3 are the compositions of once and twice burned blanket assemblies. On the type 14 cards of A.NIP3, new secondary compositions SCDRV2, SCDRV3, SCRBL2, and SCRBL3 are defined in terms of MTDRV2, MTDRV3, MTRBL2, and MTRBL3, respectively. Four additional primary compositions PCDRV2, PCDRV3, PCRBL2, and PCRBL4 are also defined in terms of each of these secondary compositions on the type 14 cards, and assigned to regions C31B, C32B, B42B, and B43B, respectively. On the type 03 card of the dataset A.BURN, the number of previous burn cycles is set to –1. The fuel management paths for the burned fuels are redefined on the type 11 cards of the dataset A.BURN using the secondary compositions for burned fuels. The type 46 cards of A.BURN provide the information on the active volume fractions of burned fuels. The

active volume fraction of the burned fuels in PATH3 and PATH4 is same to that of the fresh fuel in PATH1, while the burned fuels in PATH6 and PATH7 have the same volume fraction of the fresh fuel in PATH5.

Table A.3. Reactor Configuration of the Non-equilibrium Three-Cycle Problem Starting from a Core Loaded with Fresh and Burned Fuels

Burn Cycle	Material Contained in Each Region						
	C11B	C21B	C31B	C32B	C41B	C42B	C43B
1	Driver1 (0)	Driver2 (0)	Driver3 (1)	Driver4 (2)	Blanket1 (0)	Blanket2 (1)	Blanket3 (2)
2	Driver1 (1)	Driver4 (0)	Driver2 (1)	Driver3 (2)	Blanket3 (0)	Blanket1 (1)	Blanket2 (2)
3	Driver1 (2)	Driver3 (0)	Driver4 (1)	Driver2 (2)	Blanket2 (0)	Blanket3 (1)	Blanket1 (2)

* The numbers in parentheses are the number of previous burn cycles.

The feed enrichment was determined such that the k-eff at the end of each cycle is 1.002 as in the other problems. The required feed enrichment and the k-eff at the beginning and the end of cycle are summarized in Table A.4. The feed enrichment for the first cycle is very close to that of the equilibrium cycle with fuel shuffling as required. Even though an exact equilibrium state is not reached because of the central assembly, all three cycles well approximate the equilibrium cycle. The enrichment for the first cycle is slightly lower than that of the equilibrium cycle since the whole fuel in the region C11B is fresh. The feed enrichments for the second and third cycles are slightly higher than the equilibrium cycle value since the region C11B is loaded with burned fuel.

The same calculation was repeated by specifying the fuel management scheme using the type 35 cards of A.BURN. Figure A.6 shows the type 35 cards of this problem. The number of previous burn cycles for each of burned fuels is specified in PATH3, PATH4, PATH6, and PATH7 as a negative number. The paths PATH4A and PATH7A load fresh fuel at the beginning of cycle 2, and the paths PATH3A and PATH6A load fresh fuel at the beginning of cycle 3. PATH3A and PATH4A are defined with the fresh driver fuel, and PATH6A and PATH7A are defined with the fresh blanket fuel. The results obtained with the fuel management paths specified using type 35 cards were exactly same to those obtained with type 11 cards.

Table A.4. Feed Enrichment and Multiplication Factor of Each Cycle in the Non-equilibrium Three-Cycle Problem Starting from a Core Loaded with Fresh and Burned Fuels

Burn Cycle	Feed Enrichment (%)	k-eff at BOC	k-eff at EOC
1	27.46	1.01988	1.00202
2	27.51	1.01976	1.00198
3	27.69	1.01967	1.00200

```
35   PATH1   PCDRV1  C11B  1 3
35   PATH2   PCDRV2  C21B  1 1 C31B  2 2 C32B  3 3
35   PATH3   PCDRV3  C31B -1 1 C32B  2 2
35   PATH4   PCDRV4  C32B -2 1
35   PATH5   PCRBL1  B41B  1 1 B42B  2 2 B43B  3 3
35   PATH6   PCRBL2  B42B -1 1 B43B  2 2
35   PATH7   PCRBL3  B43B -2 1
35   PATH3A  PCDRV2  C21B  3 3
35   PATH4A  PCDRV2  C21B  2 2 C31B  3 3
35   PATH6A  PCRBL1  B41B  3 3
35   PATH7A  PCRBL1  B41B  2 2 B42B  3 3
```

Figure A.6. Type 35 Cards of A.BURN for the Non-equilibrium Three-Cycle Problem Starting from a Core Loaded with Fresh and Burned Fuels

A.3. Summary

An enrichment search capability for non-equilibrium cycle problems for partial reloading has been added to REBUS-3 to employ the LEUFBR fuel cycle analysis, and it can also extends its application to a wide range of fuel management strategies. The feed enrichment of fresh fuel can now be determined without performing the previous burn cycle analyses for an arbitrary core composed of fresh and burned fuel assemblies. Verification tests have been performed for various enrichment search options and fuel management schemes using a simple fast reactor model. Results from these tests indicated that the code changes have been correctly implemented.

Appendix B: Description of Type 03, 35, and 46 Cards of A.BURN

```
C-----------------------------------------------------------------------
CR          GENERAL PROBLEM DEFINITION DATA (TYPE 03)                  -
C                                                                      -
CL    FORMAT-----(I2,4X,I6,4E12.5,2I6)                                -
C                                                                      -
CD  #  COLUMNS          CONTENTS...IMPLICATIONS, IF ANY                -
CD  =  =======  ========================================================-
CD  1   1-2     03                                                     -
CD                                                                     -
CD  2   7-12    NUMBER OF PREVIOUS BURN CYCLES.                         -
CD                                                                     -
CD  3   13-24   SHUTDOWN TIME BETWEEN BURN CYCLES (IN DAYS).           -
CD              (NONEQUILIBRIUM PROBLEMS ONLY).                        -
CD                                                                     -
CD  4   25-36   TIME AT WHICH PROBLEM BEGINS (IN DAYS).                -
CD                                                                     -
CD  5   37-48   INITIAL TOTAL BURN CYCLE TIME GUESS (IN DAYS).         -
CD                                                                     -
CD  6   49-60   CONVERGENCE CRITERION, EPSG: ACTUAL ERROR ALLOWABLE    -
CD              IN BURNUP (SEE CARD TYPE 06 AND NOTE BELOW).           -
CD              (DEFAULT=0.001).                                       -
CD                                                                     -
CD  7   61-66   NUMBER OF SUBINTERVALS INTO WHICH THE TOTAL BURN CYCLE -
CD              TIME IS TO BE DIVIDED.                                 -
CD                                                                     -
CD  8   67-72   NUMBER OF FUEL MANAGEMENT OPERATIONS, FOR              -
CD              NONEQUILIBRIUM PROBLEMS ONLY. THIS VALUE IS 1 LESS     -
CD              THAN THE TOTAL NUMBER OF BURN CYCLES WHICH WILL BE     -
CD              COMPUTED.                                              -
C                                                                      -
CN              THE DATA CARDS OF A.BURN MAY BE DIVIDED INTO THE       -
CN              FOLLOWING FUNCTIONAL GROUPS:                           -
CN                                                  CARD TYPES         -
CN                      FUNCTION                 REQUIRED       OPTIONAL  -
CN              =========================  ===============  ===========-
CN              BASIC (NONEQUIL.) PROBLEM  03,09,11(35),24  01,02,10,25-
CN                                                                     -
CN              CHARGE ENRICHMENT SEARCH   04                          -
CN              + REQUIRED EXTERNAL CYCLE  12,13,18-22         --      -
CN                                                                     -
CN              BURNUP LIMITS              06               05,07,08   -
CN                                                                     -
CN              REPROCESSING PLANTS        15,16,17         14,23      -
CN                                                                     -
CN              IF THE FUEL MANAGEMENT IS SPECIFIED USING THE TYPE 35  -
CN              CARDS RATHER THAN THE TYPE 11 CARDS, CARD TYPES        -
CN              14, 15, 16, 17, AND 23 SHOULD NOT BE SUPPLIED.         -
CN                                                                     -
CN              THE TWO BASIC TYPES OF PROBLEMS WHICH MAY BE RUN ARE   -
CN              EQUILIBRIUM AND NONEQUILIBRIUM. AN EQUILIBRIUM PROBLEM -
CN              IS DEFINED AS ONE IN WHICH THE USER WISHES TO FIND THE -
CN              OPERATING CONDITIONS OF THE SPECIFIED REACTOR AFTER AN -
CN              INFINITE NUMBER OF BURN/DISCHARGE/REFUEL STEPS WITH    -
CN              THE CONDITIONS AND CONSTRAINTS AS SUPPLIED. SUCH       -
CN              PROBLEMS REQUIRE THE BASIC PROBLEM CARDS, THE CHARGE   -
CN              ENRICHMENT SEARCH AND EXTERNAL CYCLE CARDS, AND THE    -
CN              SPECIFICATION OF AT LEAST ONE BURNUP LIMIT.            -
CN              OPTIONALLY, ONE MAY INCLUDE REPROCESSING PLANTS IN THE -
CN              EXTERNAL CYCLE. A NONEQUILIBRIUM PROBLEM, ON THE OTHER -
CN              HAND, IS ONE IN WHICH THE BURN/REFUEL STEPS ARE        -
```

```
CN              EXPLICITLY COMPUTED IN SUCCESSION USING THE SUPPLIED   -
CN              PARAMETERS AND CONSTRAINTS. SUCH PROBLEMS REQUIRE ONLY -
CN              THE BASIC PROBLEM CARD TYPES LISTED ABOVE. OPTIONALLY, -
CN              ONE MAY SPECIFY AN ENRICHMENT SEARCH BY INCLUDING CARD -
CN              TYPE 04 AND THE REQUIRED EXTERNAL CYCLE CARDS. IF SUCH -
CN              A SEARCH IS SPECIFIED, ONE MAY ALSO SPECIFY DESIRED    -
CN              BURNUP LIMITS BY INCLUDING THE APPROPRIATE CARDS.      -
CN                                                                     -
CN              IN ORDER TO SEARCH THE FEED ENRICHMENT OF FRESH FUEL   -
CN              FOR A NONEQUILIBRIUM CYCLE PROBLEM WITH PARTIAL        -
CN              RELOADING, COLS. 7-12 SHOULD BE A NEGATIVE NUMBER.     -
CN              IN THIS CASE, THE TYPE 46 CARD NEEDS TO BE INCLUDED    -
CN              IN ADDITION TO THE TYPE 04 CARD AND THE ASSOCIATED     -
CN              EXTERNAL CYCLE CARDS. THE MATERIALS USED TO MAKE UP    -
CN              SECONDARY COMPOSITIONS ARE SPECIFIED ON THE TYPE 13    -
CN              AND 14 CARDS OF THE DATASET A.NIP3. IN DEFINING THE    -
CN              MATERIALS USED TO MAKE UP FRESH FUEL, THE ACTIVE ATOM  -
CN              DENSITIES MUST BE SET TO 1.0 AS USUAL. THE MATERIALS   -
CN              USED TO MAKE UP BURNED FUELS ARE DEFINED USING ACTUAL  -
CN              DENSITIES.                                             -
CN                                                                     -
CN              THE TOTAL BURN CYCLE TIME MAY BE DIVIDED INTO A NUMBER -
CN              OF EQUAL SUBINTERVALS, AS GIVEN IN COLS. 61-66 OF THIS -
CN              CARD. FLUX DISTRIBUTIONS WILL BE COMPUTED AT TIME ZERO -
CN              AND AT THE END OF EACH OF THESE SUBINTERVALS. EACH     -
CN              SUCH POINT IS CALLED A TIME NODE. A PROBLEM WITH N     -
CN              SUBINTERVALS THUS HAS N+1 TIME NODES. IF CONTROL       -
CN              MATERIALS ARE PRESENT, THE APPROPRIATE CONTROL SEARCHES-
CN              MAY BE CARRIED OUT TO MAINTAIN A PRESCRIBED KEFF AT    -
CN              EACH OF THESE TIME NODES. (SEE CARD TYPES 21, 22       -
CN              AND 23 OF DATA SET A.NIP3).                            -
CN                                                                     -
CN              FOR EQUILIBRIUM PROBLEMS, A MAXIMUM OF FOUR            -
CN              SUBINTERVALS IS ALLOWED. THERE IS NO LIMIT FOR         -
CN              NONEQUILIBRIUM PROBLEMS.                               -
CN                                                                     -
CN              NOTE: IF COLS. 49-60 ARE NON-NEGATIVE, THE BURNUP WILL -
CN              BE DEFINED AS THE RATIO OF FISSIONABLE ATOMS DESTROYED -
CN              BY FISSION IN THE DISCHARGED FUEL TO THE TOTAL         -
CN              FISSIONABLE ATOMS INITIALLY PRESENT IN THE FUEL.  IF   -
CN              COLS. 49-60 ARE NEGATIVE, THE BURNUP WILL BE DEFINED   -
CN              AS THE RATIO OF FISSIONABLE ATOMS DESTROYED BY ALL     -
CN              PROCESSES IN THE DISCHARGED FUEL TO THE TOTAL          -
CN              FISSIONABLE ATOMS INITIALLY PRESENT IN THE FUEL, AND   -
CN              THE ABSOLUTE VALUE OF COLS. 49-60 WILL BE USED FOR     -
CN              EPSG.  FISSIONABLE ISOTOPES ARE THOSE ACTIVE ISOTOPES  -
CN              WHICH APPEAR ON A CARD TYPE 09 WITH A 2 IN COLS. 13-18.-
C                                                                      -
C---------------------------------------------------------------------

C---------------------------------------------------------------------
CR          GENERAL FUEL MANAGEMENT SPECIFICATIONS (TYPE 35)           -
C                                                                      -
CL    FORMAT-----(I2,4X,A6,A6,3(A6,2I6))                               -
C                                                                      -
CD  #  COLUMNS          CONTENTS...IMPLICATIONS, IF ANY                -
CD  =  =======  ========================================================-
CD  1   1-2     35                                                     -
CD                                                                     -
CD  2   7-12    PATH LABEL (REPEATED ON ADDITIONAL CARDS, IF            -
CD              NECESSARY).                                            -
CD                                                                     -
CD  3   13-18   PRIMARY COMPOSITION (ZONE) OR SECONDARY COMPOSITION    -
```

```
CD              (SUB-ZONE) LABEL                                        -
CD                                                                      -
CD  4   19-24   REGION LABEL OR FUEL MANAGEMENT GROUP LABEL OR          -
CD              PRIMARY COMPOSITION (ZONE) LABEL.                       -
CD                                                                      -
CD  5   25-30   BEGINNING STAGE NUMBER FOR WHICH THE COMPOSITION        -
CD              SPECIFIED IN COLS. 13-18 RESIDES IN THE REGION OR ZONE -
CD              SPECIFIED IN COLS. 19-24.                               -
CD                                                                      -
CD  6   31-36   ENDING STAGE NUMBER FOR WHICH THE COMPOSITION           -
CD              SPECIFIED IN COLS. 13-18 RESIDES IN THE REGION OR ZONE -
CD              SPECIFIED IN COLS. 19-24.                               -
CD                                                                      -
CD  7   37-42   REGION LABEL OR FUEL MANAGEMENT GROUP LABEL OR          -
CD              PRIMARY COMPOSITION (ZONE) LABEL.                       -
CD                                                                      -
CD  8   43-48   BEGINNING STAGE NUMBER FOR WHICH THE COMPOSITION        -
CD              SPECIFIED IN COLS. 13-18 RESIDES IN THE REGION OR ZONE -
CD              SPECIFIED IN COLS. 37-42.                               -
CD                                                                      -
CD  9   49-54   ENDING STAGE NUMBER FOR WHICH THE COMPOSITION           -
CD              SPECIFIED IN COLS. 13-18 RESIDES IN THE REGION OR ZONE -
CD              SPECIFIED IN COLS. 37-42.                               -
CD                                                                      -
CD  10  55-60   REGION LABEL OR FUEL MANAGEMENT GROUP LABEL OR          -
CD              PRIMARY COMPOSITION (ZONE) LABEL.                       -
CD                                                                      -
CD  11  61-66   BEGINNING STAGE NUMBER FOR WHICH THE COMPOSITION        -
CD              SPECIFIED IN COLS. 13-18 RESIDES IN THE REGION OR ZONE -
CD              SPECIFIED IN COLS. 55-60.                               -
CD                                                                      -
CD  12  67-72   ENDING STAGE NUMBER FOR WHICH THE COMPOSITION           -
CD              SPECIFIED IN COLS. 13-18 RESIDES IN THE REGION OR ZONE -
CD              SPECIFIED IN COLS. 55-60.                               -
C                                                                       -
CN              CARD TYPES 35, 36, AND 37 ARE PERTINENT ONLY TO         -
CN              NON-EQUILIBRIUM PROBLEMS.                               -
CN                                                                      -
CN              IF BOTH TYPE 11 AND 35 CARDS ARE PRESENT, THE TYPE 11   -
CN              CARDS WILL BE IGNORED.                                  -
CN                                                                      -
CN              IF COLS. 31-36 AND/OR 49-54 AND/OR 67-72 ARE BLANK OR 0-
CN              THE ENDING STAGE NUMBER WILL BE SET EQUAL TO THE        -
CN              BEGINNING STAGE NUMBER SPECIFIED IN COLS. 25-30 AND/OR -
CN              43-48 AND/OR 61-66.                                     -
CN                                                                      -
CN              FOR A GIVEN PATH, COLS. 19-24, 37-42, AND 55-60 MUST    -
CN              EITHER BE ALL REGION LABELS, OR ALL FUEL MANAGEMENT      -
CN              LABELS, OR ALL PRIMARY COMPOSITION (ZONE LABELS).  SEE -
CN              CARD TYPE 45 FOR SPECIFICATION OF THE FUEL MANAGEMENT   -
CN              GROUPS.  IF ZONE LABELS ARE BEING USED, COLS. 13-18     -
CN              MUST CONTAIN A SUB-ZONE LABEL.  IF REGION (OR FUEL      -
CN              MANAGEMENT GROUP) LABELS ARE BEING USED, COLS. 13-18    -
CN              MUST CONTAIN A ZONE LABEL.                              -
CN                                                                      -
CN              IF ZONE LABELS OR FUEL MANAGEMENT GROUP LABELS ARE      -
CN              BEING USED TO DEFINE A PATH, COLS. 19-24, 37-42, AND    -
CN              55-60 MUST ALL CONTAIN THE SAME LABEL OR BE BLANK.      -
CN              THIS IS NECESSARY SINCE IT IS NOT POSSIBLE TO KNOW      -
CN              WHICH OF THE REGIONS ASSOCIATED WITH ONE OF THE STAGES -
CN              IS CONNECTED WITH A PARTICULAR REGION IN THE NEXT STAGE-
CN              IF THE FUEL IS BEING SHUFFLED.                          -
CN                                                                      -
```

```
CN              IN STAGE 1 OF EACH PATH, THE ZONE/REGION OR             -
CN              SUB-ZONE/ZONE CORRESPONDENCES MUST AGREE WITH THAT      -
CN              IMPLIED FROM THE DATA SET A.NIP3 TYPE 14/15 CARDS.      -
CN                                                                      -
CN              IF A NON-BLANK LABEL IS SPECIFIED IN COLS. 19-24,       -
CN              37-42, AND.OR 55-60, AND THE CORRESPONDING BEGINNING    -
CN              AND ENDING STAGE NUMBERS ARE BOTH 0, BOTH STAGE         -
CN              NUMBERS WILL BE SET EQUAL TO 1.                         -
CN                                                                      -
CN              STAGE NUMBERS MAY NOT OVERLAP IN A PARTICULAR PATH.     -
CN              THUS THE FOLLOWING DATA (IN FREE FIELD FORMAT) WOULD    -
CN              RESULT IN A FATAL INPUT ERROR...                        -
CN              35 C1 R1 1 4 R2 5 8 R3 3 3                              -
CN                                                                      -
CN              THE MATERIAL IDENTIFIED BY THE ZONE OR SUB-ZONE         -
CN              LABEL IN COLS. 13-18 CAN BE SENT TO TEMPORARY STORAGE   -
CN              BY LEAVING ITS DESTINATION (COLS. 19-24 AND/OR 37-42    -
CN              AND/OR 55-60) BLANK. THUS, IF COLS. 19-24 AND/OR 37-42  -
CN              AND/OR 55-60 ARE BLANK, THE ZONE OR SUB-ZONE            -
CN              SPECIFIED IN COLS. 13-18 WILL BE ASSUMED TO BE          -
CN              TEMPORARILY DISCHARGED FOR THE STAGES SPECIFIED IN      -
CN              COLS. 25-36 AND/OR 43-54 AND/OR 61-72.  NOTE HOWEVER,   -
CN              THE DESTINATION LABEL MAY NOT BE BLANK FOR STAGE 1.     -
CN                                                                      -
CN              THE PATH SPECIFIED IS NON-REPETITIVE SO THAT THE        -
CN              MATERIAL IDENTIFIED BY THE ZONE OR SUB-ZONE LABEL       -
CN              IN COLS. 13-18 WILL BE PERMANENTLY DISCHARGED AFTER     -
CN              THE LAST SPECIFIED STAGE.  HOWEVER, A PATH MAY BE       -
CN              REPEATED BY MEANS OF THE TYPE 37 CARDS.                 -
CN                                                                      -
CN              IF THE SMALLEST BEGINNING STAGE NUMBER FOR A PARTICULAR-
CN              PATH IS GREATER THAN 1, COLS. 13-18 MUST CONTAIN A      -
CN              PRIMARY COMPOSITION (ZONE) LABEL, AND COLS. 19-24,      -
CN              37-42, AND 55-60 MUST CONTAIN REGION LABELS.  IN THIS   -
CN              CASE, IT WILL BE ASSUMED THAT THE MATERIAL IDENTIFIED   -
CN              BY THE ZONE LABEL IN COLS. 13-18 IS INTRODUCED AS       -
CN              FRESH FUEL AT THAT STAGE IN THE PATH.                   -
CN                                                                      -
CN              FOR THE ENRICHMENT SEARCH OPTION OF A NONEQUILIBRIUM    -
CN              CYCLE PROBLEM WITH PARTIAL RELOADING, THE NUMBER OF     -
CN              PREVIOUS BURN CYCLES NEEDS TO BE SPECIFIED FOR THE      -
CN              PATHS ASSOCIATED WITH BURNED FUELS TO BE LOADED INTO    -
CN              THE REACTOR. IT CAN BE SPECIFIED ON THIS CARD BY        -
CN              PROVIDING ITS NEGATIVE VALUE AS A BEGINNING STAGE       -
CN              NUMBER WITH THE CORRESPONDING ENDING STAGE NUMBER OF 1.-
C                                                                       -
C-----------------------------------------------------------------------

C-----------------------------------------------------------------------
CR          ACTIVE VOLUME FRACTION EQUIVALENCE LIST (TYPE 46)           -
C                                                                       -
CL    FORMAT-----(I2,4X,A6,10A6)                                        -
C                                                                       -
CD  #  COLUMNS          CONTENTS...IMPLICATIONS, IF ANY                 -
CD  =  =======  ========================================================-
CD  1   1-2     46                                                      -
CD                                                                      -
CD  2   7-12    PATH LABEL ASSOCIATED WITH FRESH FUEL (REPEATED ON       -
CD              ADDITIONAL CARDS, IF NECESSARY).                        -
CD                                                                      -
CD  3   13-18   PATH LABEL ASSOCIATED WITH BURNED FUEL WHICH HAS THE    -
CD              SAME ACTIVE VOLUME FRACTION WITH THE FRESH FUEL IN       -
CD              THE PATH SPECIFIED IN COLS. 7-12.                       -
```

```
CD                                                                      -
CD  4   19-24   PATH LABEL ASSOCIATED WITH BURNED FUEL WHICH HAS THE   -
CD              SAME ACTIVE VOLUME FRACTION WITH THE FRESH FUEL IN     -
CD              THE PATH SPECIFIED IN COLS. 7-12.                      -
CD                                                                     -
CD  5   25-30   PATH LABEL ASSOCIATED WITH BURNED FUEL WHICH HAS THE   -
CD              SAME ACTIVE VOLUME FRACTION WITH THE FRESH FUEL IN     -
CD              THE PATH SPECIFIED IN COLS. 7-12.                      -
CD                                                                     -
CD  6   31-36   PATH LABEL ASSOCIATED WITH BURNED FUEL WHICH HAS THE   -
CD              SAME ACTIVE VOLUME FRACTION WITH THE FRESH FUEL IN     -
CD              THE PATH SPECIFIED IN COLS. 7-12.                      -
CD                                                                     -
CD  7   37-42   PATH LABEL ASSOCIATED WITH BURNED FUEL WHICH HAS THE   -
CD              SAME ACTIVE VOLUME FRACTION WITH THE FRESH FUEL IN     -
CD              THE PATH SPECIFIED IN COLS. 7-12.                      -
CD                                                                     -
CD  8   43-48   PATH LABEL ASSOCIATED WITH BURNED FUEL WHICH HAS THE   -
CD              SAME ACTIVE VOLUME FRACTION WITH THE FRESH FUEL IN     -
CD              THE PATH SPECIFIED IN COLS. 7-12.                      -
CD                                                                     -
CD  9   49-54   PATH LABEL ASSOCIATED WITH BURNED FUEL WHICH HAS THE   -
CD              SAME ACTIVE VOLUME FRACTION WITH THE FRESH FUEL IN     -
CD              THE PATH SPECIFIED IN COLS. 7-12.                      -
CD                                                                     -
CD 10   55-60   PATH LABEL ASSOCIATED WITH BURNED FUEL WHICH HAS THE   -
CD              SAME ACTIVE VOLUME FRACTION WITH THE FRESH FUEL IN     -
CD              THE PATH SPECIFIED IN COLS. 7-12.                      -
CD                                                                     -
CD 11   61-66   PATH LABEL ASSOCIATED WITH BURNED FUEL WHICH HAS THE   -
CD              SAME ACTIVE VOLUME FRACTION WITH THE FRESH FUEL IN     -
CD              THE PATH SPECIFIED IN COLS. 7-12.                      -
CD                                                                     -
CD 12   67-72   PATH LABEL ASSOCIATED WITH BURNED FUEL WHICH HAS THE   -
CD              SAME ACTIVE VOLUME FRACTION WITH THE FRESH FUEL IN     -
CD              THE PATH SPECIFIED IN COLS. 7-12.                      -
C                                                                      -
CN              THE PATH LABELS SPECIFIED IN COLS 7-72 MUST CORRESPOND -
CN              TO LABELS SPECIFIED ON THE TYPE 11 OR 35 CARDS.        -
CN                                                                     -
CN              THE ACTIVE VOLUME FRACTION IS THE VOLUME FRACTION OF   -
CN              THE MATERIALS INCLUDING ACTIVE ISOTOPES IN A PRIMARY   -
CN              OR SECONDARY COMPOSITION WHICH IS USED IN DEFINING A   -
CN              FUEL MANAGEMENT PATH ON TYPE 11 OR 35 CARDS OF A.BURN. -
CN              A SECONDARY COMPOSITION IS DEFINED ON TYPE 14 CARDS OF -
CN              THE DATASET A.NIP3 IN TERMS OF VOLUME FRACTIONS OF     -
CN              MATERIALS DEFINED ON TYPE 13 OR 14 CARDS OF A.NIP3.    -
CN              A PRIMARY COMPOSITION IS DEFINED ON TYPE 14 CARD OF    -
CN              A.NIP3 IN TERMS OF SINGLE SECONDARY COMPOSITION. IN    -
CN              DEFINING MATERIALS USED TO MAKE UP FRESH FUEL, ACTIVE  -
CN              ATOM DENSITIES ARE SET TO 1.0, AND THUS THE ACTIVE     -
CN              VOLUME FRACTION OF EACH COMPOSITION IS OBTAINED FROM   -
CN              THE VOLUME FRACTION SPECIFIED ON A TYPE 14 CARD OF     -
CN              A.NIP3. HOWEVER, SINCE A MATERIALS USED TO MAKE UP     -
CN              BURNED FUEL IS DEFINED USING ACTUAL DENSITIES, THE     -
CN              ACTIVE VOLUME FRACTION NEEDS TO BE PROVIDED SEPARATELY.-
CN              THIS IS DONE BY SPECIFYING THE PATH LABEL ASSOCIATED   -
CN              WITH THE CORRESPONDING FRESH FUEL.                     -
C                                                                      -
C-----------------------------------------------------------------------
```

Appendix C: Fuel Cycle Metrics Evaluation and Data Package

The performance characteristics of the three fuel cycle options are evaluated against the Fuel Cycle Evaluation Metrics of the Fuel Cycle Options Campaign. For each fuel cycle option, the reactor and fuel information and the mass flow of the equilibrium cycle are provided. The fuel cycle data package is evaluated at the equilibrium state as the evaluation considered in the nuclear fuel cycle E&S report [2]. For the purpose of fair comparison of the amounts of fuel materials used and wastes produced in each fuel cycle option, the same nuclear loss rates of 0.2% in the fresh fuel fabrication and 1% in the discharged fuel separation were assumed.

C.1. Two-stage Fast Spectrum Fuel Cycle Options Based on FR and ADS

C.1.1. First Two-Stage FR/ADS Fuel Cycle Option

The proposed two-stage fuel cycle option of continuous recycle of plutonium in FR and subsequent burning of MAs in ADS is illustrated schematically in Figure C.1.1. The first stage is a sodium-cooled fast reactor fuel cycle starting with low-enriched uranium fuel; at the equilibrium cycle, the reactor is operated using the recovered plutonium and natural uranium only without supporting LEU. Pu and uranium are co-extracted from the discharged fuel and recycled in stage one and the recovered MAs are sent to the second-stage ADS. The reactor and fuel information are presented in Table C.1.1. The mass flow data of the equilibrium cycle are shown in Table C.1.2.

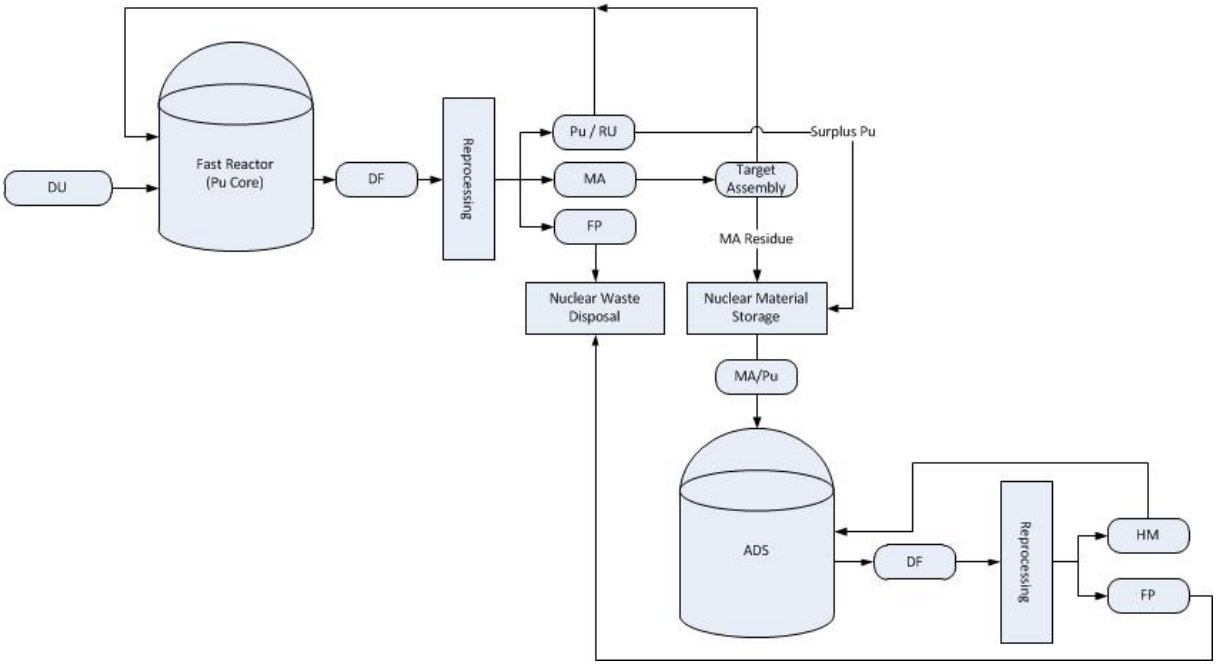

Figure C.1. Schematic Illustration of First Two-Stage FR/ADS Fuel Cycle Option

Table C.1. Reactor and Fuel Information of First Two-Stage FR/ADS Fuel Cycle Option

Technology category	Parameter		Stage number	
Nuclear power plant/ Transmutation (NPPT)	Stage		**1**	**2**
	NPPT technology identifier		**SFR**	**ADS-Burner**
	Core configuration		SFR with U-TRU-Zr	ADS with MA-Zr dispersion matrix fuel
	Core thermal power, MWth		1000	840
	Net thermal efficiency, %		40	40
	Electrical energy generation sharing, %		98.1	1.9
Nuclear fuel	Fuel type		1.1	2.1
	Fuel technology identifier		SFR-Metallic	ADS-Metallic
	Purpose		Driver	Driver
	Average discharge burnup, GWd/t		72.7	177.5
	Fuel Composition	Initial nuclear material(s)	Pu/RU/NU	MA
		(U-235+U-233)/total U, %	~0	13.0
		Th/total HM, %	0	0
		TRU/total HM, %	14.2	96.4
	Fuel residence time in reactor, EFPY		4.4	2.8

Table C.2. Mass Flow Data of First Two-stage FR/ADS Fuel Cycle Option (Metric Ton per 100 GWe-yr at Equilibrium State)

Stage		1			2			Sum
Technology		Fuel	NPPT[a]	Rep/Sep[b]	Fuel	NPPT	Rep/Sep	
Electricity, GWe-yr		98.1			1.9			100.0
Feed or product of nuclear materials (MT)								
Natural resource	NU	-102.8						-102.8
	Th							
Products from fuel or NPPT technology	DU							
	U	+1,005.0	-1,005.0		+0.3	-0.3		0.0
	Pu	+153.9	-153.9		+3.2	-3.2		0.0
	MA				+5.5	-5.5		0.0
	DF		+1,159.7	-1,159.7		+9.0	-9.0	0.0
Products from Rep/Sep technology	RU	-904.3		+904.3	-0.3		+0.3	0.0
	Pu	-154.2		+154.2	-3.1		+3.0	0.0
	MA			+1.7	-5.6		+3.9	0.0
	FP			+88.7			+1.7	+90.5
Loss[c]		+2.3		+10.7	+0.0		+0.1	+13.1

[a] NPPT = Nuclear Power Plant / Transmutation
[b] Rep/Sep = Reprocessing / Separation
[c] Loss of U, Pu and MAs

C.1.2. Second Two-Stage FR/ADS Fuel Cycle Option with MA Targets in FR

The first stage is a sodium-cooled fast reactor fuel cycle similar to that of the first FR/ADS fuel cycle option. Pu and uranium are co-extracted from the discharged fuel and recycled in stage one, but the recovered MAs are not sent to stage two directly. In order to reduce the heavy metal inventory in the second-stage ADS, the recovered MAs are made into moderated targets with zirconium hydride moderator and loaded into the fast reactor. The proposed two-stage fuel cycle option with MA and LLFP targets is illustrated schematically in Figure C.2. The reactor and fuel information are presented in Table C.3. The mass flow data of the equilibrium cycle are shown in Table C.4.

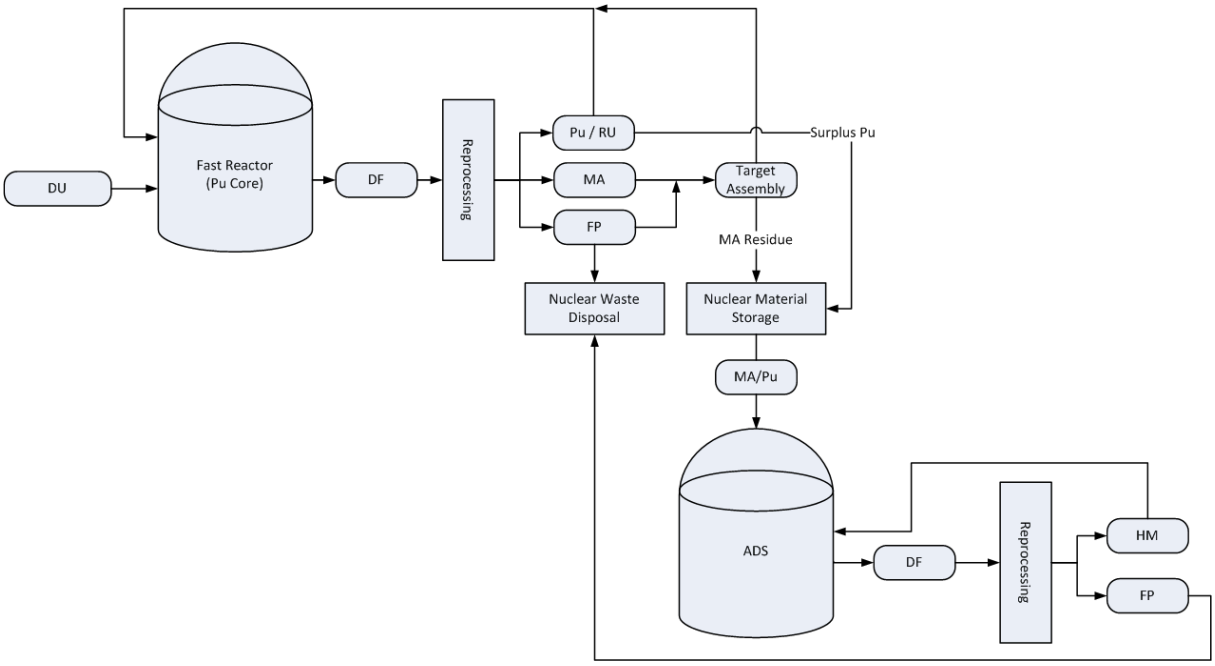

Figure C.2. Schematic Illustration of Second Two-Stage FR/ADS Fuel Cycle Option with MA Targets in FR

Table C.3. Reactor and Fuel Information of Second Two-Stage FR/ADS Fuel Cycle Option with MA Targets in FR

Technology category	Parameter		Stage number		
Nuclear power plant/ Transmutation (NPPT)	Stage		**1**		**2**
	NPPT technology identifier		**SFR**		**ADS-Burner**
	Core configuration		SFR with U-Pu-10Zr / MA-40Zr (Driver / Target)		ADS with MA-Zr dispersion matrix fuel
	Core thermal power, MWth		1000		840
	Net thermal efficiency, %		40		40
	Electrical energy generation sharing, %		99.7		0.3
Nuclear fuel	Fuel type		1.1	1.2	2.1
	Fuel technology identifier		SFR-Metallic	SFR-Metallic	ADS-Metallic
	Purpose		Driver	Target	Driver
	Average discharge burnup, GWd/t		70.5	278.1	231.0
	Fuel Composition	Initial nuclear material(s)	Pu//RU/NU	MA	MA
		(U-235+U-233)/total U, %	~0	0	13.7
		Th/total HM, %	0	0	0
		TRU/total HM, %	14.2	100.0	98.2
	Fuel residence time in reactor, EFPY		4.4	1.3	2.8

Table C.4. Mass Flow Data of Second Two-Stage FR/ADS Fuel Cycle Option with MA Targets in FR (Metric Ton per 100 GWe-yr at Equilibrium State)

Stage		1			2			Sum
Technology		Fuel	NPPT	Rep/Sep	Fuel	NPPT	Rep/Sep	
Electricity, GWe-yr		99.7			0.3			100.0
Feed or product of nuclear materials (MT)								
Natural resource	NU	-103.2						-103.2
	Th							
Products from fuel or NPPT technology	DU							
	U	+1,045.7	-1,045.7		+0.0	-0.0		0.0
	Pu	+159.2	-159.2		+0.4	-0.4		0.0
	MA	+3.3	-3.3		+0.6	-0.6		0.0
	DF		+1,209.0	-1,209.0		+1.0	-1.0	0.0
Products from Rep/Sep technology	RU	-944.6		+944.6	-0.0		+0.0	0.0
	Pu	-159.5		+159.5	-0.3		+0.3	0.0
	MA	-3.3		+3.6	-0.7		+0.4	0.0
	FP	-1.6		+90.2			+0.3	+88.9
Loss		+2.4		+11.2	+0.0		+0.0	+13.6

C.2. Single-Stage Fast Reactor Option with Homogeneous Recycle of TRU in FR

In the single-stage fast reactor option with homogeneous recycling of TRU, TRU is recycled in the driver fuel assemblies as a group without partitioning into Pu and MA streams, as shown in Figure C.3. The uranium, plutonium as well as MAs are co-extracted from the discharged fuel and recycled into FR. The reactor and fuel information are presented in Table C.5. The mass flow data of equilibrium cycle are shown in Table C.6.

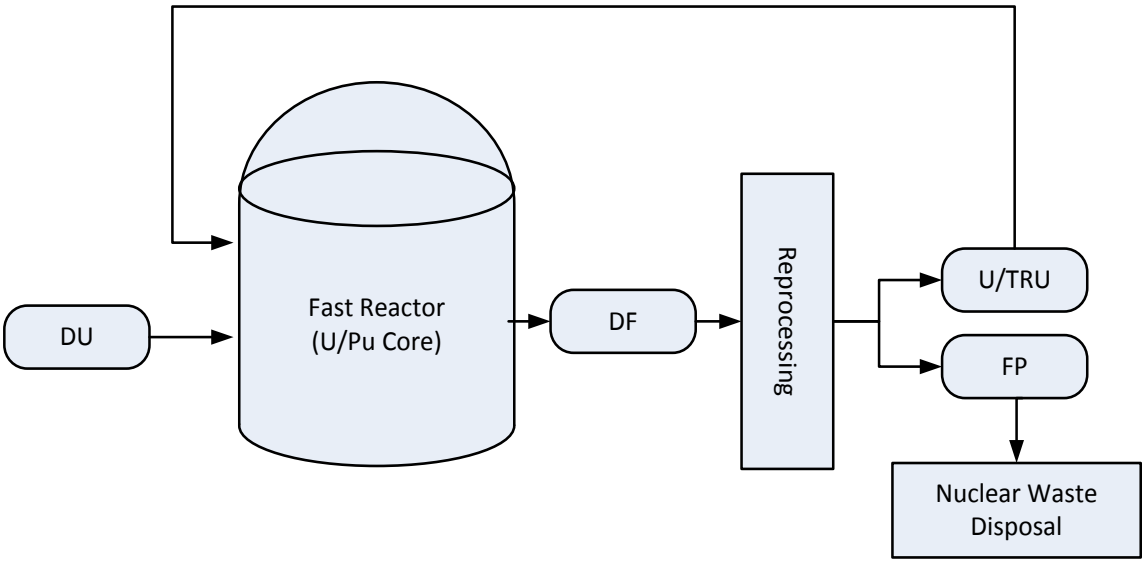

Figure C.3. Schematic Illustration of the Single-Stage Fast Reactor Option with Homogeneous Recycling of TRU

Table C.5. Reactor and Fuel Information of Single-Stage Fast Reactor Option with Homogeneous Recycling of TRU

Technology category	Parameter		Stage number
Nuclear power plant/ Transmutation (NPPT)	Stage		1
	NPPT technology identifier		SFR
	Core configuration		SFR with U-TRU-Zr
	Core thermal power, MWth		1000
	Net thermal efficiency, %		40
	Electrical energy generation sharing, %		100
Nuclear fuel	Fuel type		1.1
	Fuel technology identifier		SFR-Metallic
	Purpose		Driver
	Average discharge burnup, GWd/t		73.7
	Fuel Composition	Initial nuclear material(s)	TRU/RU/NU
		(U-235+U-233)/total U, %	~0
		Th/total HM, %	0
		TRU/total HM, %	14.8
	Fuel residence time in reactor, EFPY		4.4

Table C.6. Mass Flow Data of the Single-Stage Fast Reactor Option with Homogeneous Recycling of TRU (Metric Ton per 100 GWe-yr at Equilibrium State)

Stage		1			Sum
Technology		Fuel	NPPT	Rep/Sep	
Electricity, GWe-yr		100.0			100.0
Feed or product of nuclear materials (MT)					
Natural resource	NU	-102.6			-102.6
	Th				
Products from fuel or NPPT technology	DU				
	U	+1,003.0	-1,003.0		0.0
	TRU	+161.9	-161.9		0.0
	DF		+1,165.8	-1,165.8	0.0
Products from Rep/Sep technology	RU	-902.4		+902.4	0.0
	TRU	-162.2		+162.2	0.0
	FP			+90.4	+90.4
Loss		+2.3		+10.8	+13.1

PURDUE
UNIVERSITY

School of Nuclear Engineering
Purdue University
400 Central Drive
West Lafayette, IN 47907

www.purdue.edu